Computational modeling of the immune responses induced by both natural HPV infections and vaccination with Gardasil®

Gustavo Olivera-Botello

N° d'ordre : **THESE DE L'UNIVERSITE DE LYON** Année 2011

38 - 2011

Délivrée par

L'UNIVERSITE CLAUDE BERNARD LYON 1

Ecole doctorale

E2M2 : EVOLUTION, ECOSYSTEMES, MICROBIOLOGIE, MODELISATION

Pour l'obtention du

DIPLOME DE DOCTORAT

(arrêté du 7 août 2006)

soutenue publiquement le

18 FEVRIER 2011

par

Gustavo OLIVERA-BOTELLO

Modélisation numérique des aspects immunologiques de la réaction à l'infection à HPV et de la vaccination anti-HPV par Gardasil®

Directeur de thèse :	Pr. Jean-Pierre BOISSEL	Université Claude Bernard Lyon 1
Codirecteur de thèse :	Dr. Benoît SOUBEYRAND	Sanofi Pasteur MSD
Rapporteurs :	Pr. Vincent RODIN	Université de Bretagne Occidentale
	Dr. Randall THOMAS	Université d'Evry
Examinateurs :	Pr. Patrice MATHEVET	Université Claude Bernard Lyon 1
	Dr. Jean-Luc GOUZE	INRIA Sophia Antipolis
	Dr. Guillaume MONNERET	CHU de Lyon

RÉSUMÉ

L'infection au papillomavirus humain (HPV) est connue pour être le principal facteur causal d'une série de maladies aussi bien bénignes (condylomatose ano-génitale, papillomatose lyringée, et autres) que malignes (cancer du col de l'utérus, certains cancers ORL, et autres). Deux vaccins prophylactiques (Gardasil® et Cervarix®) sont sur la marché depuis à peu près quatre ans pour prévenir cette infection.

Le présent travail de thèse comportait trois objectifs principaux : i) étudier in-silico l'immunogénicité du vaccin Gardasil® ; ii) étudier in-silico l'histoire naturelle d'une infection à HPV et iii) évaluer in-silico le potentiel de l'hypothèse thérapeutique suivante : l'administration intramusculaire du vaccin Gardasil® chez des patients atteints d'une papillomatose laryngée induirait un effet bénéfique car l'arrivée des immunoglobulines au tissu affecté empêcherait l'HPV de compléter son cycle de vie et, par conséquent, la maladie de se propager.

Le type de modélisation que nous avons employé pour ce travail a consisté à créer une synthèse numérique des connaissances fondamentales existantes sur quelques phénomènes biologiques très précis afin d'explorer in-silico de nombreux scénarios possibles bâtis autour de leurs implications possibles en physiopathologie, rapidement et à des coûts relativement bas. Dans ce contexte nous avons développé un modèle mathématique comportant une vingtaine d'équations différentielles avec délai (dites DDEs) afin de décrire la dynamique des interactions entre plusieurs familles de cellules du système immunitaire consécutives à l'administration du vaccin Gardasil®. L'entrée du modèle est le protocole de vaccination et la sortie est l'évolution au cours du temps du titre sérique d'immunoglobulines (IgG) anti-HPV. Le système d'équations a été implémenté sur une plateforme MatLab® avant d'être calibré et validé en utilisant des données issues de la littérature. Ce premier modèle, de façon indépendante, a servi à étudier in-silico les effets sur l'immunogénicité des variations du protocole de vaccination, dans le cas particulier de Gardasil®. Cette question est

toujours d'actualité puisque, à l'heure actuelle, elle est traitée dans une douzaine d'études cliniques (en cours) enregistrées sur la base ClinicalTrials.gov.

En parallèle, un deuxième modèle a été développé en utilisant, cette fois-ci, la méthode dite des systèmes multi-agents. A l'aide de ce modèle nous avons étudié quantitativement l'avenir infectieux d'un segment de tissu muqueux (à la base sain) ayant été soumis à une exposition au papillomavirus humain. L'HPV est un pathogène plutôt furtif et silencieux et le fait qu'il puisse conquérir et rester longtemps dans un tissu dépend principalement de sa capacité à accomplir répétitivement son cycle de vie (malgré la barrière physique qu'est l'épithélium). Nous avons ainsi intégré les principaux facteurs connus pour avoir un effet sur le cycle de vie de l'HPV dans la conception de ce modèle, avant de le calibrer en utilisant des données issues de la littérature.

Les principales conclusions sont : i) pour qu'une papillomatose laryngée ne s'étende pas il faudrait, d'après nos simulations, que le taux d'IgGs sériques soit maintenu au-dessus de 200 mMU/mL ; ii) pour rester, sur une période de 10 ans, le plus longtemps possible au-dessus de ce seuil (d´effet thérapeutique), en administrant la quantité minimale de vaccin, il faudrait, d'après nos simulations, suivre le protocole suivant : l'immunisation de base (à 0, 2 et 6 mois), suivie de trois rappels successifs tous les six mois jusqu'au 24ème mois, suivis d'un rappel 18 mois plus tard ; iii) par ailleurs, il semble inutile (voire contreproductif), d'après nos simulations, de modifier le schéma traditionnel de base (0-2-6 mois) ; et iv) du point de vue de l'immunogéncité, l'effet principal de l'administration des rappels (c'est-à-dire, à partir de la quatrième dose) serait, d'après nos simulations, la montée progressive du plateau d'IgGs.

ABSTRACT

Infection with the human papillomavirus (HPV) is well known to be the origin of a series of benign (condylomata acuminata, recurrent respiratory papillomatosis, and others) as well as of malign (cervical cancer, some head and neck cancers, and others) diseases. Two prophylactic vaccines (Gardasil® and Cervarix®) have demonstrated to prevent HPV infection and have been in the market for the last four years, or so.

The three main objectives of the present project were: i) to study in-silico the immunogenicity of the vaccine Gardasil® ; ii) to study in-silico the natural history of an HPV infection, and iii) to assess in-silico the potential of the following therapeutic hypothesis : the intramuscular administration of Gardasil® to patients already suffering from a recurrent respiratory papillomatosis would result in a better prognosis thanks to the fact that the HPV-specific immunoglobulins that would bathe the affected tissue would impede the virus to complete its life cycle and, therefore, the disease to progress.

The modeling that we employed for this project consists in synthesizing, by means of a computational simulator, as much of the available knowledge on a given biological phenomenon as possible. The goal is to use such a simulator for exploring the implications of a great number of scenarios, rapidly and at relatively low costs. Within this framework, we devised a mathematical model made up of twenty delay differential equations (commonly referred to as DDEs) with the aim of describing the dynamics of the interactions between several families of immuno-competent cells, following vaccination with Gardasil®. The main input of this model is the vaccination schedule and the main output is the predicted evolution, through time, of the serum HPV-specific IgG immunoglobulin titer. This mathematical model was implemented in MatLab®, before being calibrated and validated on the basis of real data taken from literature. This first model, independently, was used to study in-silico the effect on Gardasil®'s immunogenicity of modifying

the vaccination schedule. We can affirm that this question is still relevant because it is treated in about twelve ongoing clinical trials registered in ClinicalTrials.gov.

Simultaneously, a second model was devised, based this time on a multi-agent-system kind of approach. The aim was to quantitatively study the infectious fate of a fragment of initially-healthy mucosal tissue having been exposed to HPV. The human papillomavirus is a rather silent and stealthy pathogen and the likelihood of it succeeding to settle down in a fragment of tissue mainly depends on its own capacity to repetitively accomplish its life cycle (despite the presence of a physical barrier: the epithelium). Thus, we integrated in our model the main factors known to have an effect on HPV's viral cycle, before calibrating it with real data drawn from literature.

The main conclusions are: i) according to our simulations, the minimum serum IgG titer required for hampering the progression of a recurrent respiratory papillomatosis would be 200 mMU/mL ; ii) in order to keep, within a time window of ten years, the anti-HPV IgG titer over the just-mentioned therapeutic-effect threshold, the biggest possible fraction of time and through the administration of the smallest possible number of booster doses, it would be necessary, according to our simulations, to adopt the following vaccination schedule: the basic immunization three doses (at months 0, 2 and 6), followed by three successive booster doses, every six months, until reaching the 24^{th} month, followed by a late final booster dose, 18 months later. iii) incidentally, it would seem to be inappropriate, according to our simulations, to modify the original initial vaccination schedule (at months 0, 2 and 6); and iv) from the immunogenicity point of view, the main effect of administering booster doses (i.e. from the fourth dose on) would be, according to our simulations, higher titer values for the residual IgG's plateau.

To Valéria, my daughter, the sunshine in my heart, who recently taught me that not even being 37 centimeters long and weighing 1190 grams can be an obstacle to a brave soul ...

To Adriana, my loving wife, not only for her patience (because as The Beatles once wrote and sang: this one has been a "long and winding road") but also for the many hours of very constructive discussions on the subject of this thesis ...

To Domidoro, my mother, for having taught me both to aim high and to always keep the faith ...

To Santiago, my brother, for having taught me to see things differently and for being my partner in this beautiful journey called life ...

To all my family and friends ...

SUMMARY

SECTION V: IN-SILICO SIMULATIONS – THE PRODUCT

SECTION VI: GENERAL DISCUSSION, CONCLUSIONS AND PERSPECTIVES

APPENDICES

LIST OF FIGURES

LIST OF TABLES

OVERVIEW

The present document summarizes the doctoral research work that I conducted between January 2007 and July 2010 as a member of the TEAM team (Therapeutic Effect Assessment and Modeling) of the CNRS' Biometrics and Evolutionary Biology Laboratory (UMR-5558), at Claude Bernard University, in Lyon, France.

If a single keyword had to be found to describe this project, it would have to be "multidisciplinarity". In order to come up with the simulators (section IV) that permitted us to obtain the results that we herein present (section V), it was necessary to analyze the fundamental science behind both HPV natural infections and vaccination with Gardasil® (section III). That means having to deal with state-of-the-art knowledge in vaccinology, immunology, virology, etc. On the other hand, the computational modeling of such phenomena implies having to deal with mathematical models, computational algorithms, scientific computing, etc. Although it may sound complicated, coping with such scientific diversity is not certainly so big a challenge as wanting to talk about it to the outer world. Thus, a huge effort was made when writing this document so that readers that are naive to one or several of the disciplines treated inside do not feel lost from the very first glimpse.

For starters, in the preface, I present some generalities on the human papillomavirus (experts on HPV should simply skip this part).

In section I, the starting point of my doctoral research work is introduced. In fact, this project stemmed from a still-to-date unsatisfied clinical need, which can be stated as follows: patients suffering from a recurrent respiratory papillomatosis (RRP) have no choice but to be operated several times per year to continue breathing. Thus, in chapter 1, a brief review of the literature on

this disease is presented (covering diverse aspects such as its physiopathology, the risk factors, the therapeutic strategies that have been tested so far, etc.). Since several reviews have been published on RRP (see the first paragraph in chapter 8), I decided to focus mine on those aspects that are not extensively treated anywhere else, such as the importance of the histological transformation zones in the genesis of the disease and the possible iatrogenic effect of certain surgical procedures on its progression.

In section II, some introductory insights on the computational modeling approach are presented. Even though the idea of conducting any biological research in-silico may be seen as something inconceivable for many, the fact is that the use of numerical analysis methods is not new at all in biomedical research. Evidence-based medicine, which is the paradigm on which modern western medical practice has been built, lies on intensive data collection and analysis, the latter of which implies the use of a variety of bio-statistical methods. On the other hand, as the end of the 20th century was marked by a series of technologic breakthroughs (such as the sequencing of the human genome) that deeply impacted the way life is studied, the first decade of the 21th century has seen the emergence of the resulting research specialties, such as those belonging to the –omics' family (genomics, proteomics, transcriptomics, etc.). As a consequence, bigger and bigger sets of data are being (and will continue to be) generated each day, raising the question of how to exploit such big masses of biological information. This has led to the emergence of another quantitative approach known as bio-informatics. Our modeling, unlike bio-statistics and bio-informatics, is not fully data-dependent and that is basically what we explain in chapter 5.

Chapter 6 is highly recommended for those physicians, biologists or any other kind of experts in the life sciences with little or no experience in mathematics or in any of the others computational modeling techniques that we used (multi-agent systems, genetic algorithms). This chapter is

intended to provide a brief introduction to such tools by means of a language deprived of technical terminology.

In section III we present what we call the raw material of our modeling: state-of-the-art knowledge. At first sight, this phrase may sound quite ethereal, but it is not. For decades experimental biologists have done pretty much the same every time they synthesize, in the form of a graph, what they know about a phenomenon. The novelty here is that we try to go two steps further, first by trying to figure out what the principles govern the described phenomenon are and then by trying to express such principles in a numeric language, such as (but not exclusively) mathematics. As a result, a computational model is obtained that, if conveniently calibrated, may be useful for predicting the effect of different actions on the biological system under study. Two such models are presented in chapters 9 and 11.

In section V we present the most relevant results, which can be associated: i) to the calibration of the models, ii) to the validation of the models, or iii) to the conducting of original simulations. Finally, in section VI, the implications of such results are commented and analyzed.

The public defense of my doctoral thesis should be the perfect opportunity for discussing any aspect of the research presented in this document. However, if in the future you ever get interested in exchanging any ideas on it, feel absolutely free to contact me at gust_o@yahoo.com.

In the meantime, many thanks for your interest and enjoy the reading!

PREFACE

The human papillomavirus (HPV) is a DNA virus, consisting of 8,000 base pairs, that belongs to the Papovaviridae family of viruses. HPV is both associated with a low virulence and a very high infectivity. In the United States, for example, it has been calculated that approximately 20 million people aged 15 to 49 are currently infected with HPV[1].

HPV's icosahedral capsid is composed of two molecules known as L1 and L2, the former of which has been successfully synthesized through genetic recombination techniques. The resulting particles demonstrated to have the property of self-assembling into what has been called the virus like particles (VLPs). Gardasil® is obtained by the mixture of L1-VLPs independently expressed for four different viral genotypes (HPV-6/11/16/18) via a recombinant vector called Saccharomyces pombe[2], which is a species of yeast. Besides Cervarix®, at least two other vaccines currently or once in the market share with Gardasil® the characteristic of being produced through genetic recombination techniques: the hepatitis B vaccine and the Lyme disease vaccine[3].

Gardasil® has demonstrated to provide a high degree of protection against infection due to, at least, four different HPV genotypes (6/11/16/18). Types 6 and 11 are mainly associated with 90% of cases of non-malignant genital warts, whereas types 16 and 18 are responsible for an estimated 70% of cases of cervical cancer[4,5]. In June 2006, Gardasil® was licensed by the Food and Drug Administration (FDA) with the aim of reducing the impact of cervical cancer, the second most common type of cancer among women worldwide (an estimated of 493,000 new cases and 274,000 associated deaths occurred around the world in 2002[6]). Additionally, in September 2006, Gardasil® received the marketing authorization from the European Medicines Agency (EMEA).

Today, it is known that the first step towards an HPV infection is the virus reaching its target: the basal cells of skin or mucosa[7]. For doing so, it is believed that the viral particles pass through some sort of micro-abrasion on the epithelium before reaching the stem cells, which are located in the

innermost layer. However, the identity of the receptor(s) to which the virus must bind to gain access is still unknown[8].

HPV TYPE DISTRIBUTION IN INVASIVE CERVICAL CANCER AND CIN

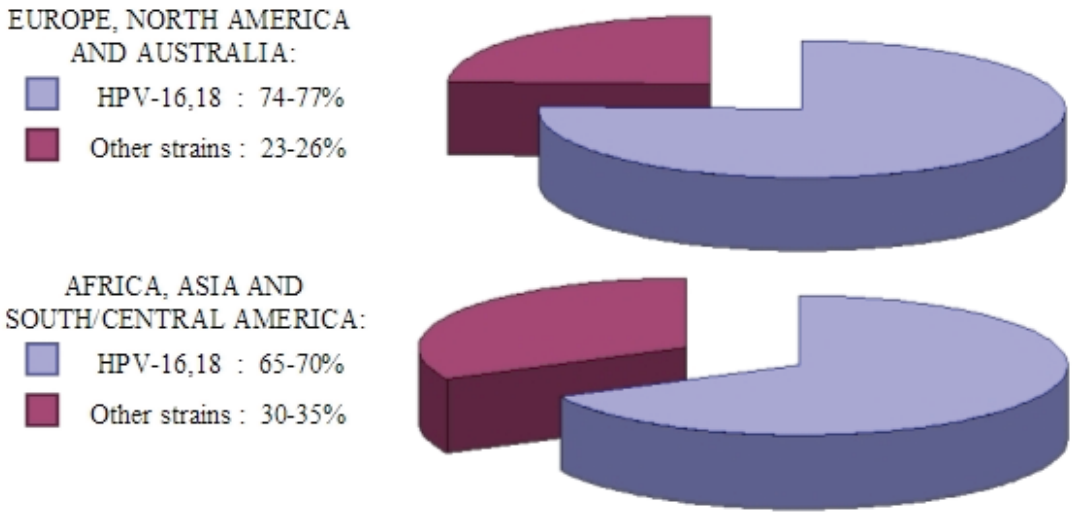

HPV is capable of infecting tissues other than the anogenital epithelium (mainly cutaneous and laryngeal epithelia). Unfortunately, the burden associated with these infections is highly underestimated, not only because they are indeed less common but also because of the lack of appropriate clinical registers. Recurrent Respiratory Papillomatosis (RRP) is a good example of this.

RRP is a chronic disabling disease that, according to some estimates[9], is diagnosed every year in approximately 2300 children and 3600 adults, only in the United States. Standard therapy is surgical removal of the papillomatous lesions that, otherwise, would obstruct the respiratory tract. A child with RRP is operated an average of 4.4 times per year, which illustrates both the poor quality of life and the economic burden associated with this disease.

Whether in the genital or in the respiratory tract, HPV infections are known for their poor immunogenicity, and the main reason for this would be the fact that, unlike many other viruses, HPV does not induce cytolysis once it has succeeded in replicating its genetic material. Thus, the accomplishment of its life cycle usually does not imply the triggering of any inflammatory signals and, therefore, activation of the immune system is unlikely to occur[10]. Another complementary explanation would be the fact that throughout its life cycle, HPV infection is not characterized by a viremic phase, which greatly reduces the probability of detection by specialized immune cells[11].

Vaccination with Gardasil® for cervical cancer prevention has shown to elicit anti-HPV immunoglobulin titers 40 times higher than those observed during a natural infection. Such a titer has been demonstrated to persist for at least 48 months after the completion of the three-dose intramuscular vaccination schedule (at months 0, 2 and 6). Several randomized controlled clinical trials have demonstrated that through this schedule a high level of protection against both infection and the associated genital lesions is obtained[12].

Currently, such protection is explained in terms of a phenomenon called immune exclusion, which refers to a non-inflammatory action (that roughly consists in blocking the entrance of the virus) attributed to the circulating specific immunoglobulins that are induced. These proteins most likely reach the genital tract by transudation, though active transport and local production are also considered as possible[13]. The immune exclusion hypothesis began to gain a great deal of credibility more than ten years ago with the publication of experimental results that showed that high levels of protection could be obtained in rabbits and dogs by the passive transfer of anti-HPV IgG antibodies.

In summary, HPV prophylactic vaccines have so far showed outstanding efficacy in preventing infection and, therefore, disease. However, patients already suffering from it still expect an analogous leap forward in terms of more efficient therapeutic procedures. This is particularly true for RRP patients, who must be operated several times per year to avoid asphyxia from the multiple (most of the time benign) little protrusions that persistently invade their respiratory tract, mostly at

the larynx level. We, and others, believe that the progression of RRP might be blocked if the quadrivalent HPV vaccine (Gardasil®) were administered intramuscularly to these patients. In order to explore the biological phenomena behind this idea, we developed a simulation platform made up of two models: the first one focuses on the immunology behind HPV vaccination, the second one on the dynamics of the HPV chronic infection behind RRP. Both of them are extensively presented in this document.

SECTION I

THE STARTING POINT

CHAPTER 1

FORMULATING THE PROBLEM

An introduction to Recurrent Respiratory Papillomatosis (RRP)

RRP is a chronic disease characterized by the apparition of multiple benign tumor-like protrusions in the respiratory tract. Traditionally, a distinction is made whether it first manifests in childhood (i.e. JORRP: juvenile-onset RRP) or in the adult age (i.e. AORRP: adult-onset RRP). The main characteristic of RRP is the patients' tendency to relapse independently of the therapeutic/surgical procedures they are subjected to.

Symptoms

RRP usually manifests through hoarseness (i.e. a vocal tone characterized by weakness of intensity and excessive breathiness), stridor (i.e. a harsh respiratory sound), while other symptoms may be persistent coughing and difficulty for swallowing.

Incidence

RRP is a rare disease. In recent years, some efforts have been undertaken in different parts of the world to develop data repository structures with the aim of providing the information needed for better orientating both RRP research and clinical practice. Some of these initiatives are: the USA national registry for juvenile-onset RRP[14], the Canadian national database of JORRP[15] and the international RRP registry created by Dr. Valentin Gerein and his colleagues at the University of Mainz, in Germany[16].

More than a decade ago both the incidence and the prevalence of RRP were estimated[17] in two USA cities (Atlanta and Seattle) from the reports of all the local otolaryngologists. The authors estimated, for the year 1996, the occurrence of 0.12–2.13 new cases of RRP per 100,000 children aged under 18 in the studied population, while the prevalence of the disease was estimated to be of 1.00–3.97

per 100,000. Another study[18] conducted in 1993 all over the USA, involving 10 times more otolaryngologists provided an estimated incidence of 4.3 cases per 100,000 children, while in adults it was estimated to be of 1.8 per 100,000. Other studies reporting estimates of either the incidence or the prevalence of RRP are scarce. An example would be the one published more than two decades ago[19] that focused on reports of adult-onset RRP, in the city of Copenhagen, over a 4-year period of time. In this study, the authors proposed an estimated incidence of 0.8 per 100,000, which is surprisingly close to the figure of 1.8 presented above. Incidentally, it has been reported that JORRP affects girls and boys equally[20].

Histology & Anatomy

Histologically, respiratory papillomata are made of highly-vascularized keratin-deprived stratified squamous epithelium. When observed under the microscope, cells seem to have suffered abnormal differentiation, most likely because of HPV intervention.

HPV has been found to be capable of infecting and conquering different locations of the respiratory tract. However, RRP appears to affect only sites where a junction between two different types of epithelia occurs. Thus, from the anatomic point of view, the most vulnerable zones are[21]: i) the limen vestibule, which is the line that demarcates the junction between the skin of the nasal vestibule and the mucosa the nasal fossa; ii) the nasopharyngeal surface of the soft palate, which marks the boundary between the oropharynx and the nasopharynx; iii) the midzone of the laryngeal surface of the epiglottis, which unlike the rest of the epiglottis (that is made of reticular cartilage) is composed of a very firm and compact but thin mucous membrane (the lamina propria); iv) the upper and lower margins of the ventricle, which separate the true and false vocal folds from each other; and v) the undersurface of the vocal folds; the carina; and the bronchial spurs.

RRP most frequently affects the vocal cords[22,23] (to the point that several decades ago the disease was commonly known as the "papillomata of the vocal cords"[24]). This results in an interference

with the normal mechanics of voice generation, which explains one of the most commonly RRP-associated symptoms: hoarseness. Both the false and the true vocal cords are known to be covered with non-keratinized stratified squamous epithelium, while the rest of the larynx is known to be lined with ciliated pseudostratified columnar epithelium. In other words, the anatomic site the most commonly affected by RRP is indeed a site of transition between two different types of epithelia.

Besides the fact that these transition zones occur naturally in different parts of the respiratory tract, it has been proposed that surgical interventions, when ablating or excising the papillomata, or when practicing a tracheotomy in the cases where the airway obstructions is too critical, can result in the generation of new squamociliary junctions. A retrospective study[25] based on the analysis of the clinical records of 448 cases of JORRP, over a 5-year period of time in a single hospital of the city of Moscow, reported 37 cases of low respiratory tract involvement in a total of 46 patients having previously been subjected to a tracheotomy (while the number of cases in the non-tracheostomized population was 3 out of 402), suggesting a iatrogenic risk increase of the disease expansion due to the surgical intervention (relative risk $\approx$ 108). Back in 1989, some authors recommended practitioners to avoid, whenever possible, the practice of tracheotomies in RRP patients on the grounds of an increased risk of developing a tracheal papillomatosis[26].

Almost invariably RRP affects the larynx (96% of the cases, according to the USA national registry for JORRP[27]), approximately in $^1/_5$ of the cases it expands to the trachea, while the rare event of expansion to the bronchi and to the lungs occurs approximately in $^1/_{20}$ of the cases (4.4% in a Polish study[28]). Some authors[29] talk of an approximate 30% of cases in which the disease spreads beyond the larynx.

Unlike the larynx, the trachea is homogeneously lined by a single type of tissue known as the pseudostratified ciliated columnar epithelium, within which dwell the non-ciliated goblet cells in

charge of mucus production. Underneath the epithelium, the trachea is made up of a layer of fibroelastic tissue and a series of (16 to 20, in the adult) cartilaginous rings, which, altogether, form its three characteristic (mucosal, submucosal and fibro-musculo-cartilaginous) tunicae. It is worth adding that the highly vascularized intermediate layer harbors aggregates of lymphoid tissue, in which it is common to find immuno-competent cells patrolling. A study was conducted[30] in which 121 biopsies, from both healthy laryngeal and healthy tracheal tissues from a total of 61 RRP patients, were analyzed in terms of HPV traces. The study concluded that the viral prevalence in both kinds of tissue was similar, refuting the thesis according to which HPV's capacity to specifically infect the larynx (but not the trachea) would explain why RRP develops preferentially in the former location. Elsewhere it has been suggested[31,32,33] that approximately 10% of both children and adults are HPV carriers at the level of the oropharynx.

In summary, even though RRP is a rare disease HPV infection in the respiratory tract is not, and the fact that the papillomatosis manifests preferentially in certain spots is neither a coincidence nor a consequence of a limited infectious capacity of the virus.

Surgical interventions (such as tracheotomies) do not seem to be the only possible cause of tissular modifications through which novel transition zones may appear. The abnormal presence of gastric juices in the upper aerodigestive tract, as occurs in patients suffering from extraesophageal reflux disease (also known as laryngopharyngeal reflux disease), is known to cause lesions through which the epithelium architecture results profoundly modified. Several studies[34,35,36] suggest that the prognosis of RRP patients may be worsen by the concurrence of extraesophageal reflux disease.

Diagnosis, Prognosis & Risk Factors

Usually, once the endoscopic exploration of the upper respiratory tract has revealed the presence of multiple abnormal protrusions, the diagnosis of RRP is confirmed through the histological analysis

of a tissue sample. Morphologically, the cytology matches with the phenotype of cells having lost the control of their differentiation process.

If untreated, the respiratory distress caused by RRP can reach critical levels threatening the patient's life. However, if under medical treatment, the risk of lethal complications is minor. The fact of being infected with HPV-11 (and not with HPV-6) has been found to be a predictive factor of rapid progression of the disease as well as of severe clinical consequences[37,38]. They are assessed in terms of the following factors: i) the number and frequency of surgeries needed, ii) the frequency of adjuvant therapy prescription, iii) the fact that the disease reaches or not the lungs, and iv) the fact that a tracheotomy results necessary. Incidentally, HPV-11-related RRP is usually diagnosed at an earlier age than HPV-6-related RRP, and it has been suggested that the younger the patient when RRP first diagnosed, the higher the amount of sites affected in the respiratory tract[39].

HPV, the causative agent

Sir Morell Mackenzie, the father of British laryngology, is said to have been the first to identify the presence of papillomata in the larynx of children by the end of the XIX century[40]. The role of HPV as the causative agent of RRP began to be elucidated 70 or 80 years later, firstly on histological grounds[41], then through the direct observation of the HPV viral particles by electron microscopy[42], afterwards through immuno-cytochemistry techniques that permitted to demonstrate the presence of HPV-specific antigens in laryngeal papilloma tissues[43], and finally through the direct cloning and molecular characterization of the virus[44].

Laryngeal papillomata are commonly associated to HPV-6, 11 genotypes. However, a closer look to some of the studies[45,46,47] in which a viral DNA characterization was conducted has led us to highlight some interesting facts: i) the amount of cases in which no HPV detection was possible at all is not negligible and varies from 7 out of 14 in the first study, to 1 out of 14 (i.e. 7%) in the

second one; ii) in the third study, it was reported that up to 41% of the 27 cases of laryngeal papillomata under analysis were not associated to any of the four viral genotypes that were tested (i.e. HPV-6, 11, 16, 18). Should this be explained only in terms of a possible lack of sensitivity of the underlying biochemical techniques?

In the course of RRP, it is thought that the viral DNA replicates episomally and that the rare event of the viral genome integrating to the host cell's genome is a determining factor for the disease eventually evolving to malignancy.

Besides the multiple surgical interventions necessary for keeping the patient's airways free (an average of five surgeries per year in the case of JORRR[48]), several adjuvant therapies (cidofovir, interferon, etc.) have been tested so far. Nonetheless, through none of them has it been possible to cope with the problem of latency. The risk of deleterious off-target side effects and the high cost associated with the chronic prescription of these adjuvant therapies limit their utilization. Once the adjuvant therapy stopped, whether the clinical outcome is going to be remission or relapse and, in the latter case, how much time will pass before it occurs, remains unpredictable. Three different criteria have been proposed to define the state of latency in the course of a RRP: i) DNA traces can be found in the respiratory tract; but ii) no clinical manifestation of the disease can be observed; and iii) the viral activity, assessed in terms of the production of viral mRNA and/or in terms of the expression of the E6 – E7 proteins, is considerably reduced. Whether latency depends exclusively on the virus (through factors such as the viral variants involved, the viral load and the fact that it gets to integrate into the host cell's genome or not), exclusively on the host (through genetic susceptibility factors), or on a mixture of factors, is still uncertain.

It has been proposed that, in the case of RRP, a higher tendency to relapse may be associated with the patient's immune system incapacity to mount effective responses either against the virus itself or against the HPV-infected cells. The immune system's branch that would be concerned by such a

state of immunodeficiency would differ between these two scenarios. However, several facts would make the balance tilt towards the hypothesis of the host exhibiting a defective cellular immunity: i) First of all, HPV is well known for being a stealthy intruder, capable of accomplishing its life cycle without killing the cells it infects, and therefore without triggering any immune "alarm signals", which means that neither in normal nor in pathologic conditions could the immune system easily "sense" and therefore get rid of it; ii) clinical evidence suggests that patients presenting different types of immuno-paralyses (because under treatment after having received a transplant, or because suffering from AIDS or from other kind of immunodeficiency) not only tend to develop more easily HPV-related diseases but also have a greater tendency to remain refractory to treatment[49,50,51], which would be mainly explained in terms of an impaired cell-mediated immunity[52,53]. Incidentally, clinical data suggest that women suffering from RRP will present a worse clinical manifestation of the disease if pregnant[54], which would be a consequence of the changes in the immune function that occur for guaranteeing the protection of the fetus[55]. Such changes include, but are not limited to, a remarkable shift in the physiology of the Th1/Th2 balance[56,57,58].

Possible HPV transmission modes in RRP

Various transmission modes have been proposed to explain the origin of the HPV infections responsible for RRP. Among these we can cite, for juvenile onset RRP, mother-to-newborn transmission during birth and mother-to-fetus transmission during pregnancy (through viral migration into the uterus). In the case of adult-onset RRP, the only possible explanation seems to be direct mucosal contact during oral sex with an infected partner.

It has been estimated[59] that 7 out of 1,000 children vaginally delivered from mothers suffering from a genital HPV infection will develop juvenile-onset RRP. On the other hand, children born to women suffering from RRP as well as RRP patients' sexual partners seem to have absolutely no risk of contracting and developing the disease[60].

Besides the fact of being born to an HPV-infected woman, three risk factors commonly associated to developing JORRP in the first years of life are: i) being a firstborn, ii) having been delivered vaginally, and iii) having been born to a rather young (< 20 years old) woman[61,62]. It has been proposed[63] that a possible explanation for this would be the fact that when delivering their first baby women tend to have longer periods of labor, which would represent, for the newborn, longer periods of time in contact with fluids potentially containing HPV. Additionally, the age factor would be related to the fact that in recently acquired HPV infections there would be a greater tendency of viral shedding into the genital fluids than in longtime established ones.

Therapeutic approaches

To date, numerous therapeutic approaches have been tested clinically: from the dated prescription of chemotherapy[64] and antibiotics[65], to the more modern use of indole-3-carbinol[66], alpha-interferon[67,68], and the intralesional administration of cidofovir[69]. Although some encouraging clinical results have been obtained through these treatments, it has not been possible, so far, to avoid the risk of relapse whenever they are interrupted. In fact, it may be necessary to do so because of the potential induction of deleterious off-target side effects, which is the case of indole-3-carbinol[70]; because of the risk of iatrogenic complications due to the invasiveness of the procedure itself, which is the case of cidofovir [71]; or simply because of the high cost associated to the treatment if prescribed chronically, which is the case of alpha-interferon[72]. As a consequence, the surgical excision of the papillomata remains the standard procedure worldwide.

Experts on JORRP seem to agree that the reason why all treatments have failed in preventing relapse is the fact that none of them is capable of coping with latent infection. Unfortunately, the mechanisms underneath HPV's latency and reactivation in JORRP remain poorly understood[73] and therefore unpredictable.

We believe that the progression of the disease could be halted (or at least hampered) if the affected tissues were continuously bathed with anti-HPV-6,11 immunoglobulins (produced through the

intramuscular immunization with the quadrivalent HPV vaccine, Gardasil®). Even without fully understanding how and when viral reactivation occurs, we hypothesize that a better clinical outcome should be obtained if the HPV virions had difficulties in completing their life cycle, thanks to the already-known neutralization capacity of such immunoglobulins.

Whether prescribing Gardasil® to patients suffering from JORRP would result in a clinical benefit is hard to foresee. Traditional approaches cannot provide much insight into this issue: i) in vitro models are not feasible because HPV cannot be cultured in a laboratory; ii) animal models for studying the human papillomavirus do not exist because papillomaviruses are species-specific; iii) other animal models, such as the canine oral papilloma model for studying JORRP[74], usually leave more questions than answers because the experiments are conducted with a closely-related yet distinct virus, and because infection occurs in a kind of tissue that differs from the one affected in JORRP[75]. iv) clinical studies are difficult to conduct because of JORRP's low incidence and the lack of standardized registers of patients.

Thus, the aim of this project has been to devise, develop and exploit a simulation platform in which to predict the clinical benefit (if any) of the above-described hypothetical therapeutic procedure. If the simulations confirm our expectations, in terms of the vaccine administration having a positive effect, the second goal has been set to be the optimization of the clinical protocol (i.e. number of doses and the vaccination schedule – especially in relation to the different stages of the disease).

SECTION II

THE IN-SILICO APPROACH

CHAPTER 2

AN ALTERNATIVE APPROACH FOR FILLING A GAP… WHAT GAP?

In general terms, what we pursue is the promotion and the development of computational modeling of biological phenomena as a possible means for achieving therapeutic (or prophylactic) innovation.

The main reasons for wanting to do that are:

- It could permit to save great amounts of time and money.
- It could permit to tackle the problem of having to "search needles in a hay stack".
- Traditional approaches seem to have difficulties in coping with several modern medical challenges, especially in the field of immunology and infectious diseases.

Computational modeling could permit to save great amounts of time and money

Between 1970 and 2005 an average of 25 new molecules per year were approved for human use by the FDA. Behind those 25, there were approximately 100 others that entered once the clinical studies phase but that resulted in failure somewhere between phases I and III. It has been calculated that for each one of them, the preclinical studies must have cost an average of 335 million dollars per molecule and must have taken an average of 4.3 years of research[76]. This means that the pharmaceutical industry lost (and continues to lose) 33,500 million dollars per year in fruitless preclinical research, which is more than the gross domestic product of at least a hundred countries around the world. If the computational modeling approach could help prevent at least a small fraction of these losses, the resources needed today for boosting its development would be largely compensated.

Computational modeling could permit to tackle the problem of having to "search needles in a hay stack"

Current efforts towards drug (and vaccine) discovery mainly depend on a (clinical)-trial-and-error kind of approach, which means that the exorbitant resources spent in the development of a new drug (or vaccine) are mainly associated with its testing (in-vitro, in animal models and finally in human beings). The problem is that the chemical space (which is the universe of molecules that could theoretically be synthesized and that might have a biological activity of interest) is so vast, and there are so many additional variables that must be taken into account (the administration route, the doses, the side effects, the therapeutic effect if concomitantly used with other drugs), that wanting to find out a shortcut, for not having to spend lots of time and money in a myriad of clinical trials, seems just natural. The idea is not to replace evidence-based medicine; the idea is render it more efficient.

Unfortunately, evidence-based medicine, as it is applied today, does not leave much space to the emergence of any complementary approaches. By folding into itself, evidence-based medicine would not seem to worry much about the costs and delays associated with the proofs it demands. It would not seem to care much either about the lack of efficacy of the methods currently used for drug discovery, nor about the unsatisfied needs of millions of patients around the world.

Traditional approaches seem to have difficulties in coping with several modern medical challenges, especially in the field of immunology and infectious diseases

- Thousands of patients suffering from a septic shock around the world are treated pretty much in the same way as they were thirty years ago, and the likelihood of surviving to such a critical condition has not significantly varied over this period of time.
- In 2007, two million people were newly infected and two other million were killed worldwide by the AIDS pandemic that has been hitting the planet for the last quarter century. That same

year, research on the most promising anti-HIV vaccine candidate (MRK-Ad5) was abandoned after the announcement of failure in a phase-III clinical trial.

- About one billion people around the world are affected by, at least, one of the ten major tropical diseases (malaria, dengue, tuberculosis, etc.)
- Approximately 10 million people worldwide are diagnosed every year with a cancer. The least invasive conceivable way of treatment would be the stimulation of the patient's own immune system to control the progression of the malignancy (active immunotherapy). However, up to date, none of these experimental procedures has shown any clinical success.

In the midst of this somber panorama one might wonder why in spite of the ever-growing quantity of available knowledge (it has been indeed calculated that the volume of scientific literature doubles approximately every 12 years) such problems remain unsolved.

Through history, many sciences have experienced the revolution of using numerical models as a means for synthesizing knowledge. I am convinced that the sciences of life will soon know this revolution. I remember one day, while talking with a biologist about the perspectives of systems biology, I heard something like: "yeah, OK, but the difference is that biology is a soft science". To which I automatically replied: "Do you really not believe that some centuries ago someone must have said something similar when referring to sciences such as astronomy, physics or chemistry?" I think that the "consistency" of a science is not an inherent property, but rather a consequence of the abstraction level reached by the observer. Abstraction, in the Aristotelian sense of the term, which means: "the process through which one passes from particularities to generalities". The word abstraction actually comes from the Latin "abstraher", which means to extract.

In a world largely dominated by evidence-based medicine, we could hardly imagine how things would be if other sciences laid on the same kind of principle. Here are some examples:

The Millau viaduct: a marvelous piece of engineering of two and a half kilometers of length, which had already been crossed between 3 and 4 million times by the end of its second year of operations. A total of 14 years of conception and designing, 3 years of construction and 400 million dollars were needed to make it real. Its development undoubtedly required the analysis of several hundreds of variables. However, we never saw any cohort of viaducts parading over the Tarn valley in order to gather enough data so that a team of statisticians could work the problem out.

Idem for the Ludwigshafen chemical complex: 10 square kilometers of facilities harboring 200 factories connected through a 2000-kilometer pipeline network. Hundreds of physicochemical transformations per minute, possible today thanks to the theoretical study of thousands of variables during the conception and designing stage. Idem for many other examples that one can easily find everywhere.

I think that life sciences are mature enough to quit the highly descriptive and extensive phase in which they are nowadays, to evolve to a more abstractive, theoretical, analysis-driven kind of phase. Some time will be necessary for the numerical modeling tools to evolve and to adapt themselves to the particularities of the biological world. Once this done, the conditions will be all set, and the transition will occur spontaneously.

In summary, and because in our days it is generally well accepted to speak in terms of evidence, let us say that a great deal of evidence demonstrates that most sciences have embraced the numerical modeling approach to overcome the obstacle of experimentation being unrepresentative in relationship to all that could be experimented. It seems logical to believe that life sciences will not be an exception.

CHAPTER 3

IN-SILICO RESEARCH IN THE RECENT HISTORY OF BIOLOGY

In this chapter I present a snapshot of the theoretical, computational and mathematical approaches most commonly associated with the general idea of conducting in-silico research in medicine and biology. They are listed alphabetically and at least one illustrative example is included for each one of them so that the reader can have a better idea of the kind of results that can be obtained. Of course, many of these disciplines may overlap, but the idea is not to generate an endless debate on where the boundaries should be set. The objective is just to provide the reader with a general picture of the different attempts that are being undertaken worldwide to address the need for multidisciplinarity in the study of life.

Abstract relational biology

- Definition: Consists in defining networks of linked physiological and biochemical functions of living cells and multi-cellular organisms; such sets are then assembled in set-related mathematical constructions by making abstraction of the underlying, physical and molecular structures.
- Associated fields: Graph theory, reliability theory.
- Example: The study of senescence[77].

Biocybernetics

- Definition: It is the discipline that deals with the study and modeling of control and communication systems in living organisms.
- Associated fields: Control systems.
- Example: Hormone replacement studies[78].

Bioinformatics

- Definition: It is the discipline that deals with the gathering, storing, handling, analyzing and interpreting of biological information, especially the related to molecular biology.
- Associated fields: Genomics, taxonomy, database mining.
- Example: The gathering, storing, handling, analyzing and interpreting of the data obtained from the sequencing of the whole genome of a pathogen, such as Helicobacter pylori[79].

Biological engineering

- Definition: It is the discipline that seeks to integrate the molecular and cellular biosciences with a quantitative, systems-oriented, engineering-analysis approach to advance fundamental understanding of how biological systems operate.
- Associated fields: Transport phenomena; biomolecular engineering; cell and tissue bio-mechanics.
- Example: Effect of the mechanical forces associated to blood flow in the development of atherosclerosis[80].

Biophysics

- Definition: Interdisciplinary science that uses the methods of physics and physical chemistry to study biological systems.
- Associated fields: Thermodynamics, X-ray crystallography, NMR spectroscopy, atomic force microscopy, quantum biology.
- Example: The quantum mechanics analysis of the origins of cancer[81].

Biosemiotics

- Definition: It is the discipline that studies both communication and signification in living

- systems by analyzing the representation, meaning and sense of codes and sign processes, from genetic code sequences to intercellular signaling processes.
- Associated fields: Molecular biology, cognitive science, semiotics.
- Example: The study of the reasons why a family of membrane receptors known as the GPCRs (G protein-coupled receptors) tend to oligomerize[82].

Biostatistics

- Definition: It concerns the collection, storage, retrieval, analysis, and interpretation of health data.
- Associated fields: Inferential statistics, epidemiologic statistics, clinical trials, survival analysis, statistical genetics, meta-analyses.
- Example: A meta-analysis, based on 14 clinical trials, intended to investigate the effect of physical exercise on the course of type-2 diabetes mellitus[83].

Complex systems analyses

- Definition: It concerns the study of the properties of a system that emerge from the whole and that cannot be described in terms of the properties of the individual interconnected parts.
- Associated fields: Systems theory, complexity theory, systems ecology.
- Example: The in-silico analysis of the deleterious effects of maternal alcohol intake on fetal condition[84].

Computational biology

- Definition: It is the discipline that seeks to apply different mathematical and computational techniques, originally developed for other completely different application fields (such as engineering, economics and sociology) to provide a comprehensive analysis of the vast amounts of biological data that are being generated in the post-genomic era.

- Associated fields: Computational genomics, gene mapping, statistics.
- Example: A study in which the genomes of two siblings, suffering from two rare genetic diseases, and the genomes of their parents, were entirely sequenced and analyzed in order to identify the responsible genes[85].

Computational and mathematical epidemiology

- Definition: It is the discipline that seeks to analyze the spread and control of infectious diseases.
- Associated fields: Computer science, mathematics, epidemiology, public health, biology, geography.
- Examples: Daniel Bernoulli's mathematical analysis of smallpox in 1760[86], the in-silico study of the herd-immunity effect associated to a vaccination campaign[87].

Mathematical biology

- Definition: It concerns the application of mathematical modeling to solve problems in biology and physiology. The goal is to contribute significantly to the understanding of the biological world and the processes involved in disease.
- Associated fields: Physiology, interacting-population models, enzymatic reactions kinetics models, electrophysiology models, biological oscillators models, reaction-diffusion models, chemotaxis models.
- Examples: A mathematical model of the beating heart[88]; a mathematical model developed to explain why sperm swim in circles[89].

Molecular evolution modeling

- Definition: Aims to describe the patterns of DNA base substitution and amino acid replacement as a means for achieving reconstruction of phylogenetic trees from molecular data.
- Associated fields: Markov models, mathematics, genetics.

- Example: A novel simulator for reconstructing phylogenies from molecular sequence data[90].

Network biology

- Definition: It is the discipline that seeks the emergence of detailed computational models of the biochemical pathways involved in normal physiological processes as well as in disease.
- Associated fields: Computational modeling, high-throughput proteomics, genomics, and metabolomics, protein engineering, microbiology.
- Example: A network-based analysis of systemic inflammation in humans[91].

Protein structure prediction

- Definition: It is the discipline that seeks the prediction of a protein's tertiary structure from its primary structure.
- Associated fields: Theoretical chemistry, drug design, enzymology.
- Example: Computational prediction of the 3D structure of a G protein-coupled receptor, followed by experimental validation[92].

Synthetic biology

- Definition: It is the discipline that seeks to design and construct new biological entities such as enzymes and genetic circuits, or to redesign the existing biological systems.
- Associated fields: Biology, chemistry, engineering, DNA sequencing, modeling.
- Example: A simulation platform for the study of synthetic genetic constructs[93].

Systems biology

- Definition: It is the discipline that seeks to integrate experimental and computational approaches to study and understand biological processes in cells, tissues, and organisms. When applied to human health, systems biology models are intended to predict physiological behavior in

response to natural and artificial perturbations and thereby contribute to the understanding and treatment of human diseases.

- Associated fields: Biology, mathematics, computational science, engineering, physics.
- Example: A predictive model for the transcriptional control of physiology in a free living cell[94].

Systems genetics

- Definition: It is the discipline that seeks to integrate experimental and computational approaches to study genetic complexity, first by developing network-based computational models to predict the states generated by complex genetic networks and then by in-silico studying the effects of gene variants on the network's dynamics.
- Associated fields: Genetics, systems biology, network biology.
- Example: An integrative genomics approach to infer causal associations between gene expression and disease[95].

Systems immunology

- Definition: It is the discipline that seeks to apply systems biology to the study of immunology, in order to obtain a more integrated perspective on how entities participate at different levels to the immune function.
- Associated fields: Systems biology, immunology, infectiology, vaccinology, mathematics, engineering.
- Example: Systems biology approach predicts immunogenicity of the yellow fever vaccine in humans[96].

Systems pharmacology

- Definition: It is the discipline that seeks the application systems biology to the study of drugs,

- drug targets, and drug effects, combining large-scale experimental studies with computational analyses.
- Associated fields: Systems biology, network biology, pharmacology, drug discovery.
- Example: An in-silico approach to better understand drug side effects and adverse events[97].

CHAPTER 4

STATE OF THE ART IN THE COMPUTATIONAL MODELING OF IMMUNOLOGY- AND INFECTIOLOGY-RELATED PHENOMENA

The purpose of this chapter is to present a general picture of what has been done and accomplished by others in the application of in-silico modeling techniques to biological topics somehow related to the subject of this doctoral thesis. As one may expect, several articles have been published[98,99,100,101,102,103,104] that include very detailed reviews of the different in-silico approaches that have been tested in these fields. However, the information they provide on the individual original articles is highly heterogeneous and most of the times inexistent for several key aspects such as the origin of the parameters and the validation (if any) of the models. So, I decided to conduct my own research of the literature by first defining a series of criteria I would particularly pay attention to, then by defining a series of requests that I would make to the PubMed database (see appendix 1) and finally by selecting some of the articles for which the targeted information was presented as completely as possible. The result is presented here below:

Example No 1

- Title: A systems perspective of host-pathogen interactions: predicting disease outcome in tuberculosis[105].
- Published in: 2010.
- Level of access: Just the abstract.
- Aim: To study the host-pathogen interactions both at the cellular and at the molecular level.
- In the specific case of: Tuberculosis.
- Type of modeling: A Boolean network.
- Size of the model: 75 nodes, corresponding to host and pathogen molecules, cells, cellular states or processes.

- Origin of the parameters: This information could not be accessed.
- Was the model fed by or confronted to real data? This information could not be accessed.
- What is the main conclusion of the article? The simulations suggest that disabling defense mechanisms such as phagocytosis would result in more persistent infections, while removing bacterial defense proteins such as SapM would result in higher clearance rates.
- Simulation platform used: This information could not be accessed.

Example No 2

- Title: Energy cost of infection burden: an approach to understanding the dynamics of host-pathogen interactions[106].
- Published in: 2006.
- Level of access: Full text.
- Aim: To study in-silico the evolution of an infection in terms of both the energetic cost associated to the damage caused by the pathogen and the energetic cost associated to getting rid of it.
- In the specific case of: Pneumonia.
- Type of modeling: A set of ordinary nonlinear delay-differential equations.
- Size of the model: 10 equations.
- Origin of the parameters: The model comprises about 40 parameters which were estimated following an optimization process, in which: i) a "permissible values range" was first defined for each one of them, ii) real data describing what they call a "generalized picture of pneumonia" was then used as the targeted behavior, iii) a mathematical function was used to minimize "the distance" between what the model predicts and what the data show.
- Was the model fed by or confronted to real data? Besides the already-mentioned use of data for calibrating the model, no other data-based operation (such as a validation one) was reported.

- What is the main conclusion of the article? According to the energetic analysis conducted, the authors conclude that some chronic infections may be the result of the host taking the optimal decision of not spending great deals of energy trying to get rid of a pathogen that most likely will be able to re-infect it and that, in the end, does not represent a major threat for it.
- Simulation platform used: Undisclosed information.

Example No 3

- Title: Decay dynamics of HIV-1 depend on the inhibited stages of the viral life cycle[107].
- Published in: 2008.
- Level of access: Full text.
- Aim: To study the effect of pharmacologically targeting different viral life cycle stages on the therapeutic effect clinically observed.
- In the specific case of: HIV.
- Type of modeling: A set of ordinary differential equations.
- Size of the model: 7 equations.
- Origin of the parameters: The model comprises 15 parameters; all of them were "chosen to be consistent with previously reported measurements".
- Was the model fed by or confronted to real data? During the calibration process, the model's output was compared to the "viral dynamics observed in integrase inhibitor trials". Besides that, no validation stage was reported in the article.
- What is the main conclusion of the article? The later a drug acts in HIV's life cycle, the greater its tendency to induce a therapeutic effect. Based on this work, the authors suggest that "future drugs acting at later stages of the HIV-1 life cycle may be capable of producing even faster decay rates than the most potent protease, reverse transcriptase, or integrase inhibitors."
- Simulation platform used: Matlab.

Example No 4

- Title: HIV recombination: what is the impact on antiretroviral therapy? [108]
- Published in: 2005.
- Level of access: Full text.
- Aim: To study the role of genetic recombination in the development of drug-resistance.
- In the specific case of: HIV.
- Type of modeling: A set of differential equations.
- Size of the model: 35 equations.
- Origin of the parameters: Most of the parameters were taken from the literature, while some others were estimated so that the model complies to a set of rules define by the authors ("the super-infection parameters are adjusted such that the pre-treatment equilibrium distribution of multiple cell infections is π_1=0.1, π_2=0.3 and π_3=0.6, that is, the mean multiplicity of infection is 2.5").
- Was the model fed by or confronted to real data? No.
- What is the main conclusion of the article? "The principal conclusion is that the clinical response to a particular antiretroviral drug regimen depends on the location of the associated resistance mutations on the HIV genome".
- Simulation platform used: Undisclosed information.

Example No 5

- Title: Simulating the effect of vaccine-induced immune responses on HIV infection[109].
- Published in: 2003.
- Level of access: Full text.

- Aim: "To predict what characteristics a preventive or therapeutic vaccine should possess to be immunogenic, and what are the key factors that most likely will affect its ability to control the spread of an infection."
- In the specific case of: HIV.
- Type of modeling: A set of delay Volterra integral equations.
- Size of the model: 3 equations.
- Origin of the parameters: "The kinetic parameters used for solving the model are those of HIV-1 infection obtained from experimental and clinical observations".
- Was the model fed by or confronted to real data? No data-based calibration or validation operation is reported in the article.
- What is the main conclusion of the article? "Control of the chronic infection by a therapeutic vaccine appears to be possible, but it is strongly influenced by the infectivity of the virus and by the strength of the vaccine."
- Simulation platform used: Matlab.

Example No 6

- Title: Predicted 30-year protection after vaccination with an aluminum-free virosomal hepatitis A vaccine[110].
- Published in: 2010.
- Level of access: Full text.
- Aim: To predict the duration of the protection conferred by a prophylactic vaccine.
- In the specific case of: Hepatitis A.
- Type of modeling: "A linear mixed mathematical model".
- Size of the model: One equation.

- Origin of the parameters: They are obtained through a regression in which a method known as the restricted maximum likelihood estimation procedure is employed.
- Was the model fed by or confronted to real data? Yes. Real data regarding the serum antibody titers induced by vaccination was used for the regression. Besides, "concentrations measured at 9–11 years after booster were compared with the predicted concentrations based on the linear mixed model".
- What is the main conclusion of the article? "a two-dose Epaxal regimen confers in healthy adults a real-time protection of at least 9– 11 years; this protection is predicted to last at least 30 years in over 95% of individuals.".
- Simulation platform used: Undisclosed information.

Example No 7

- Title: Do we need 3 doses of hepatitis B vaccine? [111]
- Published in: 1999.
- Level of access: Full text.
- Aim: To analyze the mechanisms behind the immune responses elicited by a multi-dose vaccination procedure.
- In the specific case of: Hepatitis B.
- Type of modeling: A set of differential equations.
- Size of the model: Three equations.
- Origin of the parameters: Some parameters where directly taken from the literature, while some others were indirectly estimating by making them vary until the model fits real immunogenicity data.
- Was the model fed by or confronted to real data? Yes, real data was used for calibrating the model but there is no report of such a kind of operation for validation purposes.

- What is the main conclusion of the article? "The interpretation of immunogenicity data, using the mathematical model, should give greater confidence in the results from vaccine efficacy trials which show that 3 doses of HBV vaccine are not necessary."
- Simulation platform used: The mathematical model was solved using a 4th order Runge Kutta routine but the nature of the simulation platform was not disclosed.

Example No 8

- Title: Agent-based modeling of endotoxin-induced acute inflammatory response in human blood leukocytes[112].
- Published in: 2010.
- Level of access: Full text.
- Aim: "To study the underlying complexity of the acute inflammatory response".
- In the specific case of: No specific pathology was chosen to conduct this analysis.
- Type of modeling: An agent-based kind of modeling, in which different types of biological entities were considered: immunocompetent cells (mainly macrophages), immunostimulator molecules (mainly LPS), membrane-bound receptors (mainly TLR4) and intracellular signaling molecules (mainly NF-kB).
- Size of the model: A single "virtual cell" contains more than 400 agents. For conducting each simulation, the authors employed a virtual environment comprising 4 "virtual macrophages".
- Origin of the parameters: Many different sets of parameters were tested and the criterion for selecting one was the following: "A set of parameters is considered satisfactory if the model is capable of simulating the dynamics of a self-limited inflammatory response (resolution within 24 hr post-LPS administration)".
- Was the model fed by or confronted to real data? The authors mention a set of data that is widely known if the study of inflammation: the transcriptomic analysis of a systemic

inflammatory response in healthy individuals following the intravenous administration of LPS, which was conducted and published by the consortium "Inflammation and the Host Response to Injury" (www.gluegrant.org) in the USA. However, in the present article, such data do not seem to intervene in the calibration/validation process.

- What is the main conclusion of the article? "The hypothetical scenarios explored in this study would potentially improve our understanding of how manipulating the behavior of the molecular species could manifest into emergent behavior of the overall system."
- Simulation platform used: "NetLogo (Center for Connected Learning and Computer-Based Modeling, Northwestern University, Evanston, IL), a freeware that constructs agent based models."

Example No 9

- Title: Modeling endotoxin-induced systemic inflammation using an indirect response approach[113].
- Published in: 2009.
- Level of access: Full text.
- Aim: To study the dynamics of inflammation by "coupling extracellular signals with essential transcriptional responses through a receptor mediated indirect response model".
- In the specific case of: No specific pathology was chosen to conduct the analysis.
- Type of modeling: A set of differential equations.
- Size of the model: 10 equations.
- Origin of the parameters: Approximately 20 parameters were estimated using data-based "standard parameter estimation techniques".

- Was the model fed by or confronted to real data? The authors mention the same data set previously described for example No 8. Such data seem to intervene in the model's calibration process but no validation operation seems to have been conducted.
- What is the main conclusion of the article? "The temporal profiles of the essential inflammatory components under an unresolved inflammatory state highlight the potential importance of early effective therapeutic interventions, e.g. 2–4 h whilst after 4 h the system seems to have lost any potential for attenuation."
- Simulation platform used: Undisclosed information.

Example No 10

- Title: Mathematical model to simulate the cellular dynamics of infection with human herpesvirus-6 in EBV-negative infectious mononucleosis[114].
- Published in: 2003.
- Level of access: Full text.
- Aim: "To study the effects of viral infection on cells of the immune system".
- In the specific case of: The human herpesvirus-6.
- Type of modeling: A set of differential equations.
- Size of the model: Approximately 30 equations.
- Origin of the parameters: A total of 17 parameters were estimated indirectly by using a data-driven optimization procedure described somewhere.
- Was the model fed by or confronted to real data? The data used for calibrating the model correspond to the follow-up of several groups of patients in which both the viral load and the T-cell count were registered over an 8-month period of time. On the other hand, the authors stated that at the time of the publication there were on-going studies that had been designed to validate this in-silico model.

- What is the main conclusion of the article? "After completion of the validation studies and standardizing physiological parameter values, the mathematical model presented can be used for monitoring all T-cell populations under pathological conditions such as in chronic persistent viral infection with cellular aplasia or atypical proliferation."
- Simulation platform used: Matlab.

Example No 11

- Title: Mathematical model of antiviral immune response. I. Data analysis, generalized picture construction and parameters evaluation for hepatitis B[115].
- Published in: 1991.
- Level of access: Full text.
- Aim: To describe in-silico the course of a viral disease as well as the intervention of the immune system.
- In the specific case of: Hepatitis B.
- Type of modeling: A set of non-linear delay differential equations.
- Size of the model: 10 equations.
- Origin of the parameters: "Data of immunological experiments in vitro and experiments with animals are used to obtain the estimates of permissible values of parameters."
- Was the model fed by or confronted to real data? Apart from the calibration process, no other data-based operations, such as the model calibration, are reported. By the end of the article, the authors state "To refine the crude initial estimates of parameters of the mathematical model for antiviral immune response, the identification of parameters according to quantitative data on acute viral B hepatitis and biological validation of the model are required."

- What is the main conclusion of the article? "The developed model allows us to quantitatively simulate the basic features of the antiviral immune response during acute hepatitis B and some closely related phenomena."
- Simulation platform used: Undisclosed information.

Example No 12

- Title: Mathematical model of a three-stage innate immune response to a pneumococcal lung infection[116].
- Published in: 2011.
- Level of access: Full text.
- Aim: To analyze in-silico the innate immune response to a bacterial infection.
- In the specific case of: Pneumococcal pneumonia.
- Type of modeling: The model comprises a set of ordinary differential equations and a set of delay differential equations.
- Size of the model: 18 equations.
- Origin of the parameters: Some parameters were taken from the literature while some others were indirectly estimated by using experimental data that the authors themselves collected by using a murine model.
- Was the model fed by or confronted to real data? Yes, for calibration purposes. However, no calibration operation was reported in the article.
- What is the main conclusion of the article? The authors state the following: "our model quantifies the contributions of cytotoxicity and immune-mediated damage in pneumococcal pathogenesis". However, I could not find any details of how this was done or how such an analysis could be conducted.
- Simulation platform used: Matlab.

Example No 13

- Title: Lifelong dynamics of human CD4+CD25+ regulatory T cells: insights from in vivo data and mathematical modeling[117].
- Published in: 2010.
- Level of access: Full text.
- Aim: To study in-silico the dynamics of regulatory T cells for getting some insights on how these cells are controlled by the immune system.
- In the specific case of: There is no particular disease associated with this study. It deals with a very precise and fundamental question on the physiology of the immune system.
- Type of modeling: A set of ordinary differential equations.
- Size of the model: Three equations.
- Origin of the parameters: "We employ a modeling technique that alleviates the parameter estimation problem by considering parameters as random variables having a priori distributions (as in Bayesian approaches). This approach allows us to evaluate simultaneously several values, to produce results that depend little on the exact values, and therefore to diminish the probability of errors due to wrong parameter estimates".
- Was the model fed by or confronted to real data? Yes. Human regulatory T cells were isolated from blood samples and their reactions to different antigenic stimuli were studied in-vitro for validating the model's predictions.
- What is the main conclusion of the article? "Although the antigen-driven proliferation of regulatory T cells is essential for the development of a pool of mature Tregs, it is not a critical issue for the lifelong maintenance of this compartment."
- Simulation platform used: Matlab.

CHAPTER 5

DEPICTION OF OUR MODELING STRATEGY

In general terms (see this article[118] for deeper methodological insights on our modeling approach), we seek to predict in-silico the way an ensemble of pathological and/or therapeutic stimuli elicit a biological response in an organism. We do so by synthesizing, through a numerical formalism (e.g. a set of equations), as much of what is known about the related biological phenomena as possible. Then, we use data either to calibrate the in-silico model (i.e. we realize that it does not comply to reality, so we intervene) or to validate it (i.e. let us see if you – the model – can predict this fragment of reality that we know pretty well and that we are hiding from you), but never as the raw material from which to build the model (inferential statistics).

Unlike the traditional approaches used to treat biological knowledge, ours is:

- Integrative, which means that it takes into account the fact that the properties of a system, as a whole, usually cannot be known by simply adding what is known about its components.
- Quantitative, which means that it goes beyond the binary relationships commonly used in biology (e.g. does A activate B? yes or no).
- Dynamic, which means that it considers the fact that the inputs/outputs may evolve through time.
- Transversal, which means that it permits to integrate knowledge/data obtained at different observation scales.
- Anticipative, which means that it would permit the rapid exploration of a vast universe of possible scenarios, reducing the costs associated to experimentation.

Our modeling usually implies eight steps, which are:

- E1 – Formulation of objectives, which are usually associated to unanswered clinical questions, like in our case: i) what would be the most likely clinical outcome if a patient suffering from RRP was treated with Gardasil®?; or ii) what would be the most likely consequence, in terms of immunogenicity, if Gardasil®'s vaccination schedule was modified?

OUR COMPUTATIONAL MODELING STRATEGY

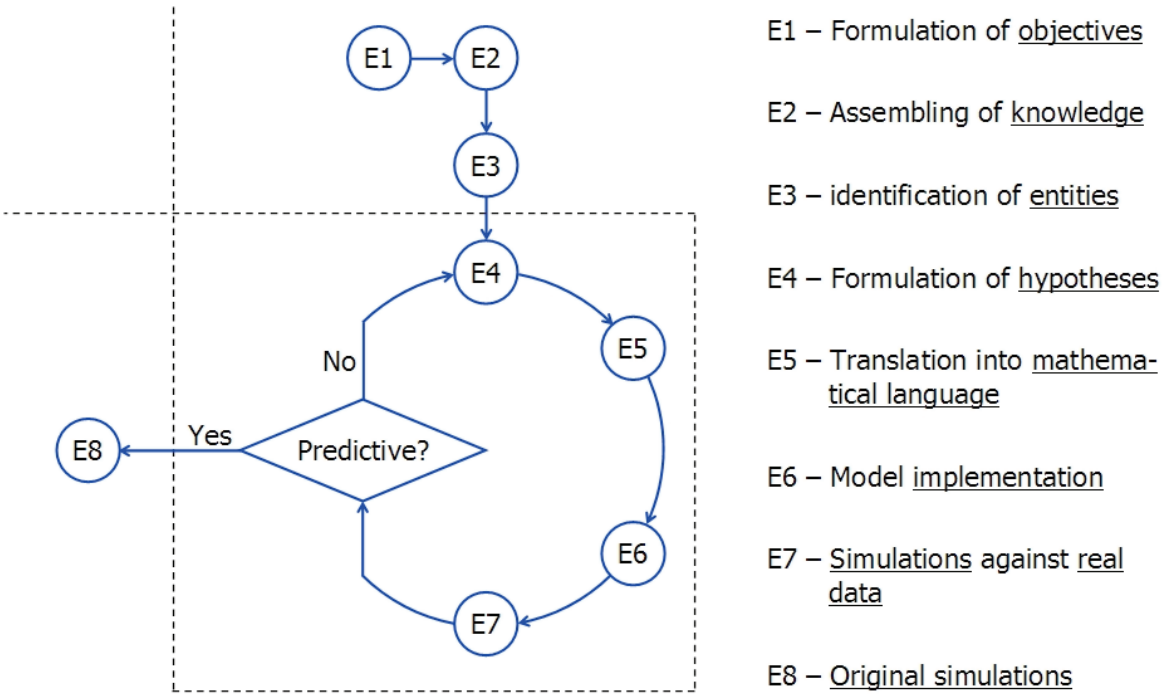

- E2 – Assembling of knowledge, which consists in: i) an exhaustive analysis of the scientific literature, and then ii) in the direct interaction with experts of the field. In our case, we interacted with various world-renowned HPV experts, such as: Pr. Margaret Stanley

(Cambridge University, UK); Pr. Pierre Coursaget (François Rabelais University, Tours, FR) and Dr. Nubia Muñoz (National Institute of Cancer of Colombia).

- E3 – Identification of entities. In the case of our mathematical model some of the selected biological entities were: the antigen presenting cells and the CD4+ helper T cells. Some others were once considered, for example the CD25+ regulatory T cells but, in the end, were excluded from the model. In fact, one of the biggest challenges we had to face is to find the right balance for including as many entities as possible without generating a too-hard-to-handle mathematical model.
- E4 – Formulation of hypotheses, which are necessary because: i) there are knowledge gaps, or ii) because the models need to be simplified so that they remain solvable.
- E5 – Translation into mathematical language, which is the core of the whole process. Defining the modeling technique greatly depends on the nature of the biological phenomenon, as exemplified in this project in which two different kinds of modeling were employed.
- E6 – Model implementation, which means taking each model from the scratch paper where it was created to a computer where it will be solved.
- E7 – Simulations against real data, first for calibrating the model and then to assess its predictive power.
- E8 – Original simulations, which means completely unplugging the model from any source of previously existing data to let it explore novel scenarios.

Since ours is definitely an unorthodox approach, we are aware of the fact that faithful partisans and radical opponents could spend hours and hours debating over its pertinence and relevance to modern research. However, we believe that it will be the facts rather than the rhetorics that should be used for settling the question. An ideal way of assessing our models' worth would be to make some in-silico predictions and then to gather clinical data to confirm or disproof what the models predict. Unfortunately, the conducting of such "validating clinical studies" was not included in the

formulation of the present project. Nonetheless, what does lie within its boundaries, and what we actually did, is to compare some of the model's predictions to already-published non-used-for-calibration-purposes data. By doing so, we are actually tackling the major pitfall of the computational modeling approach, which is: the risk of lack of connection between the simulations and the biological reality they are supposed to represent.

Finally, we would like to insist on how important it is for us to interact with experts in the biological and clinical fields related to our projects. In fact, the major precepts that govern the way we interact with the outer world are: i) the mathematics and all the computational methods that we use are quite useful tools, but they constitute neither the goal nor the reason of being of our work; ii) we are aware of the fact that our in-silico modeling approach is not the only one and we certainly believe in the need of confronting different approaches, but we think that it is a debate that must be carried in function of the models' predictive power and not in function of the authors' rhetorical ability; iii) our goal is definitively to be predictive with our models, not just for the pleasure of proclaiming it, but for translating such kind of breakthroughs into novel therapeutic and/or prophylactic actions; and iv) we preferentially pursue an impact on the international scientific communities concerned by the biological/clinical side of our multidisciplinary projects (in this case: the HPV, the immunologists' and the otorhinolaryngologists' communities). In fact, throughout these years, we presented posters of this work in different international conferences, including:

- In 2008 – Vaccine's 2nd Global Congress. December 7-9, Boston, MA, USA.
- In 2009 - The 25th International Papillomavirus Conference. May 8-14, Malmö, Sweden.
- In 2010 - Nature Medicine's Colloquium on Systems Biology and HIV Vaccine Development. February 8-10, Peachtree City, GA, USA.

CHAPTER 6

DEPICTION OF OUR MODELING TOOLS

Differential equations

Probably the shortest path for understanding what a differential equation is consists in thinking of an algebraic equation. Let us take the following simple algebraic equation as an example: $3x - 2 = 0$. Solving this equation means finding a value or set of values for the variable x so that what lies on both sides of the equal sign results equivalent. In this particular case, there exists a unique solution, which is $x = 2/3 = 0.66$. One can state that the information originally contained in the equation was enough for solving it out. In the case of a differential equation, the goal is not the find out the value or values that satisfy a given condition but to find out the function or family of functions that do so. For example, one may write $y' = 2x + 1$, which one can identify as being a differential equation only through the apostrophe that accompanies the variable y. This symbol is used to represent what is called the derivative of a function, which in common language denotes a rate of change. For instance, it is commonly said that the acceleration is the derivative of the speed. But let us get back to our example of differential equation to say that its solution is the following equation: $y = x^2 + x + c$, where c denotes an undefined constant. But how come the solution of an equation is another equation? As illogical as it may sound, that is how it works. And even though things do not seem much clearer after having found the solution, the fact is that they are. Let us suppose that x represents the variable “time” and that y represents the variable “number of cells on a Petri dish”. A scientist may be interested in parameterizing this equation, which means determining that for his own cell-culture experiment c equals “3 million cells”, for then testing several values of x. This would permit our scientist to foresee how long it would take to have the number of cells of his interest, let us say 100 million cells. At this point, one might wonder what the chances are of this event happening exactly as predicted through the calculations. In other words one may want to know the validity of the model (and we may call it that because that sole differential equation may

constitute, by itself, a model). The answer to this question is: the validity of this model will mainly depend on how well the differential equation y' = 2x + 1 fits into the phenomenon that wants to be modeled. One can imagine that next to the scientist that was conducting the experiments there was a mathematician or an engineer that proposed the equation and it is mainly on this choice that the reliability of the predictions will depend.

Genetic algorithm

It is a computational tool used for conducting optimization operations. An example of such an operation would be the following: let us suppose that it has been established that by mixing reactants A, B and C at some given conditions of pressure (P), temperature (T) and pH it is possible to obtain the highly valuable compound D. Let us suppose that for each one of the 6 variables (the concentration of the three reactants, P, T and the pH) a range is known within which the reaction takes place but only for a very specific set of values it would result in an optimal quantity of D being produced. Let us define the "search space" as the totality of sets of values that satisfy the condition of keeping all of the six variables within the already mentioned ranges. In our example, let us say that the amount of possible combinations is so vast that wanting to test them all in a laboratory would be something unconceivable. As an alternative, a guided exploration of this "search space" may be proposed. A genetic algorithm is a computational tool that may play the role of "guide" in this story, which means that based on the results of a few experiments it may be able to suggest what "regions" of the "search space" should be privileged, giving origin to an iterative process in which multiple experimental and computational phases are alternated. In the end, the goal is to establish what the optimal set of values is after having invested the smallest amount of time and resources conducting experiments. The first requirement for implementing a genetic algorithm is to devise a method for translating into binary code (i.e. a succession of 1s and 0s, for instance, "111010101") any value potentially assigned to a single variable. For example, if the range for the variable temperature had been set to be 30 to 240 Celsius degrees and if we were

punctually interested in testing the value 90 degrees, we should be able to translate this value into a binary number in such a way that the relationship remains bi-univocal, which means that for this particular value there must be only one possible binary number and vice versa. The amount of binary digits used for representing a single variable is what we call the "resolution". Let us say that, in our example, we select a resolution of 3. This automatically implies that there would be only 2^3 = 8 evenly distributed testable values for the variable temperature (30, 60, 90, 120, 150, 180, 210 and 240 Celsius degrees). It also implies that the sole possible representation for the value 90 degrees would be the 3-digit binary number "010". Translating all of the just-mentioned 8 testable values into binary language would yield the following: "000", "001", "010", "011", "100", "101", "110" and "111", respectively. At this point, let us introduce a parallel between any of these fragments of binary code and a gene. In our example, putting together all the binary-code fragments needed to represent a complete set of values for the 6 variables would result in an 18-digit binary array (i.e. the number of variables multiplied by the "resolution" = 6 x 3 = 18). Let us call this array the "genome" of the "individual". Now, let us imagine that we randomly create a single "individual", let us say "110.100.001.110.101.111" and that we translate this "genome", "gene" by "gene", into a set of values that we respectively assign to the 6 variables [A], [B], [C], P, T and the pH. Then, we go to the laboratory and conduct the experiment to find out that the yield of the reaction is quite modest, let us say 15%. This would not be surprising because the likelihood of randomly falling into the optimal set of values in the very first attempt would be extremely small. Let us imagine that now we repeat the same operation (random generation of a set o values followed by the experimental determination of the associated chemical reaction yield), let us say, 20 times. Thus, we would find ourselves with a population of twenty 18-bit binary vectors, each one of which would have a "fitness" indicator associated, within a range of, let us say, 5% to 30%. The next operation would consist in separating the "strongest individuals" (i.e. the binary vectors with the highest "fitness" indicators) from the "weakest individuals". The latter would then be eliminated before using the former as precursors for generating new individuals in such a way that the total population

remains stable. The same procedure is repeated over and over again permitting the system to evolve towards the optimal set of parameters. In the end, let us suppose that the genetic algorithm will have proposed, let us say, a hundred sets of parameters before finding the optimal one, which is negligible when compared to total amount of possible combinations, in this case, $2^{18} = 262,144$.

Multi-agent system

It is a modeling technique that consists in creating a "virtual environment" in which computational entities called "agents" evolve with a certain degree of liberty. Depending on the modeling scale chosen, such entities may represent different kinds of biological constituents, such as cells, proteins, genes, etc. The main two reasons for wanting to employ such a modeling approach over a more conventional mathematical modeling kind of approach are: i) the likelihood of success of the latter greatly depends on the validity of each one of the model's equations. In other words, equations are very restrictive in the behavior they describe. If the biological system under study happens to behave differently, or if it happens to possess the capacity of modulating its behavior, the mathematical model would simply lack of validity. A multi-agent system is not subjected to such constraints. ii) The second reason would be that unlike many others, biology is an information science. And the problem is that the variables contained in a mathematical model are the most suitable way for representing magnitudes, but not information. A multi-agent system may permit to handle both simultaneously.

From the informatics point of view, the development of a multi-agent system begins with the definition of the "classes" or "family of agents" to be represented. For instance, let us suppose that we are interested in studying the dynamics of a biochemical pathway that begins with the stimulation of a membrane-born receptor and that results in the expression of a particular gene. Let us suppose that between them there are 25 different types of molecules that are concerned. These would constitute the families of agents in our hypothetical model. Let us take as an example the

molecule STAT3 (which is a “signal transducer and activator of transcription”). The information fields that would be shared by all the agents belonging to this “family” should now be defined. For example, let us define the field “type” for indicating the kind of molecule, the field “id” for stocking the agent’s identity and the field “state” for indicating the fact of the molecule would be active or not (i.e. “state=1” or “state=0”). Let us now suppose that we are interested in simulating a system containing 1,000 agents of the STAT3 family. Computationally, this would result in 1,000 “packages of information”. For instance, the agent representing “STAT3 molecule number 547” would have the following information associated to it: “type = STAT3”, “id = 547” and “state = 1”. Let us now define a bi-dimensional coordinates system (x, y) that would permit us to add spatial information to each agent. For instance, for “STAT3 molecule number 547”, the one in our example, it might look something like this: “x = 317”, “y = 117”. Some of the information contained in an “agent” may be completely static: for instance, we may want to establish that the identity of an agent should remain the same remain all over the simulation. On the other hand, we may be interested in letting the information regarding the position of the agent to vary. How this information may evolve is the kind of question that needs to be answered by the person in charge of conceiving the model. For instance, one may define that the movement of each “virtual molecule” should have a random Brownian kind of behavior within a restricted region of the “virtual space”. This is what we call a “rule”. Thus, conducting a “virtual experiment” implies three main stages: i) creating each one of the agents; let us suppose, in our example, that we decide to create 1,000 “individuals” for each one of the 25 classes of biological entities, which would give us a total of 25,000 agents. ii) Defining the rules; such as, for example, the one previously explained for the entities’ movement. Another type of rule could be related, for example, to the interaction between agents of a different kind that may conduct to one of them changing the value contained in the “state” field of another one, from inactive to active or vice versa. iii) And finally, after having set all the initial conditions up, the third and final stage would be simply to let the system evolve freely.

Usually, the rules beneath a multi-agent system are associated with quantitative parameters for which optimal values must be. In our example, the fact that the 25,000 agents exhibit a Brownian-movement kind of behavior in a simulation implies that some parameters must exist that define the frequency and the intensity of every single movement for each one of the agents. Thus, in spite of the differences between a mathematical and an agent-based kind of modeling, the question of having to determine the optimal values for the underlying parameters remains a common affair. On the contrary, only a multi-agent based kind of modeling would permit the user to handle complex sets of rules. Let us suppose, for instance, that for making our example more interesting we decide to integrate other families of agents to represent the genes that may be concerned by the biochemical pathway under study. Transcriptomic data reflecting the expression patterns of such genes could then be used for defining the set of rules related to the regulatory networks involved. Wanting to directly exploit such kind of data by means of a mathematical model would simply be unnatural.

SECTION III

BIOLOGICAL KNOWLEDGE –

THE RAW MATERIAL

CHAPTER 7

UNDERSTANDING THE IMMUNE RESPONSES INDUCED BY THE INTRAMUSCULAR IMMUNIZATION WITH AN HPV VACCINE

Gardasil® and Cervarix® in the history of vaccines

Along with antibiotics, vaccines remain one of the most successful forms of intervention in the history of medicine. In the last century or so, vaccines have permitted to drastically reduce the burden (in terms of mortality, morbidity, handicap and health-care associated costs) caused by several infectious diseases, including diphtheria, measles, mumps, pertussis, polio, rubella, tetanus and many others. Factors such as the simplicity of the intervention, its little invasiveness, the extremely rare undesired effects, the usually long-lasting protective effect as well as their usually relatively low cost, make of vaccines an ideal means for fighting disease. This is so true that in the last couple of decades or so, researchers in several other fields (such as cancer, diabetes, multiple sclerosis, Alzheimer's disease and many others) have pursued (fruitless, so far) their own Eldorado in the form of the so-called field of "therapeutic vaccines".

The success of vaccines in the fight of infectious diseases can be mainly explained by the fact that they perfectly mimic a natural phenomenon, which is: the long–lasting protective effect frequently induced when an organism encounters a pathogen and succeeds in getting rid of it. Way before Edward Jenner's late-eighteenth-century breakthrough (immunity against smallpox induced through cowpox infection), the human being had already been aware of this phenomenon. Medical historians believe that back in the year 1,000 of our era Chinese "may have practiced inoculation by scratching matter from a smallpox sore into a healthy person's arm"[119]. Since then, multiple technological advances have permitted scientists to harness this practice in such a way that the ratio between the probability of inducing protection and the probability of inducing adverse effects has been demonstrated to be quite high. However, the old principle of administering a vaccine in which the pathogen is presented entirely or partially, attenuated or killed, has not been enough to obtain

the same kind of results for several highly-devastating infectious diseases (such as AIDS, malaria, cholera and others). In fact, some authors believe that the remaining low-hanging ready-to-grasp fruits in this field must be rather rare nowadays. As a consequence, the discipline of vaccinology has moved on to explore alternative paradigms and it has done so mainly oriented by the advent of modern technological breakthroughs, such as genetic recombination. The first two vaccines produced through this technique were the hepatitis B (1981) and the Lyme disease (1998) vaccines. Both HPV prophylactic vaccines (Gardasil® and Cervarix®) added their names to this list when approved in 2006 and 2009, respectively. Besides the fact that their active principles are obtained through genetic recombination, these four vaccines share other interesting features: i) they are all administered intramuscularly, ii) their recommended administration schedules differ slightly the ones from the others, iii) the protection they confer is tightly associated with the high circulating immunoglobulin titers that they induce.

The uniqueness of HPV vaccines

One of the particularities of both HPV vaccines is that physically they mimic the wild virus but physiologically they do not mimic an HPV infection.

HPV's viral capside is made out of a complex lattice of two elementary proteins known as L1 and L2. When artificially produced in a laboratory, the L1 proteins have the spontaneous capacity to self-assemble giving origin to artificial capsids (commonly known as virus-like particles, or VLPs). They physically resemble the original ones but possess no infectious capacity at all.

On the other hand, and despite its high infectivity, HPV is well known for being poorly immunogenic[120]. The main reasons for this are: i) a classical pathway through which viruses elicit immune responses is the recognition of their double-stranded RNA intermediates by the toll-like receptor 3[121], but in HPV's life cycle there are not any; ii) HPV's non-structural proteins (E1, E2, E4, E5, E6 and E7) are expressed at very low levels, restraining its immunogenicity to just a couple of proteins (L1 and L2); iii) HPV only infects epithelial cells, where a predominantly non-

inflammatory environment reigns (mainly mediated by IL-10 and TGF-β); iv) for accomplishing its life cycle, HPV is not forced to kill the cells it infects, which implies than none of the danger signals associated to such event are generated; and v) HPV's life cycle does not imply a viremic phase, which largely limits the likelihood of recognition by the immune system.

As a consequence, one would expect that if administered locally (as if trying to mimic a natural infection) a VLP-based kind of vaccine should result in poor immunogenicity, which in fact seems to be the case, at least according to what can be drawn from a murine model[122].

Thanks to the fact that they are administered intramuscularly, both Gardasil® and Cervarix® induce long-lasting serum anti-HPV IgG immunoglobulin titers, much higher than those observed during a natural infection. The resulting protection can be explained in terms of such immunoglobulins being able to transude through the epithelium to create a protective barrier at the cervical level.

Understanding HPV vaccines' immunogenicity

Coarsely speaking, an immune response can be classified on the basis of the following six criteria: i) the antigen's origin (autologous / heterologous); ii) the antigen's location when detected by the host (intracellular / extra-cellular) iii) the branch or branches of the immune system that is/are concerned (innate / adaptive / or both of them); iv) the modality of action (humoral / cellular / or both of them); v) the site of induction of the response (systemic / mucosal / or both of them); and vi) the site of action (systemic / mucosal / or both of them). Thus, a parallel between an HPV infection and vaccination with either Gardasil® or Cervarix® would result in the following:

- **Antigen's origin**. In both cases the antigen is heterologous.
- **Antigen's location**. Infection: the predominant way in which the host detects the viral antigens is intracellularly, through the intervention of the MHC-I complex. Vaccination: the vaccine's active principle is recognized extracellularly by the immuno-competent cells locally recruited after the induction of an inflammatory response.

- **Branch(es) of the immune system that is(are) stimulated**. Infection: the induction of an adaptive response is possible but remains relatively weak. Vaccination: it is definitively an innate response followed by an adaptive response that, as usual, requires some weeks to take place.
- **Modality of action**. Infection: a modest humoral response has indeed been observed, but it is principally a cell-mediated kind of immune action that explains why most HPV infections are naturally controlled and cleared. Vaccination: both vaccines were actually conceived and formulated to induce strong humoral responses. This is achieved thanks not only to the high immunogenicity of the virus-like particles themselves but also to the excellent complementary contribution of the adjuvant.
- **Site of induction**. Infection: since the virus never crosses entirely the epithelium, all the possibly observed immune reactions are induced at the mucosal level. Vaccination: since the vaccine is administered intramuscularly, the resulting immune responses are induced systemically.
- **Site of action**. Infection: the induced (mainly cell-mediated) immune responses act locally trying to get rid of the HPV infected cells. Vaccination: even though the immune response is induced systemically, the protective effect takes place locally, at the cervical level.

Cellular versus humoral immune responses

In general terms, whether an immune response is oriented towards a humoral or a cellular kind of action is partly reflected in the phenotype of a subset of T lymphocytes, known as the CD4+ helper cells. Depending on whether they differentiate to Th1 or Th2 cells, they secrete different sets of cytokines, predominantly IFN-γ and IL-2 in the former case and IL-4, IL-5, IL-6 in the latter. Thus, the Th1/Th2 balance promotes, almost exclusively, a defensive action mediated either by cytotoxic T cells (Th1 phenotype) or by immunoglobulin-secreting B cells (Th2 phenotype). In fact, in the

case of HPV cervical infections several studies have shown[123,124] that Th1 responses are predominantly important in controlling the virus.

In the case of HPV vaccination, data on the role of the Th1/Th2 balance in the induced immune reactions are scarce. A study[125] in which such an analysis was conducted concluded that the observed cytokine and chemokine profiles did not permit to state that a Th2 phenotype was predominant. However, besides the fact that the experimental vaccine they used for the study was a monovalent one, the biggest difference was the absence of adjuvant, which is well known for playing a major role in the humoral responses induced both by Gardasil® and Cervarix®.

Systemic versus mucosal immune responses

To date, at least ten vaccines for human use have been licensed that stimulate the immune system directly at the mucosal level (e.g. the live attenuated polio vaccine). As already stated, this is not the case of HPV vaccines. The different mucosae (gastrointestinal, respiratory, and genitourinary) constitute specialized sites where the immune reactions are induced in a different way from systemic immune responses. This is manly due to the fact that in such zones the body must constantly tolerate the presence of foreign matter, such as food and the different bacterial florae that populate the human body. In addition, the physicochemical characteristics of the local environment also influence the way the immune systems responds at the mucosal level. For instance, in the gastrointestinal tract it is more common to find immunoglobulins type A then any other isotype, which is due to the fact that IgAs better resist being surrounded by the intestinal fluids. On the other hand, it is well known that both semen and cervicovaginal fluids contain more IgG's than IgA's. However, a feature that is common between the systemic and the mucosal immune responses is that they are both associated to highly-specialized centers in which the innate and the adaptive immune system cells find each other to interact and to induce common responses. In the systemic immune system, such sites can be, for instance, the lymph nodes. In the case of the gastrointestinal tract, they take the form of the Peyer's patches, while in the respiratory system they form what is known

as the lymphoid tissue aggregation sites in the bronchial tract. In the case of the reproductive system, the study of the migration patterns of both T and B cells, through highly sophisticated tracing techniques, has permitted to identify the internal and external iliac lymph nodes as being some of the associated immune-response induction and maturation sites[126].

In the case of the intramuscular administration of either of the HPV vaccines, the virus-like particles (VLPs) are firstly recognized by the innate immune system, which constitutes the second line of defense against pathogens (the first one being the physical barriers such as the mucosa and the skin and the third one being the adaptive immune system). Several types of innate-immune cells (macrophages, neutrophils, dendritic cells and others) are capable of capturing foreign matter shortly after it has crossed the epithelial barrier. Most of these cells possess toll-like receptors that permit them to sense their environment and to discriminate between self and non-self proteins. Once identified as belonging to the latter kind, they are endocytosed and processed, the purpose being to produce short peptides, usually 8 to 10 amino-acid long, to be later presented by the MHC-I molecules. As a consequence, the antigen-presenting cells get activated and migrate to the already-mentioned specialized immune-response induction centers[127]. The reason for doing this is twofold: i) first, there they find the microenvironment they need for maturing and therefore acquiring the phenotype they need for becoming totally functional; and ii) there they find and activate different lymphocyte populations such as B cells, which will later differentiate and become either immunoglobulin-secreting plasma cells or long-lived memory cells. The activity of the former is directly associated with the immunoglobulin titer curves observed after vaccination, which constitutes the outcome of our mathematical model.

CHAPTER 8:

UNDERSTANDING THE HOST-PATHOGEN INTERACTIONS FOLLOWING A MUCOSAL HPV INFECTION

From a general point of view, chronic HPV infections can affect a variety of anatomic sites in the body, such as i) the skin, where they can induce several types of predominantly-benign lesions: common warts (verruca vulgaris)[128,129], plantar warts (myrmecias)[130], flat warts (verruca plana)[131], verruciform epidermal dysplasia (epidemodysplasia verruciformis)[132]; ii) the head and the neck, where they are associated to a subset of squamous cell carcinomas[133,134,135,136]; iii) the oral cavity, where they may induce focal epithelial hyperplasia[137,138,139] or leucoplakia[140,141]; iv) the nasal cavity, where they can give rise to inverted papillomata[142,143,144]; v) the respiratory tract, especially the larynx, where they may cause recurrent respiratory papillomatoses[145,146,147,148] (see these references for excellent reviews on RRP); vi) the upper gastrointestinal tract, where they may cause esophageal squamous papillomatosis[149,150,151]; and vii) the genitourinary tract, where the HPV-associated diseases may be either benign (condyloma acuminatum) or pre-cancerous (cervical intraepithelial neoplasia, adenocarcinoma in-situ).

So far, more than 100 HPV types have been identified. Of these, it is known that at least 40 are susceptible of establishing long-lasting infections in human beings. HPV types are commonly divided into high-risk and low-risk genotypes. The former (mainly HVP-16, 18, 31, 33, 35, 39, 45, 51, 52, 56, 58, 59[152]) are best known for their implication in the genesis of several types of cancer (from which cervical cancer is the most widely known and studied), while the latter (mainly HPV-6, 11, 40, 42, 43, 44, 54, 61, 70, 72, 81) are generally associated to the occurrence of genital warts. Multiple epidemiologic studies[153,154,155,156] have been conducted to demonstrate that approximately 70% of the cases of cervical cancer are linked to HPV-16, 18 chronic infections. The molecular

demonstration of this causal relationship was obtained and published in the 1980s[157,158,159], and 25 years later was rewarded with the Nobel Prize in Physiology or Medicine.

An interesting characteristic of HPV's natural history is that even if it can be found in a great number of sites, it only seems to induce disease when the infection affects the so-called "transformation zones" (as in the case of the cervix, the anus, the tonsils, and some others), which are particular anatomical spots that constitute the transition between two different kinds of tissue[160,161].

For completing its life cycle HPV must first gain access to its target cells: the basal epithelial cells. The stratified squamous epithelium is made up of about 20 layers of cells, of which only those forming the innermost layer have the capacity of permanently multiplying themselves. For reaching their target cells, HPV virions must cross the epithelium through the microscopic breaches they may eventually find within an otherwise continuum of epithelial cells. Under normal conditions, daughter cells emerging from the innermost layer undertake a journey that takes them to the outermost layer where they spontaneously disintegrate and die. As soon as they quit the basal zone, daughter cells turn their replicating machinery off to swap into a differentiation program. The problem is that, when infected by HPV, these cells are no longer capable of coordinating their replication / differentiation programs.

The human papillomavirus is made up of two envelope (L1 and L2) and six constitutional (E1, E2, E4, E5, E6 and E7) proteins, the whole being coded by a bare single-stranded DNA genome with a relatively modest size of 8,000 pair of bases. The mechanisms through which HPV interferes with the normal life cycle of the epithelial cells it infects is thought to vary profoundly between the high- and the low-risk genotypes. In the case of the former, the late-expressed viral E6 – E7 proteins are thought to bind specifically to the proteins coded by a couple of genes (p53 and the retinoblastoma

tumor suppressor gene) known to play a major role in the regulation of the cell cycle. In the case of the latter, it is known that the mechanism is different, but its nature remains uncertain.

SCHEMATIC DEPICTION OF HPV'S NATURAL HISTORY

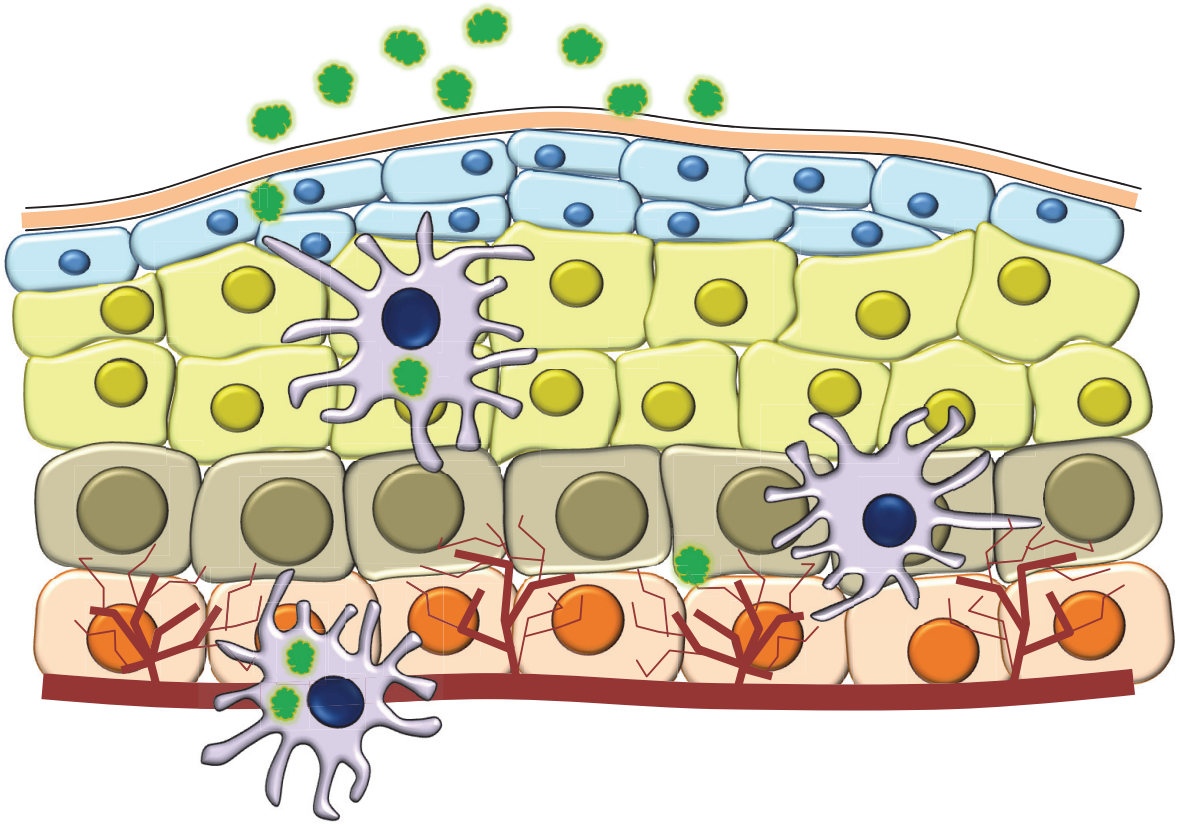

Besides infection with the human papillomavirus, several risk factors[162] have been identified that can be associated with the development of a cervical cancer. They can be divided in three groups: i) environmental factors, which include the use of hormonal contraceptives, tobacco smoking and coinfection with other sexually transmitted pathogens; ii) viral factors, which include coinfection with other HPV types, viral load and viral integration; and iii) host factors, which include various

tumor suppressor gene) known to play a major role in the regulation of the cell cycle. In the case of the latter, it is known that the mechanism is different, but its nature remains uncertain.

SCHEMATIC DEPICTION OF HPV'S NATURAL HISTORY

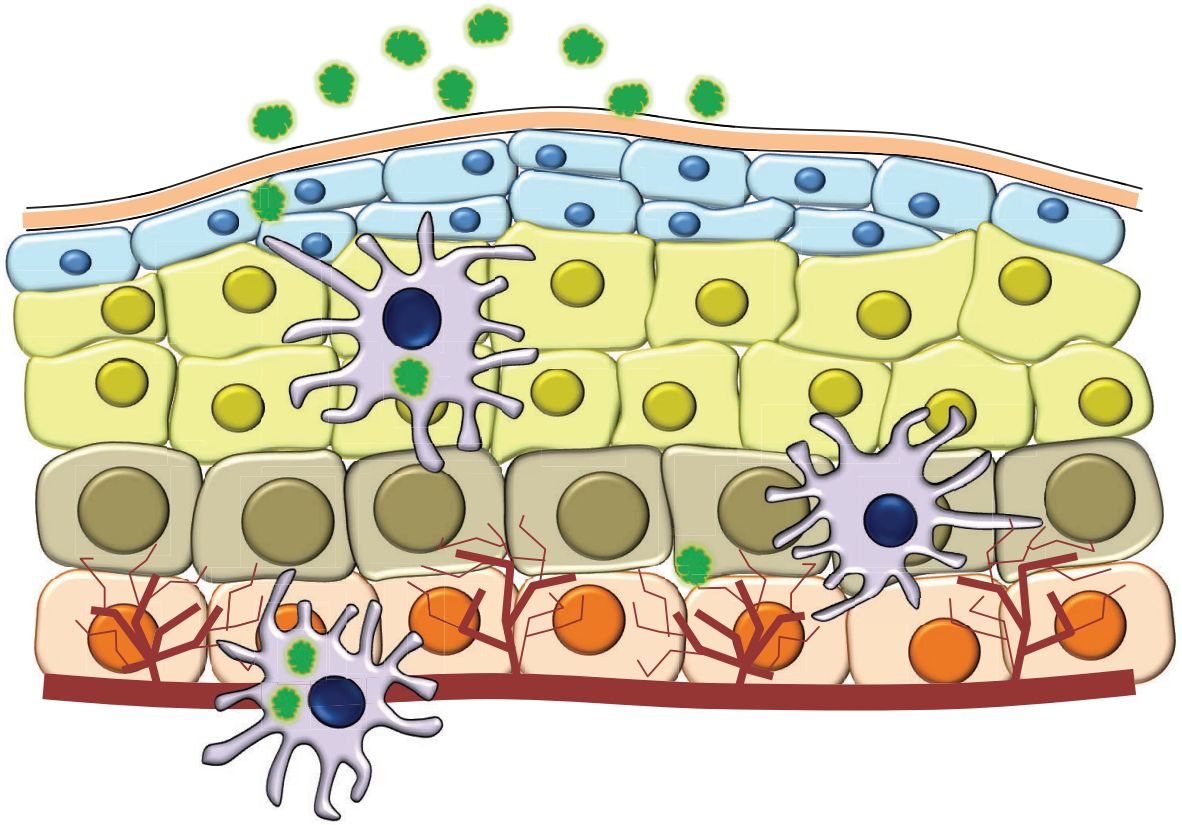

Besides infection with the human papillomavirus, several risk factors[162] have been identified that can be associated with the development of a cervical cancer. They can be divided in three groups: i) environmental factors, which include the use of hormonal contraceptives, tobacco smoking and coinfection with other sexually transmitted pathogens; ii) viral factors, which include coinfection with other HPV types, viral load and viral integration; and iii) host factors, which include various

genetic factors (especially those associated with the immune system) as well as the unbalanced activity of certain endogenous hormones.

In fact, the physiology of the female genital mucosa is strongly influenced by hormonal cycles. First of all, the dynamics of the epithelial-cell turnover is impacted by the fact that the higher the estrogen levels the thicker the genital epithelium and the more abundant the intra-cytoplasmic glycogen[163]. Moreover, these hormonal cycles have been found to affect the local levels of cytokines as well as the expression of several receptors on epithelial cells[164,165] implicated in immune-related functions, such as the transit of both immunoglobulins and immuno-competent cells through the genital mucosa.

In spite of the considerable progress that has been made in understanding the natural history of HPV infections, it is still unknown whether or not, after having successfully coped with a first infection, the organism acquires the capacity of protecting itself against new exposures to the virus (i.e. the capacity of developing protective immunity)[166], as occurs with other epithelial pathogens such as the influenza virus[167]. In the case of HPV, there is no experimental way to elucidate this question in human beings. Nevertheless, there are some animal models that suggest that the resolution of a primary infection can lead to some degree of protective immunity. Additionally, both in animal models and in humans regression of HPV-associated lesions has been associated with the activity of T lymphocytes, which suggests that a cell-mediated immune response must have been induced. This would be a key aspect for explaining the relapsing nature of RRP, which is thought to be associated to some kind of immune impairment in the host.

SECTION IV

COMPUTATIONAL MODELS –

THE MACHINERY

CHAPTER 9

COMPUTATIONAL MODELING OF THE IMMUNE RESPONSES INDUCED BY THE INTRAMUSCULAR IMMUNIZATION WITH AN HPV VACCINE

Here we present a mathematical model intended to describe the dynamics (in terms of activation, migration, multiplication, differentiation, interaction with others and death) of the major cell types involved in the immune response following the intramuscular administration of the quadrivalent HPV vaccine (Gardasil®).

More than four years have now passed since the approval of Gardasil®, which was the first prophylactic HPV vaccine to reach the market. Since then, the officially recommended schedule consists of three doses, at months 0, 2 and 6. But, what would be the consequence, in terms of the induced immunogenicity, if the vaccination protocol happened to be modified (as in the case of lack of compliance, for instance)? No one can really answer this question today for the immunological phenomena behind are not fully understood. Moreover, in the specific case of HPV vaccines not much has been published so far on this regard, which does not imply that the question lacks of relevance. Currently, at least 12 clinical trials registered in ClinicalTrials.gov and using immunization with the quadrivalent HPV vaccine as the main intervention form include within their objectives the question of the effects of schedule modifications on the immunogenicity (see table 1).

The problem is that the number of conceivable ways of (intentionally or unintentionally) modifying the original 0-2-6-month schedule is so vast that wanting to figure this question out on the basis of a clinical-trial strategy would represent a highly time- and money-consuming choice. We, on the contrary, propose computational simulations, not with the intention of replacing the evidence-based approach but as a possible means of rendering more efficient.

	ClinicalTrials.gov Identifier	Vaccination protocols (months)	Results published in (expected for)
1	NCT00339040	0,2,6,24	June 2010
2	NCT00501137	Undisclosed	February 2008
3	NCT00520598	0,2,6 vs. 0,6	February 2011
4	NCT00524745	0,2,6; 0,3,9; 0,6,12; 0,12,24	January 2010
5	NCT00572832	0,2,6 vs. 0,2,12	August 2010
6	NCT00829608	The information is contradictory 0,4,8 (?) 0,2,4 (?)	June 2010
7	NCT00923702	0,2,6 vs. 0,6	May 2014
8	NCT00925288	0,2,6 vs. 0,3,6	October 2010
9	NCT00949572	0,1,4	December 2010
10	NCT01031069	0,1.5,6	May 2013
11	NCT01184079	0,2,6 vs. 0,2,12	January 2012
12	NCT01030562	2nd dose on time / 3rd dose late vs. 2nd dose late / 3rd dose on time vs. 2nd dose late / 3rd dose late vs. On-time administration	December 2012

Table 1. Currently ongoing clinical trials in which the question of the effects of the vaccination schedule modifications on the resulting immunogenicity is treated for HPV prophylactic vaccines.

The model's variables

The present model focuses on the dynamics of the following four key aspects of the induction of an immune response through intramuscular vaccination: i) the antigen recognition, capture and processing as a hallmark of the innate immune system intervention[168,169]; ii) the migration and maturation of the activated antigen-presenting cells (APCs)[170,171]; iii) both the primary (T-cell

THE VACCINE	V^N	Concentration of the HPV-L1 virus-like particles in the non-lymphoid compartment.
	V^L	Concentration of the HPV-L1 virus-like particles in the lymphoid compartment.
	A^N	Concentration of the adjuvant in the non-lymphoid compartment.
	A^L	Concentration of the adjuvant in the lymphoid compartment.
APCs	P_N^N	Cell-population density of the naive antigen-presenting cells in the non-lymphoid compartment.
	P_T^L	Cell-population density of the immature (primed but non-reactive) antigen-presenting cells in the lymphoid compartment.
	P_T^N	Cell-population density of the immature (primed but non-reactive) antigen-presenting cells in the non-lymphoid compartment.
	P_R^L	Cell-population density of the mature (primed and reactive) antigen-presenting cells in the lymphoid compartment.
T CELLS	H_N^L	Cell-population density of the naive HPV-L1-specific CD4+ helper Th2 lymphocytes in the lymphoid compartment.
	H_P^L	Cell-population density of the primed HPV-L1-specific CD4+ helper Th2 lymphocytes in the lymphoid compartment.
	H_P^N	Cell-population density of the primed HPV-L1-specific CD4+ helper Th2 lymphocytes in the non-lymphoid compartment.
B CELLS	B_N^L	Cell-population density of the naive (non-effector, non-proliferating) HPV-L1-specific B lymphocytes in the lymphoid compartment.
	B_O^L	Cell-population density of the pre-primed (non-effector, proliferating) HPV-L1-specific B lymphocytes in the lymphoid compartment.
	B_F^L	Cell-population density of the fully primed (non-effector, proliferating) HPV-L1-specific B lymphocytes in the lymphoid compartment.
	B_S^L	Cell-population density of the HPV-L1-specific plasmacytes (effector non-proliferating) in the lymphoid compartment.
	B_K^L	Cell-population density of the memory-precursor (non-effector, non-proliferating) HPV-L1-specific B lymphocytes in the non-lymphoid compartment.
	B_M^L	Cell-population density of the circulating memory (non-effector, non-proliferating) HPV-L1-specific B lymphocytes in the lymphoid compartment.
	B_L^L	Cell-population density of the stationary long-lived bone-marrow-residing (effector, non-proliferating) HPV-L1-specific B lymphocytes .
IgGs	C^L	Concentration of the HPV-L1-specific IgG immunoglobulins circulating in the lymphoid compartment.
	C^N	Concentration of the HPV-L1-specific IgG immunoglobulins circulating in the non-lymphoid compartment.

Table 2. List of the 20 variables contained in the mathematical model, including a brief description of the phenotypes.

independent) and the secondary (T-cell mediated) priming of B lymphocytes[172,173]; and iv) both the initial (short-term, highly-intensive) and the subsequent (long-term, more-modest) immunoglobulin production and secretion phases[174,175,176].

We inspired ourselves from an already-published model[177] to come up with a system of twenty delay differential equations (DDEs) devised to describe the dynamics of three cellular (APCs, CD4+Th2 and B cells) and three molecular entities (the virus-like particles or VLPs – which constitute the vaccine's active principle, the adjuvant and the HPV-specific circulating IgG immunoglobulins). Each one of these six entities (which are respectively represented by the capital letters P, H, B, V, A and C) may adopt a series of functional phenotypes (naive cells, pre-primed cells, fully-primed cells, etc.), represented by capital letters in subscript. The molecular entities were studied in terms of molecular concentrations (i.e. number of moles per unit of volume), while for the cellular entities we used population densities (i.e. number of cells per unit of volume). Thus, the model consists of twenty variables, each of which is defined as the concentration / cell-population density of a given species (a species being defined as an entity that adopts a functional phenotype) divided by the volume of the theoretical (either lymphoid or the non-lymphoid) compartment, at a given instant of time. The added volume of both compartments is considered to be sixty liters. The full list of variables, including a brief description of the functional phenotypes, is presented in table 2.

Assumptions behind the model

In figure 1, all the considered interactions between the different species are depicted. Briefly, we consider that the vaccine's active principle (i.e. the HPV-L1 VLPs) can directly activate both APCs and B cells. We assume that APCs need to migrate to a lymphoid maturation center where they encounter and prime T cells, which later provide the complementary antigen-specific signal needed by B cells to become plasmacytes. We hypothesize that these short-lived cells secrete high rates of HPV-L1-specific IgG immunoglobulins, while the long-lived circulating memory B cells (as well

SCHEMATIC REPRESENTATION OF THE IMMUNE RESPONSES INDUCED BY VACCINATION WITH GARDASIL®

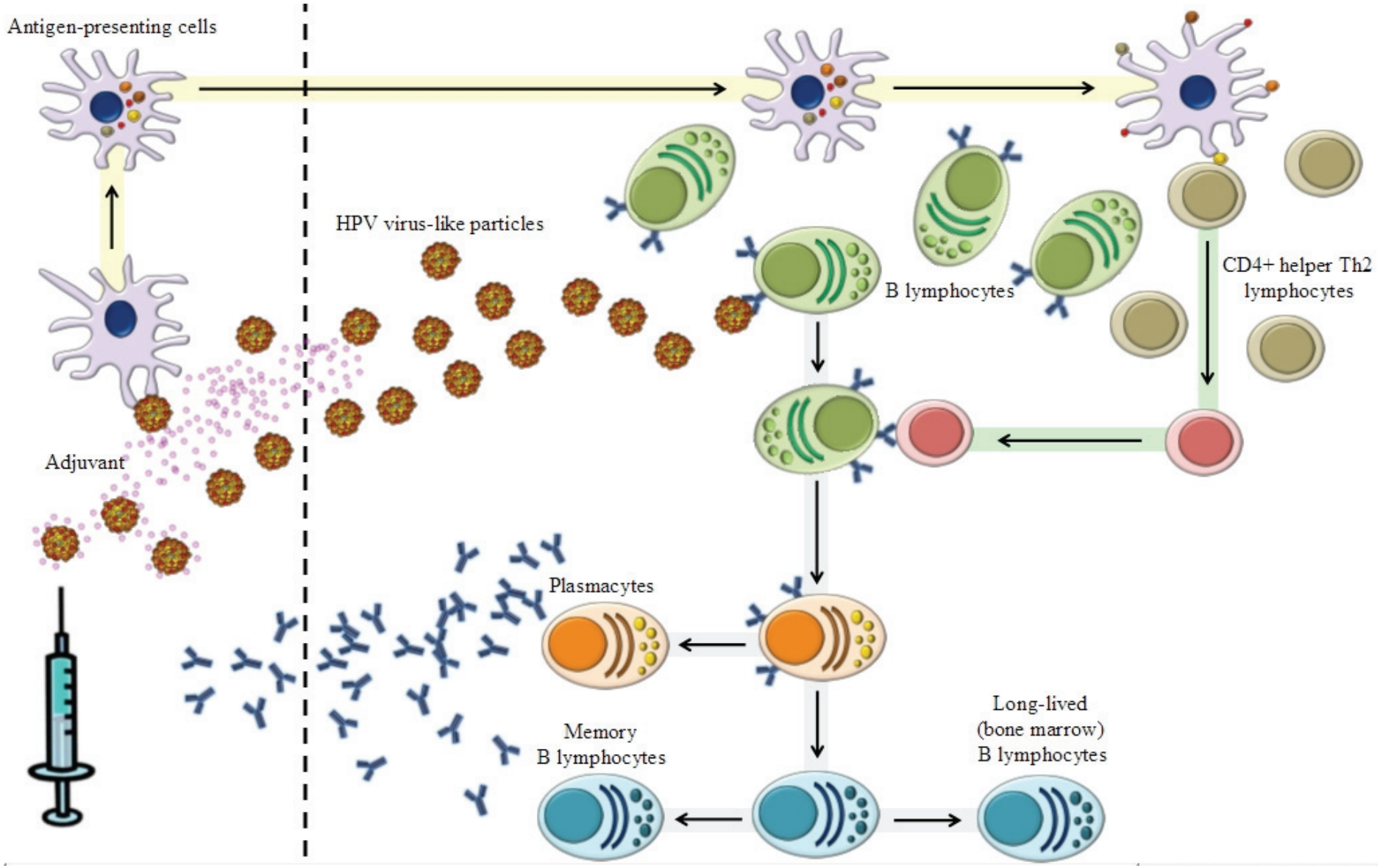

as the long-lived stationary bone-marrow-residing B cells) secrete the same kind of immunoglobulins but at much lower rates.

We consider that the quantitative fate of each species is defined by: i) its own tendency to die, decay or become non-functional; ii) by its own tendency to migrate to the complementary (lymphoid / non-lymphoid) compartment; iii) by its own tendency to evolve to other phenotypic states either independently or through the interaction with other species; v) by its own capacity to multiply itself; vi) by the system's capacity to offset loss through the production of new individuals of the same species.

A major precept underneath our model dictates that the way the whole system (i.e. the set of twenty variables) evolves at a given instant of time is fixated by both the state of the system at the same instant of time and by the state of the system at one (or several) previous instant(s) of time, which explains the use of DDEs. In fact, a major feature of this kind of differential equations consists in the introduction of a series of terms, commonly referred to as the tau (τ) terms, which are a mathematical means for taking into account such a multiple dependence on time. By doing so, it is the inertia inherent to the system that is taken into account (in our case, we consider that such inertia stems from the fact that the immune system takes some time to satisfy punctual needs, such as, for example, the monoclonal expansion of a given cell lineage[178]). Additionally, in our model, the system can be occasionally perturbed by punctual step-like functions affecting one, or more, of the variables (as when simulating, for example, the administration of a vaccine dose).

Other, secondary, biological precepts underneath our model are: i) We assume that the supply of both VLPs and the adjuvant is exclusively fixated by the vaccination protocol; and that there is no source of HPV-L1-specific circulating IgG immunoglobulins other than the one associated with the administration of the vaccine. For APCs, helper-T and B lymphocytes, we suppose that the rate at which they are supplied (through hematopoiesis) is independent of the state of the system at any

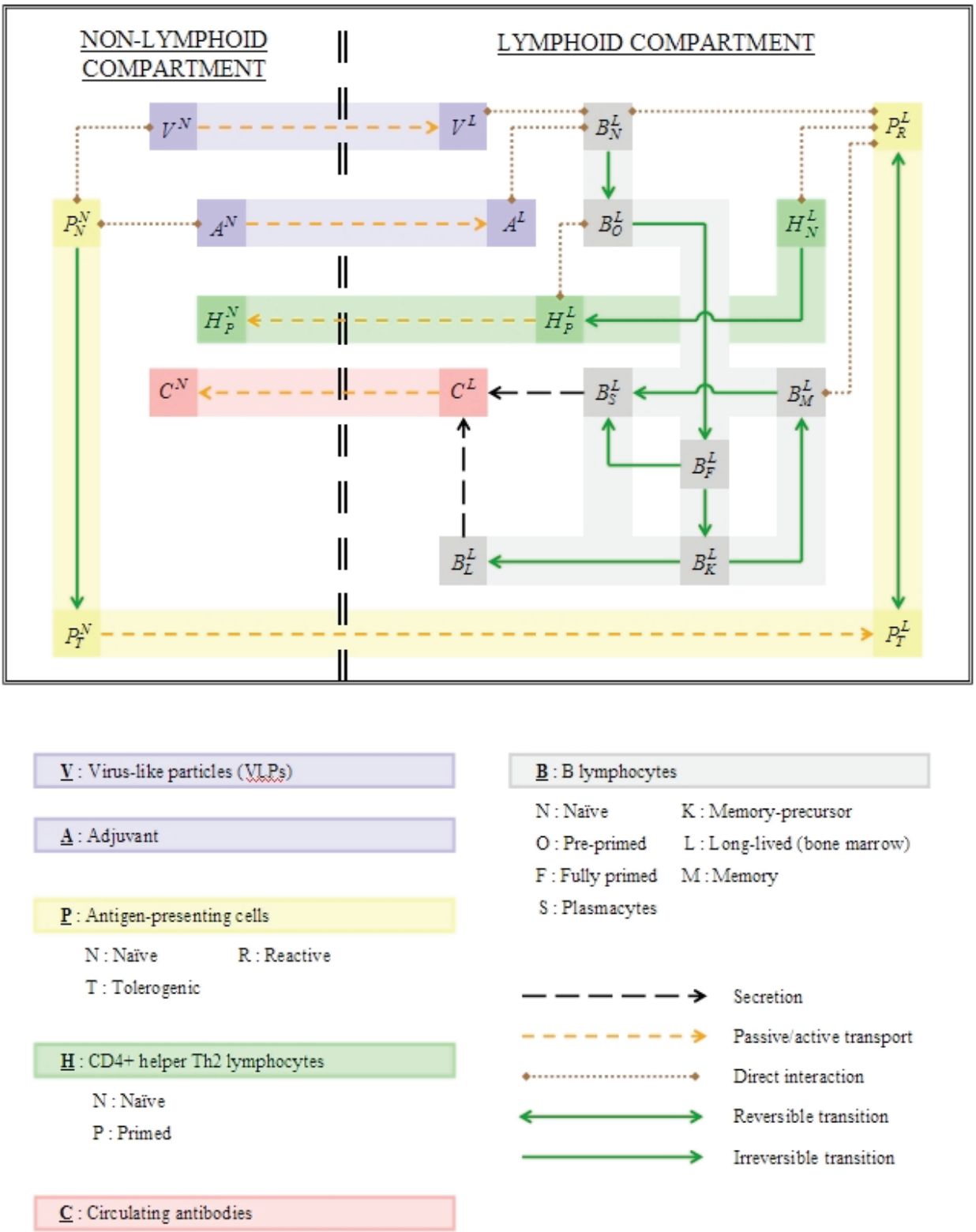

Figure 1. Schematic representation of the interactions included in the mathematical model. Each variable is represented by a square that contains a central capital letter, which defines the corresponding biological entity (T cells, or B cells, or APCs, etc.). The letter in subscript indicates the particular phenotype (naive, or activated, or suppressed, etc.), while the letter in superscript represents the location (in either the lymphoid or the non-lymphoid theoretical compartment).

given instant of time (i.e. the model does not take into account any possible feedback signals susceptible of modulating the dynamics of hematopoiesis[179]). ii) We hypothesize that for each species the death/decay rate (as well as the inter-compartmental flow rate) depend only on its own concentration at any give instant of time. We suppose that each species disappears (or diffuses into the complementary compartment) following an exponential dynamics (i.e. the higher its concentration, the higher its death/decay rate and the higher its inter-compartmental flow rate). This assumption constitutes a mathematical abstraction of the immune system's tendency to maintain homeostasis, which, when studied in detail, is found to involve extensive and complex biologic networks, as in, for example, the case of T lymphocytes[180]. iii) We consider that the rate at which a species evolves from one phenotypical state to another (through the interaction with other species), follows a second-order kinetics law, which means that it is proportional to the product of its own concentration and the concentration of the stimulating species. iv) The model takes account of the fact that, upon activation, some species have the capacity of multiplying themselves. We presume that the magnitude of this clonal expansion is proper to every cellular type and does not change during the course of the vaccine-induced immune response, which means that the model does not take into account any mechanisms known for affecting the pace at which immuno-competent cells multiply (e.g. the intervention of regulatory T cells[181]). v) We suppose that the adjuvant renders the process of APC-mediated lymphocyte activation more efficient. Mathematically, we describe this effect as a function of the adjuvant's active concentration, as showed schematically in figure 2. In this graphic, the lower threshold reflects the assumption that even if the adjuvant's active concentration is set to be zero, APCs remain capable of priming lymphocytes (as demonstrated by the fact that, when administered with no adjuvant, the vaccine remains highly immunogenic[182]). On the other hand, the upper threshold reflects the presumed existence of a critic value beyond of which no increase in the adjuvant's active concentration would result in any increase of the lymphocyte activation rates (as though reaching a saturation state).

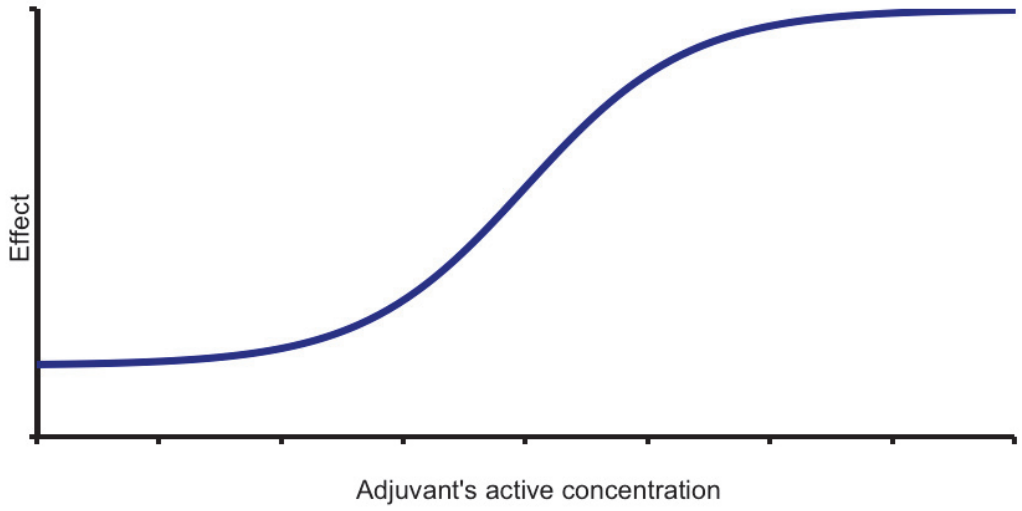

Figure 2. Schematic representation of the relationship used for computing the adjuvant's effect on the induced immune response. By using this empirical function we hypothesize the existence of a lower and an upper threshold. The former should reflect the fact that even when administered with no adjuvant the vaccine remains immunogenic, while the latter indicates the existence of a limit beyond of which no increase in the adjuvant's concentration would result in a higher immunogenicity. The quantitative characterization of this relationship constitutes one of the major challenges for the model's calibration process.

Implementing the model

The model contains a total of fifty-six parameters, which constitute the bricks permitting the establishment of quantitative relationships (equations) between the twenty variables. Once all the equations finely chipped and crafted, and the dimensional coherence of each one of them verified, the model (extensively presented in appendix 4) found itself ready for being implemented, calibrated and exploited. For doing so, we employed a Matlab® (2006R) simulation environment.

Conducting a simulation implies four fundamental steps: i) Attributing each one of the fifty-six parameters a value. ii) Defining the system's history (i.e. the behavior of each one of the twenty variables for any $t < t_0$; $t_0 = 0$). We did so by assuming that before any perturbation occurs (i.e. before the vaccine administration is simulated) the system finds itself in a steady state in which all the variables exhibit constant values (estimated through a procedure later explained in this

document). iii) Defining the system's initial conditions, which correspond to the values of the twenty variables at $t = t_0$. Here, we consider that all of them inherit their values from the system's history, with the exception of those accounting for both the vaccine's active principle and the adjuvant (whenever a dose administration is simulated at $t = t_0$). iv) Solving the mathematical system, which we did with the aid of a slightly modified version of the Matlab®'s dde23 routine, originally developed by others[183]. This ready-to-use tool uses a Runge-Kutta-like numerical method that permitted us to obtain, whenever the convergence towards a solution was possible, the simulated evolution of each one of the twenty variables, through a discretized axis of time.

The model's parameters

The fifty-six parameters contained in the model can be grouped in twelve families, which are presented in table 3 (a more detailed presentation can be found in appendices 2 and 3). From the fifty-six parameters, four were driven from the literature (d_P[184], d_H[185], d_B[186] and d_C[187]), four others ($k_{V/P}$, $k_{V/B}$, $q_{V/P}$ and $q_{V/B}$) were found to be dependent on other parameters through the expressions presented here below. Three other parameters (s_B, s_H and s_P) were indirectly calculated as explained later, twenty others were directly estimated on the basis of a series of assumptions presented in the paragraph below, and the twenty-five remaining were indirectly estimated through a calibration process (later detailed in this document) in which Gardasil®-induced-seroconversion data (taken from literature) were used as the numeric target the mathematical model was "guided" to comply to.

$$k_{V/P} = k_{P/V} \cdot q_{P/V} \qquad k_{V/B} = k_{B/V} \cdot q_{B/V}$$

$$q_{V/P} = \left(q_{P/V} \right)^{-1} \qquad q_{V/B} = \left(q_{B/V} \right)^{-1}$$

Symbol	Types of parameters	Amount
d	Spontaneous death/decay rates	12
f	Inter-compartmental migration rates	5
k	Kinetic coefficients	8
q	Stoichiometric coefficients	8
z	Clonal expansion coefficients	4
n	Average numbers of cell cycles occurring during clonal expansions	4
v	B-lymphocytes differentiation rates	4
s	Supply rates of naive cell populations	3
k	Empirical constants used for computing the effect of the adjuvant	2
ω	Fractions of the naive (B and T) lymphocytes populations naturally specific for HPV-L1 epitopes	2
m	Maturation rate of antigen-presenting cells	1
r	anti-HPV-L1 IgG immunoglobulin secretion rates	2
τ	Average duration time of a cell division cycle	1
	Total amount of parameters	56

Table 3. List of the 13 types of parameters contained in the mathematical model

The assumptions behind the direct estimation of some of the model's parameters are the following: i) We hypothesize that the vaccine's active principle, i.e. the HPV-L1 VLPs, has a moderate tendency to persist in the vaccinee's organism (in-silico half-life ≈ 60 days), which is an intermediate position between the theories that support[188,189,190] and those that contradict[191,192,193], the idea of long-term antigen persistence as a requirement for immune memory. ii) We consider that there is no difference, in terms of their pharmacokinetic behavior, between the vaccine's active principle and its adjuvant. Even though some animal studies[194] suggest a peripheral blood half-life of a couple of days for aluminum adjuvants, others[195] talk of a localized depot effect through which both the immunogen and the aluminum adjuvant would remain in the site of the injection for, at least, a couple of months. iii) We presume that the differentiation of B lymphocytes implies shorter

life spans, thus, we suppose that both the pre-primed and the fully-primed B cell populations have a half-life of approximately $^1/_4$ of that of naive B cells, while in the case of plasmacytes the ratio (still to naive cells) is supposed to be of the order of $^1/_{16}$. In fact, some animal studies[196,197] suggest that most plasmacytes residing both in the spleen and in the lymph nodes have a life span of less than 3 days, which is quantitatively compatible with our assumptions. iv) We hypothesize that the magnitude of a B-cell clonal expansion is the same whether its origin is the activation of naive or memory cells. We consider that the difference between the two cases lies in the fact that in the former the concurrence of T cells is required for B cells to reach the state of plasmacytes, while in the latter not. This assumption was introduced on simplicity grounds in spite of the fact that it has been suggested[198] that memory B cells can undergo both T-cell dependent and independent reactivation. v) We presume that, from the stoichiometric point of view, i.e. the quantitative ratio between the activating and the activated species needed for the activation to take place, all the cell-to-cell interactions are of the 1:1 kind. For the amount of immunogen needed for activating either an APC or a B lymphocyte, we suppose an order of magnitude in the scale of picograms and we hypothesize that APCs possess a greater capacity of endocytizing VLPs than B-cells do (in-silico values: $q_{P/V} = 10^{2.1}$ pg/cell, $q_{B/V} = 10^{0.4}$ pg/cell). vi) We suppose that approximately one in a million naive B / T cells happen to be naturally specific for the predominant epitopes in the vaccine's immunogen (the HPV-L1-VLPs).

The case of APCs

In our model, the early event of the immunogen being recognized by and therefore leading to the activation of the innate immune system was modeled in terms of the capacity of the circulating monocytes to respond to the vaccination-induced inflammatory signals, by crossing the vascular barrier, by differentiating and adopting an antigen-processing phenotype, and by capturing, endocytizing and processing the viral pseudoparticles. In order to compute the effect (over the whole vaccination-induced immune cascade presented in figure 1) of APCs accomplishing the just-

mentioned series of tasks in a more or less promptly manner the model employs a kinetic coefficient, k_{PV}, which is one of the twenty-five parameters indirectly estimated through the calibration process.

The initial (i.e. for any $t \leq t_0$; $t_0 = 0$) cell-population density of naive APCs was estimated on the basis of a cell count of 400 circulating monocytes per micro-liter of blood in a regular healthy individual, as well as on the assumption that the total blood volume for the same average person would be of approximately six liters.

Based on the already-explained assumption that the hematopoietic supply of fresh cells occurs at a rate independent from the state of the system, we proceeded to estimate s_P, which represents the fresh monocytes' production rate. We did so by taking equation 5, by temporally suppressing the third term (the one accounting for APC's activation), by equalizing the derivative to zero, by considering that, for any $t > t_0$, $P_N^N = P_N^N|t = t_0$ (i.e. the initial value is supposed to remain constant) and, finally, by solving the equation. The result is $s_P = 1.85 \times 10^4$ monocytes per day and per milliliter of the non-lymphoid compartment. According to these in-silico estimates, an average human being should produce an approximate of 555 million fresh monocytes every day ($s_P \cdot v_N = 5.55 \times 10^8$), which is rather compatible with the widely accepted figure of 1×10^{10} fresh white cells produced every day (considering that approximately 5% of them are monocytes). The exact same procedure was applied to estimate the supply rates of helper T as well as of B cells (which, respectively, correspond to parameters s_H and s_B in our model).

CHAPTER 10

ESTIMATING THE UNKNOWN PARAMETER VALUES WITH THE AID OF A GENETIC ALGORITHM

In order to come up with the best possible estimation for a total of twenty-five parameters, we proceeded first to restrict each one of them to a range. For doing so, it was hypothesized that, due to the intimate relationship between the mathematical model and the biological knowledge from which it was created, any set of parameters leading to a mathematically incoherent version of it (i.e. the one for which the numerical method does not converge to a solution) should be discarded because such mathematical insolvability must be an indicator of biological incoherence within the model. Thus, by making vary all the twenty-five parameters simultaneously, and by confining the model to those "zones" where it would remain solvable, the aforementioned ranges were obtained. Then, we used clinical data regarding the seroconversion dynamics (i.e. the evolution of HPV specific immunoglobulin titers, in serum, after vaccination) for indirectly estimating the most adequate value for each parameter within these ranges. We extracted these not-explicitly-disclosed data by analyzing and processing figure 2 from an article[199] published in 2007, and by later assessing the accuracy of our data-extraction procedure by comparing them with those partially unveiled in another article[200] published in 2006 (table 4). Both publications deal of course with the same clinical trial, known as Merck's protocol V501-007. Briefly, in this study, a total of 552 16-to-23-year-old women received either Gardasil® (same formulation and same 3-dose protocol as prescribed everywhere nowadays, i.e. 3 shots at 0, 60 and 180 days) or placebo (1:1 ratio), and were engaged over a 3-year follow-up (an additional 2-year follow-up was conducted in approximately 50% of the participants). Serum samples were collected periodically and analyzed to obtain anti-HPV-6,11,16,18 immunoglobulin levels through a technique known as competitive luminex immunoassay. Since HPV-6 has been reported[201] to be slightly more common in infants suffering from JORRP (HPV-6 ≈ 53%, HPV-11 ≈ 40%, other types ≈ 7%), we decided to focus on this viral

Time (months)	Extracted data (milli-Merck units per mL of blood)				Real data (mean values within their confidence intervals)				Extraction error			
	HPV-6	HPV-11	HPV-16	HPV-18	HPV-6	HPV-11	HPV-16	HPV-18	HPV-6	HPV-11	HPV-16	HPV-18
0	6,1	6,1	10,0	6,0								
2	32,2	32,5	152,5	15,6								
3	438,3	437,7	2849,5	313,8								
6	167,4	163,6	1073,9	95,5								
7	557,5	633,2	3812,1	748,5	559,7 ± 18,3%	642,4 ± 19,3%	3889,1 ± 21,3%	755,5 ± 26,3%	0,4%	1,4%	2,0%	0,9%
12	164,6	169,4	1210,7	158,0								
18	103,5	105,4	550,8	80,8								
24	80,0	81,0	307,8	51,9								
30	100,0	100,0	514,4	61,4								
36	88,7	78,2	440,9	51,9	88,1 ± 22,4%	78 ± 24,0%	441,3 ± 23,3%	50,5 ± 32,5%	0,6%	0,2%	0,1%	2,8%
54	82,8	72,9	418,9	41,9								
60	68,5	70,4	404,8	45,3	66,5 ± 24,3%	67,6 ± 28,3%	395,4 ± 26,9%	43,7 ± 35,8%	3,0%	4,1%	2,4%	3,5%
61	697,1	2629,3	5749,2	1257,0								
								Average 25,2%			Average	1,8%

Table 4. Clinical data used for calibrating the model. Mean serum anti-HPV-6,11,16,18 IgG titers following 3-dose vaccination (at months 0, 2 and 6) with the quadrivalent HPV vaccine. The values were computationally extracted (second column) from a published graphic and then compared to the partially unveiled values (third column) that we found in a published table somewhere else. The error associated to the extraction procedure was calculated and is reported in the fourth column.

type for calibrating our model. At this point, one practical way of thinking of it would be to imagine a processor, that receives an input signal (the vaccination protocol) and that delivers an output signal (a curve predicting the serum immunoglobulin titer over time). The calibration process is an iterative operation that consists in feeding the processor with a well studied input signal (in this case, the 0-60-180-day vaccination protocol), in comparing the resulting output against the known biological behavior to obtain a "deviation" or "error", and, finally, in tuning the processor, in such a way that, after each iteration, the "deviation" or "error" becomes smaller. Such a tuning work was accomplished by an optimization tool, developed in our laboratory, which employs a genetic-algorithm kind of approach (see chapter 6 for an introductory note on this topic).

The genetic algorithm

The resolution of the search (herein called r) is a factor that defines the amount (2^r) of possible values, within the previously defined ranges, that might be potentially attributed to a single parameter. Thus, for the genetic algorithm, each parameter is represented by an r-bit binary number. Even though r could vary between parameters, we decided to use a single constant value (r = 5) in all our simulations. The search space is then defined as the collection of all the possible sets of parameters and its dimension can be calculated as follows: 25 "flexible" parameters * 5 bits per parameter (i.e. the resolution, r) = 125 bits per set of parameters; size of the search space = 2^{125} = 4.3×10^{37}. When executed, the genetic algorithm starts by randomly selecting a small number (32) of sets of parameters within this gigantic search space, all of which are evaluated in terms of their "fitness", defined in function of their capacity to reproduce the targeted output behavior (i.e. the seroconversion dynamics following vaccination). Then, the genetic algorithm gets rid of the "weakest" sets of parameters before using the strongest ones as precursors to generate a new "population" of ready-to-test sets of parameters. After a certain number of iterations (in our case 250), the process is halted, and the "fittest" set of parameters is retained and stocked for later

analysis. Considering the magnitude of the search space, only a tiny fraction of it is explored in a single execution of the genetic algorithm, which is rather convenient because we are not forced to use extremely sophisticated computing equipments (all our in-silico work was conducted in a conventional 8-core workstation), neither are we constrained to deal with monstrous calculation times (a typical run of our genetic algorithm lasts only a couple of hours). However, a pitfall of our approach could be the possible dependence on fate, for the power of the optimization process might depend strongly on what zones of the search space are initially randomly selected by the genetic algorithm. To overcome this problem, we repeated the same procedure over an over again (a total of 26 times) giving it the opportunity to have completely distinct starting points from which to launch the optimization process.

BINARY REPRESENTATION OF THE MODEL'S PARAMETERS

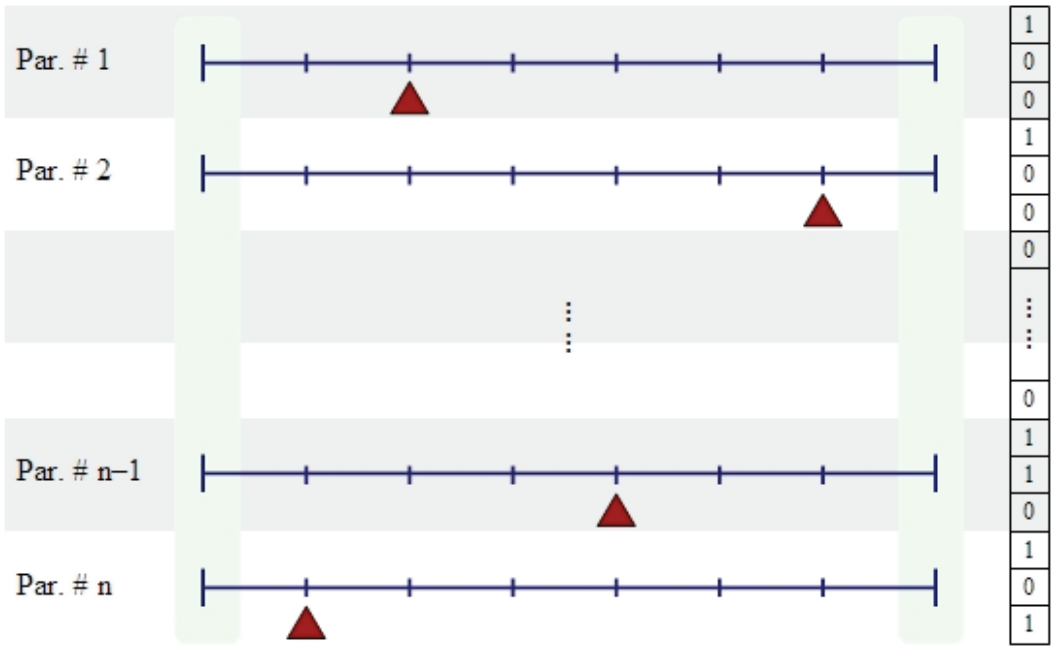

CHAPTER 11

COMPUTATIONAL MODELING OF THE HOST-PATHOGEN INTERACTIONS FOLLOWING A MUCOSAL HPV INFECTION

A multi-agent system was developed in order to quantitatively simulate the interactions between the human papillomavirus and the host's epithelial cells. For doing so, four different classes of agents were defined: the epithelial cells, the viral particles, the immunoglobulins, and the space where all of them exist and interact. The space, which is two-dimensional, is divided into three zones: i) the upper or northern zone (also called hereafter the "upper free space") which represents the mucous milieu lining the outer surface of the epithelium; ii) the middle zone, which represents the tissue; and iii) the lower or southern zone (also called hereafter the "lower free space") which represents the inner surface of the epithelium, the one that is in direct contact with the micro-vessels.

An introductory note on the principles behind and the interest of conducting a multi-agent based kind of modeling can be found in chapter 6.

From the informatics point of view, an agent is a computational entity (technically called an object) characterized as follows: i) it belongs to one of the previously defined four classes; ii) it possesses a unique identity (for example, in our simulator, an agent called "vp1" represents the first individual of the viral-particle class; another different agent, of the same class, called "vp2", represents the second individual, and so on); iii) it can be created and deleted; iv) it stocks a package of information that may evolve over time (for example, its position (x,y) in the two-dimensional Cartesian coordinate system). In the following paragraphs, we are going to describe the information associated with each one of the four classes of agents employed in our simulations.

SCHEMATIC REPRESENTATION OF THE MULTI-AGENT SYSTEM

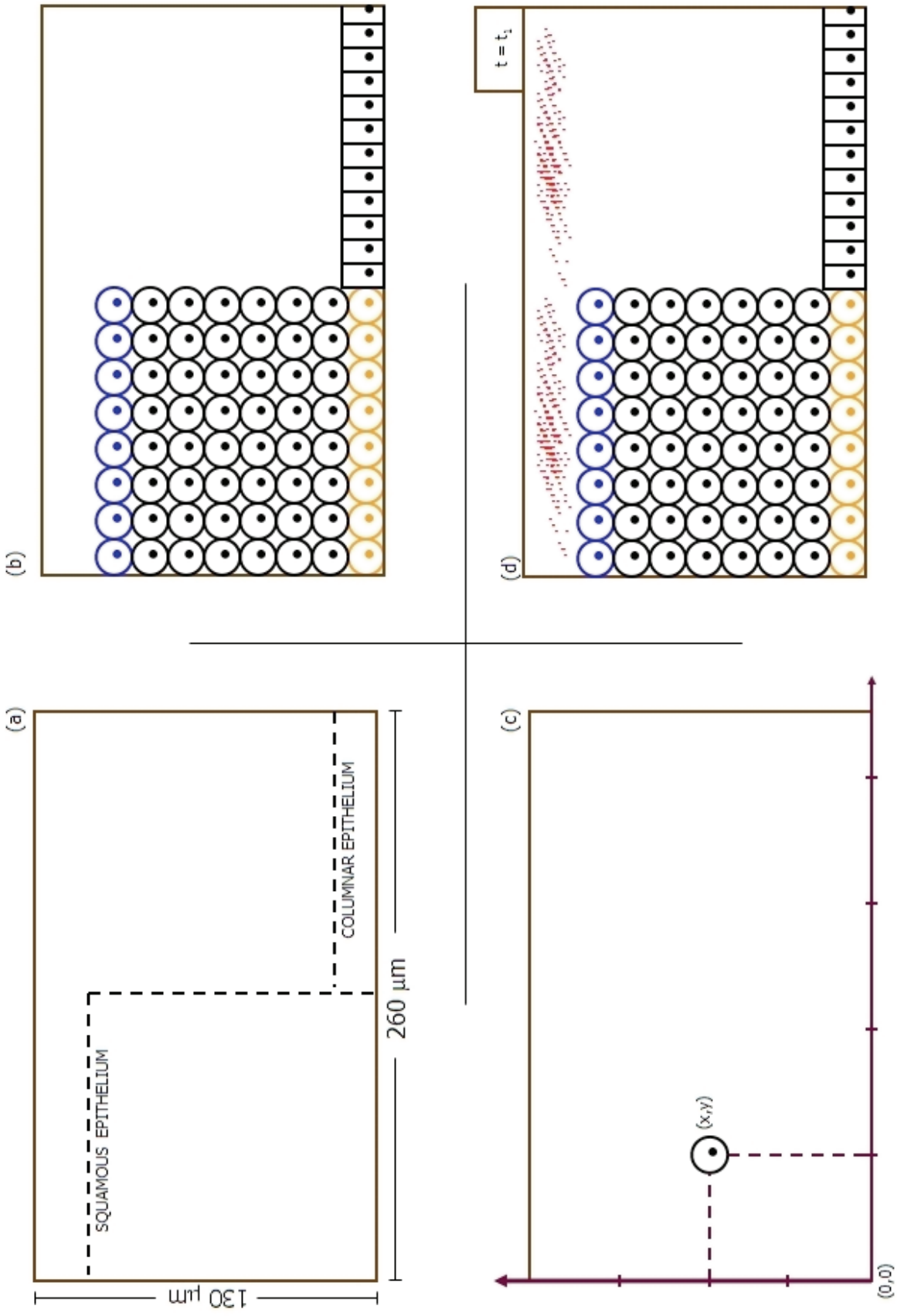

The first class of agents: the epithelial cells

The representation of a single cell implies the existence of a two-dimensional matrix in which it occupies a circular portion of the space (diameter = 115 pixels). Each pixel corresponds to a single position, defined by its Cartesian coordinates (x,y), in the matrix. Thus, the boundaries of each cell are defined: i) by the coordinates of each one of its four poles (northern, eastern, southern and western) and ii) by the coordinates of each one of the points that constitute its "membrane" (56 points for each fourth of circumference).

Thus, the information contained in each agent representing a cell is the following:

- "id": unique integer defining the identity of the cell.
- "type": binary number that shows whether it is a stem cell or not.
- "x": the x coordinate of the cell's center.
- "y": the y coordinate of the cell's center.
- "x_poles": array that contains the x coordinates of the cell's four poles (northern, eastern, southern and western).
- "y_poles": array that contains the y coordinates of the cell's four poles (northern, eastern, southern and western).
- "membrane": 4-row matrix that stocks the vertical coordinates of the points that constitute the cell's membrane. Each row corresponds to one fourth of the circumference.
- "birthday": integer that registers the instant of time when the cell was created.
- "mother_id" = integer that registers the identity of the stem cell from which it originated.
- "alive": binary number that shows whether the cell is alive or not.
- "multiplying": binary number that shows whether the cell is multiplying itself or not.
- "latency_start": integer that registers the instant of time when a stem cell enters a latency phase (i.e. it stops multiplying itself).
- "latency_end": integer that registers the instant of time when a stem cell exits a latency phase.

- "moving": binary number that shows whether the cell is moving or not.
- "receptors": 4-row matrix containing binary numbers that identify every single point on its membrane specifying if it constitutes a receptor for the viral particles, or not.
- "infected": binary number that shows whether the cell is infected or not.
- "viral_load": integer that accounts for the cell's viral load.
- "viral_id": array that contains the identity of the viral particles infecting the cell.

The second and third classes of agents: the viral particles and the immunoglobulins

Each one of these entities is represented by means of the smallest possible unit of size in our multi-agent system: one pixel, which corresponds to a single position (x,y) in the matrix representing the space. The information contained in each one of these entities is the following:

- "id": unique integer defining the identity of the viral particle or immunoglobulin.
- "x": the x coordinate corresponding to the viral particle's or the immunoglobulin's location.
- "y": the y coordinate corresponding to the viral particle's or the immunoglobulin's location.
- "birthday": integer that registers the instant of time when the viral particle or the immunoglobulin was created.
- "death_day": integer that registers the instant of time when the viral particle or the immunoglobulin will stop being active and disappear.
- "active": binary number that shows whether the viral particle or immunoglobulin is still active or not.
- "free_particle": binary number that shows whether the viral particle or immunoglobulin is free, or if, on the contrary, it is "embedded" in the tissue.
- "id_cell": integer that registers the identity of the cell that has been infected by the viral particle.
- "multiplying": binary number that shows whether the viral particle is multiplying itself or not.
- "latency_start": integer that registers the instant of time when a viral particle enters a latency phase (i.e. it stops multiplying itself).

- "latency_end": integer that registers the instant of time when a viral particle exits a latency phase.
- "diffusion": array of binary numbers (size=4) that serves to represent the direction of diffusion of a viral particle or immunoglobulin. If the array is full of zeros it means no movement at all; if there is a 1 in the first spot it means movement towards the north; if there is a 1 in the second spot it means movement towards the east, and so on.
- "closest_cell": integer that registers the identity of the cell to which the distance is the smallest.

The fourth class of agent: the space

Three different populations can be represented in our multi-agent system: i) a population of cells, arranged in such a way that they represent a self-renewing epithelial tissue, ii) a population of viral particles, possessing the capability of infecting the cells and of multiplying themselves, iii) a population of immunoglobulins, possessing the capability of neutralizing the viral particles. The fourth class of agent is the space and unlike the others it corresponds to a unique agent. The information contained in it is the following:

- "length": integer that corresponds to the number of pixels used to represent the epithelial tissue, horizontally. It is obtained from multiplying the number of stem cells included in the first layer by the number of pixels needed to represent a single cell horizontally (i.e. 115).
- "thickness": integer that corresponds to the number of pixels used to represent the epithelial tissue, vertically. It is obtained from multiplying the number of layers by the number of pixels needed to represent a single cell vertically (i.e. 115).
- "free_space": integer that corresponds to the number of pixels used to represent the free spaces over and under the epithelial tissue, vertically. The upper free space is used as the arrival zone for viral particles when simulating a viral exposure, while the lower has the exact same function for immunoglobulins.

- “first_matrix”: it is a two-dimensional [m x n] matrix, by default full of zeros in every position. Representing a single cell in it consists in writing the identity number of the cell in every spot occupied either by each one of the 4 poles or by each one of the 224 points of the membrane. The same matrix also serves to harbor the viral particles, each one of which is represented by its identity number, multiplied by -1.
- “second_matrix”: it is a two-dimensional matrix [m x n], by default full of zeros in every position. It is used for representing the immunoglobulins. This is made by writing, in a single (x,y) spot, the identity number of the immunoglobulin, multiplied by -1.
- “graphic_matrix”: it is a three-dimensional matrix [m x n x 3], by default full with the number 255 in every position. It is used for graphically representing the three kinds of agents (i.e. cells, viral particles and immunoglobulins). For doing so, the matrix stocks in every (x,y) spot an array (size=3) corresponding to the color of each type of agent in a RGB color code. Thus, an array {255, 255, 255} would represent a white-colored pixel representing the absence of any type of agent; an array {0, 0, 0} would represent a black-colored pixel belonging to a cell; an array {255, 0, 0} would represent a red-colored pixel, a viral particle; and, finally, an array {0, 0, 255} would represent a blue-colored pixel, an immunoglobulin.

An epithelial tissue is simulated by disposing a group of [p x q] cells in a rectangular arrangement. The first layer of such an arrangement is composed exclusively of stem cells, whereas the rest of the layers are composed exclusively of non stem cells. Each one of the agents type “cell” possesses the capacity to:

- Move vertically, heading north.
- If it is a stem cell, it has the capacity to replicate itself giving birth to a new “cell”.
- It has the capacity to sense its environment, i.e. if, when wanting to move, it lacks of space, it has the capacity to put the action off, to identify the encumbering agent and to transmit a “message” to the latter saying “could you please move on?”. In the same way, if it senses that it

has reached the upper limit of the tissue, it is programmed to disappear, releasing all the containing viral particles, if any, into the upper free space.

The agents representing the viral particles are created, into the upper free space, according to a "schedule" of exposures to the virus. Each one of these agents has the capacity to:

- Move vertically, heading south.
- Infect a stem cell in the basal layer. This occurs when the viral particle finds itself in a location that permits it to interact with its specific membrane receptor. The location of such receptors is an attribute of each stem cell.
- Reproduce itself once it has gained access into a stem cell.

The agents representing the immunoglobulins are created in the lower free space in such a way that they reproduce the anti-HPV IgG's serum titer. Each one of the agents type "immunoglobulin" has the capacity to:

- Move vertically, heading north.
- Neutralize the viral particles they encounter.

When conducting a simulation, it is first necessary to define the size and the architecture of the tissue segment that will be simulated. This implies to determine the number of stem cells to be set in the basal layer and to determine whether it will represent a homogeneous stratified squamous kind of epithelium, in which all the columns have the same number of cells, or if it will represent an epithelium containing a squamo-columnar junction, in which the number of cells per column may vary.

During the simulation, the virtual stem cells will continuously multiply themselves as a means for assuring the natural cell turnover on the surface. Additionally, they have the capability of pushing cells in upper layers to obtain the space they need for successfully dividing. The signal that induces

cell movement is transmitted vertically until it reaches the superficial layer, inducing cell death and desquamation.

Each simulation is visually followed with the aid of a video that registers both the spatial and the temporal evolution of the infection in the virtual tissue. Additionally, several variables, such as the viral load, can be followed up for later analysis.

In summary, the input of the model is defined by:

- The total duration of the simulation.
- The number of stem cells in the first layer.
- The number of layers.
- "The viral exposure schedule" (number of exposures to the virus, instant of time, viral load, etc).

The main output of the model is defined by:

- The temporal evolution of the viral load (per cell / per zone / total viral load).

SECTION V

IN-SILICO SIMULATIONS –

THE PRODUCT

CHAPTER 12

IN-SILICO SIMULATIONS OF THE IMMUNE RESPONSES INDUCED BY THE INTRAMUSCULAR IMMUNIZATION WITH AN HPV VACCINE

In this chapter we explain how the mathematical model, extensively presented in chapter 9, was exploited. First, we present the results corresponding to the calibration process, then we present the results of the model being confronted to some "validating" data, and by the end we present some predictions.

Calibrating the model

The parameter optimization process (or model calibration) was conducted by iteratively comparing the model's output against the clinically observed evolution of the serum immunoglobulin titers following intramuscular vaccination with Gardasil®. In figures 3, 4 and 5, the red dots represent the mean immunoglobulin titers induced by a 3-dose immunization schedule, at t = 0, t = 60 and t = 180 days (graphically represented by the red arrows). Three different sets of parameters (A, B and C) were retained after having executed the parameter optimization process several times. Each set of parameters represents a different way in which the mathematical model "adapts" itself to the biological phenomenon described by the red dots. You may think of it as a data-based training process. Three different criteria were defined to assess the outcome of such process: i) the way the model reproduces the relatively high values of the second and the fourth red points (i.e. the short-term intense reactions following the administration of the second and the third doses); ii) the way the model reproduces the values of the third and the fifth red points, which represent the relatively rapid waning of the just-mentioned intense responses; and iii) the way the model reproduces the residual long-term plateau. While the three sets of parameters (A, B and C) serve to satisfy the first criterion, it is worth to note that they do it differently, predicting different values for the immunoglobulin titer peaks. Sets of parameters A and C, which predict the titer peaks as being

considerable higher than those observed thirty days after the second (and after the third) dose administration are incapable of satisfying the second criterion. The third criterion, on the other hand, is invariably satisfied by the three sets of parameters.

First round of validation

Our mathematical model, independently fed with sets of parameters A, B and C, was then asked to predict the outcome of administering a late fourth-dose (at t = 60 months), which is represented by the green arrow in figures 6, 7 and 8. The clinically observed value (the green dot), which was drawn from the same clinical study used for the model-calibration stage, can be directly compared to the in-silico predicted value (blue line). In the light of these results, we decided to discard parameter sets A and C, to continue working only with parameter set B.

Quantitative characterization of the predicted immunogenicity

We devised a simple method for quantitatively characterizing the serum immunoglobulin titer curve. Such procedure consists of four steps, which can be better understood if you refer to figure 9. i) First, all the critical points (i.e. peaks, troughs, points of abrupt slope change, etc.) are identified and their respective coordinates stocked; ii) Then, the time axis is split into two zones: an initial zone, A, in which a double bell-shaped behavior is observed, and a posterior zone, B, in which a plateau predominates; iii) For zone A, the area under the curve is calculated and then normalized (i.e. the value obtained for the 0-60-180-day protocol is considered to be 1.0); iv) For zone B, the mean antibody titer is calculated and then normalized (i.e. the value obtained for the 0-60-180-day protocol is considered to be 1.0).

Second round of validation

We decided to investigate, with the aid of our model, the effect of administering the second dose (the one usually administered at t = 60 days) sooner or later. We did so by making vary the

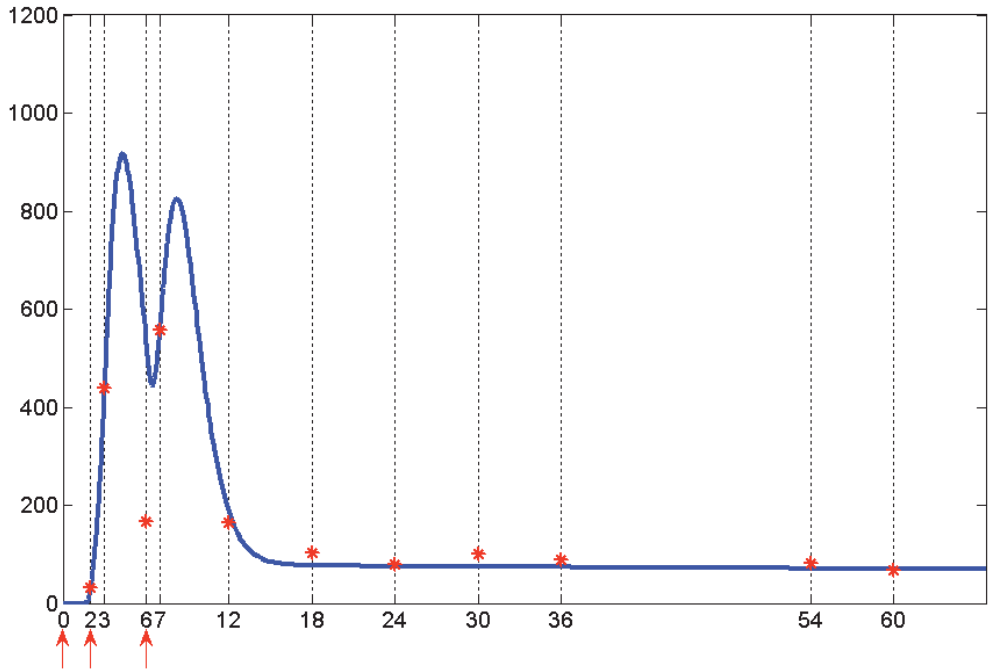

Figure 3. In-silico modeled (blue line) versus observed (red dots) immunogenicity of the quadrivalent HPV vaccine. **x-axis**: time, in months. **y-axis**: serum HPV-specific IgG titers, in milli-Merck units per mL. This curve was obtained during the model **calibration** process by using **set of parameters A**. (The red arrows represent the simulated vaccination schedule).

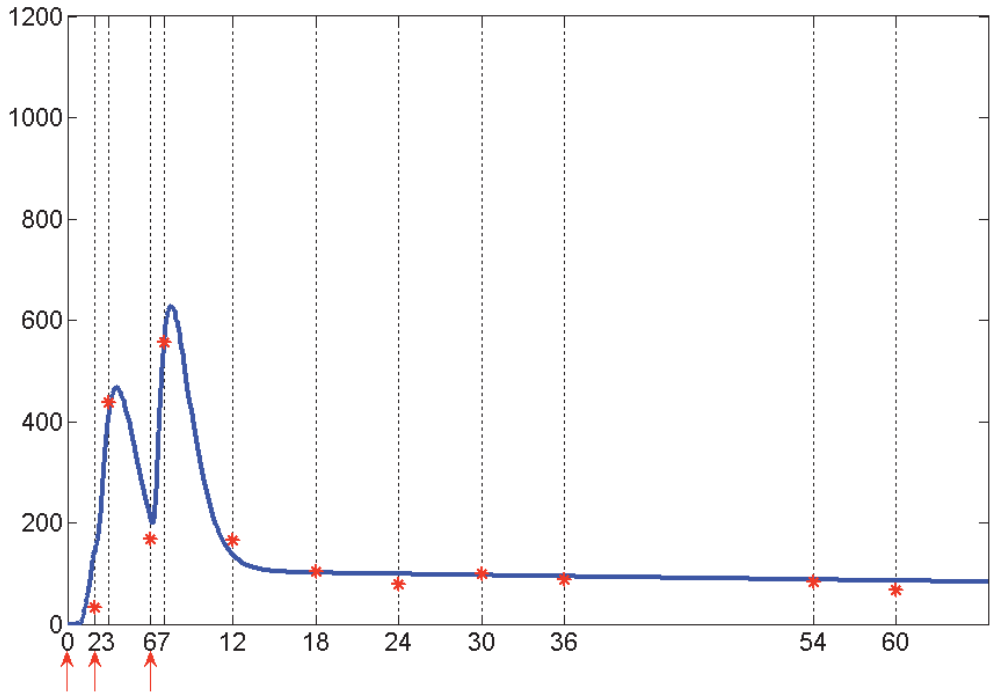

Figure 4. In-silico modeled (blue line) versus observed (red dots) immunogenicity of the quadrivalent HPV vaccine. **x-axis**: time, in months. **y-axis**: serum HPV-specific IgG titers, in milli-Merck units per mL. This curve was obtained during the model **calibration** process by using **set of parameters B**. (The red arrows represent the simulated vaccination schedule).

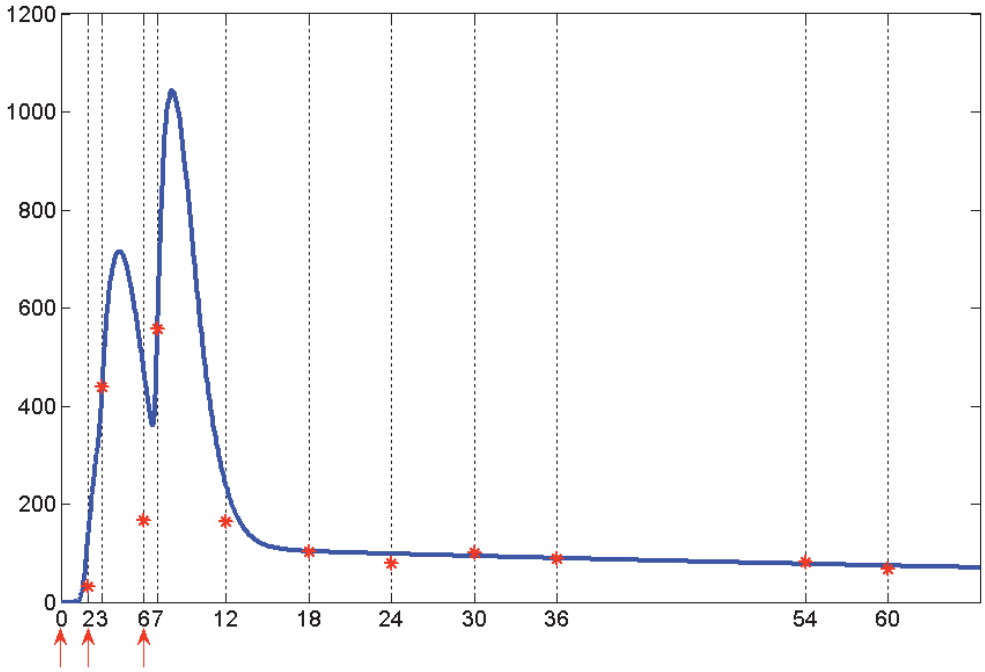

Figure 5. In-silico modeled (blue line) versus observed (red dots) immunogenicity of the quadrivalent HPV vaccine. **x-axis**: time, in months. **y-axis**: serum HPV-specific IgG titers, in milli-Merck units per mL. This curve was obtained during the model **calibration** process by using **set of parameters C**. (The red arrows represent the simulated vaccination schedule).

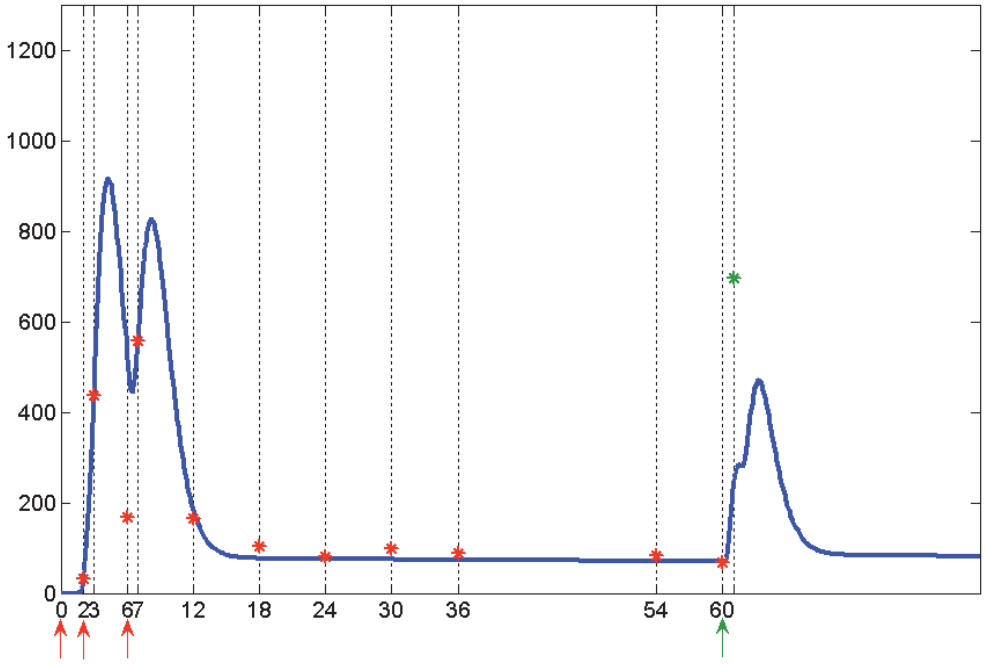

Figure 6. In-silico modeled (blue line) versus observed (green dot) immunogenic response following the late administration of a fourth dose (green arrow) of the quadrivalent HPV vaccine. **x-axis**: time in months. **y-axis**: serum HPV-specific IgG titers, in milli-Merck units per mL. This curve was obtained during the model **validation** process by using set of **parameters A**.

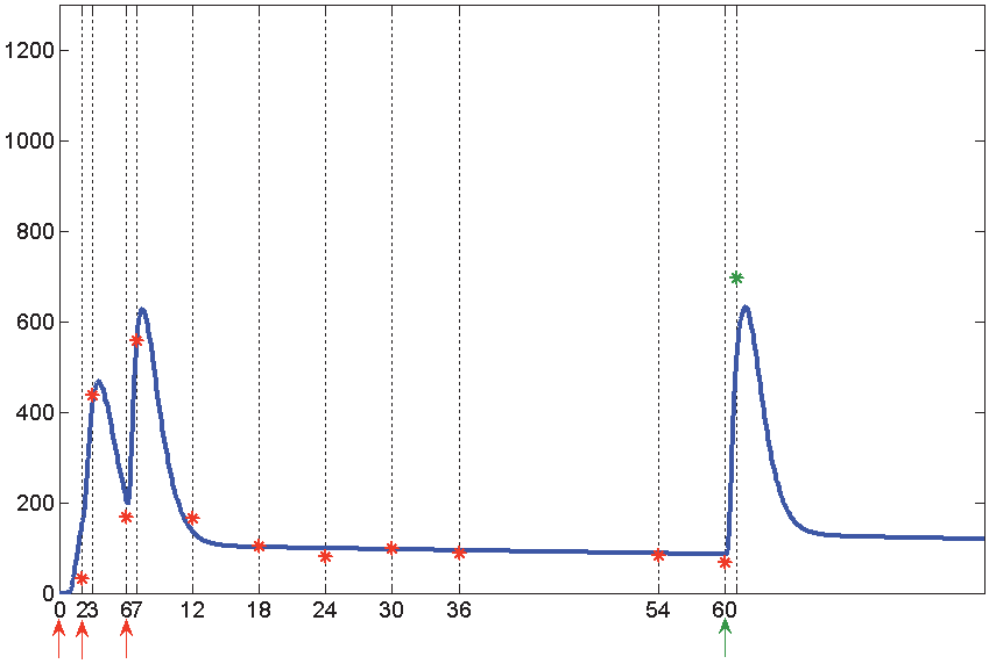

Figure 7. In-silico modeled (blue line) versus observed (green dot) immunogenic response following the late administration of a fourth dose (green arrow) of the quadrivalent HPV vaccine. **x-axis**: time in months. **y-axis**: serum HPV-specific IgG titers, in milli-Merck units per mL. This curve was obtained during the model **validation** process by using set of **parameters B**.

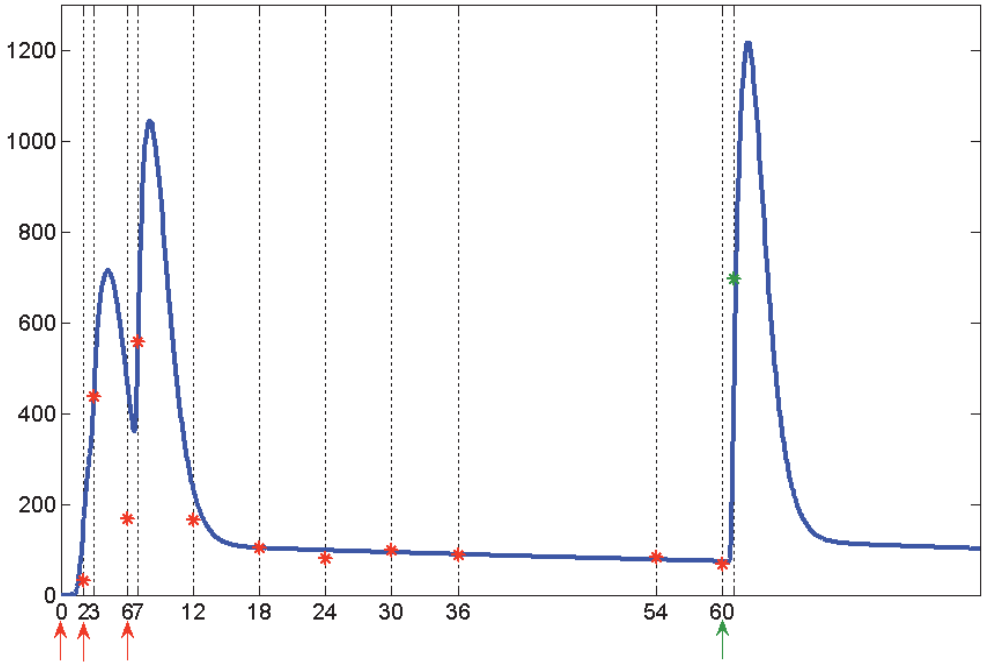

Figure 8. In-silico modeled (blue line) versus observed (green dot) immunogenic response following the late administration of a fourth dose (green arrow) of the quadrivalent HPV vaccine. **x-axis**: time in months. **y-axis**: serum HPV-specific IgG titers, in milli-Merck units per mL. This curve was obtained during the model **validation** process by using set of **parameters C**.

vaccination protocol (0-λ-180 days), by obtaining for each hypothetical protocol an in-silico prediction of the seroconversion curve, by quantifying both the area under the curve (for the zone A) and the plateau's mean value (for the zone B), and by normalizing them with respect to the 0-60-180 protocol. Results are presented in figures 10 and 11. Additionally, a direct comparison between two protocols of interest is presented in figure 12.

Predictions

JORRP is a disease that seems to have a rather well-defined lifespan: while it is commonly diagnosed at around the age of five, adolescence seems to be the most favorable period of life for spontaneous remission to occur. That is why, in the paragraphs below, we will refer to simulations made over a 10-year period of time, in which different strategies for boosting the anti-HPV humoral response were tested. In fact, by following the reasoning behind the therapeutic hypothesis presented in chapter 1, the idea would be to consider a 5-year-old-or-so infant, who has just been diagnosed with JORRP, to vaccinate him/her with Gardasil® following the traditional 0-60-180-day schedule, and then to boost the humoral response as frequently as needed to avoid surgery, until adolescence comes and the intensity of the disease spontaneously fades out. The biggest obstacle towards the concretion of this idea resides in the fact that the serum immunoglobulin titer threshold from which the just-described clinical benefit would be obtained is completely unknown, which is not surprising at all if you consider the fact that such a threshold is not even known for the much-more-studied case of Gardasil® (and CervarixTM) being prescribed to prevent cervical dysplasia[202]. Our multi-agent-system model, which deals with the natural history of JORRP, proposes that for maximizing the likelihood of a Gardasil®-associated clinical benefit in patients with JORRP the serum immunoglobulin titer would have to remain on a level of 200 milli-Merck units par milliliter of blood, or above (see chapter 13). If a classic (i.e. a 0-60-180-day) vaccination schedule were prescribed alone, the patient would only benefit from it, according to what the model predicts, 6% of the time over the 10-year span (figure 13).

Figures 14 and 15 show what the model predicts for two different 3-dose boosting schedules arbitrarly defined: with injections every 6 months and every 24 months after the completion of the 0-2-6-month initial vaccination schedule. In order to predict the optimal way of boosting the immune response so that the amount of time passed over the "therapeutic threshold" results maximized (with the minimum possible quantity of boosting doses), we employed our genetic-algorithm-based optimization tool. The most suitable boosting schedule is presented in figure 16, for which an average JORRP patient would remain over the therapeutic threshold 98% of the 10-year period of time, as a result of prescribing of 6 boosting doses (represented by the red arrows).

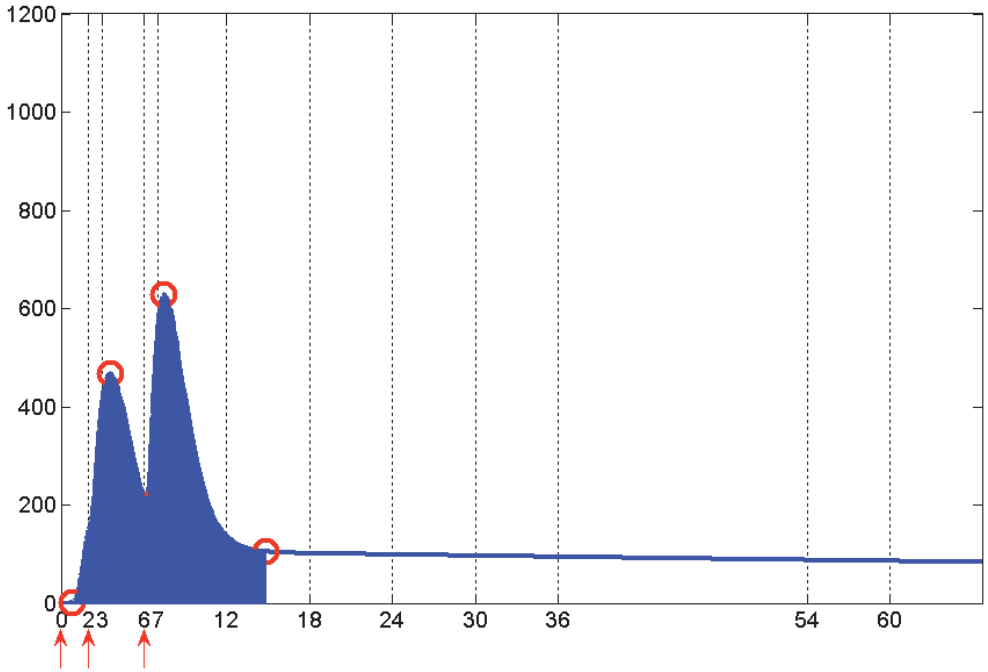

Figure 9. Schematic representation of the procedure used for quantitatively characterizing the modeled immunogenicity induced by the quadrivalent HPV vaccine. **x axis**: time, in months. **y axis**: serum HPV-specific IgG titers, in milli-Merck units per mL. Zone A (the blue shaded area) is defined as the double bell-shaped portion in which the highest IgG titers are observed. Zone B is defined as the remaining portion in which a less-intense plateau-like behavior takes place. The quantitative characterization consists in calculating the area under the curve for zone A and in calculating the mean IgG titer for zone B.

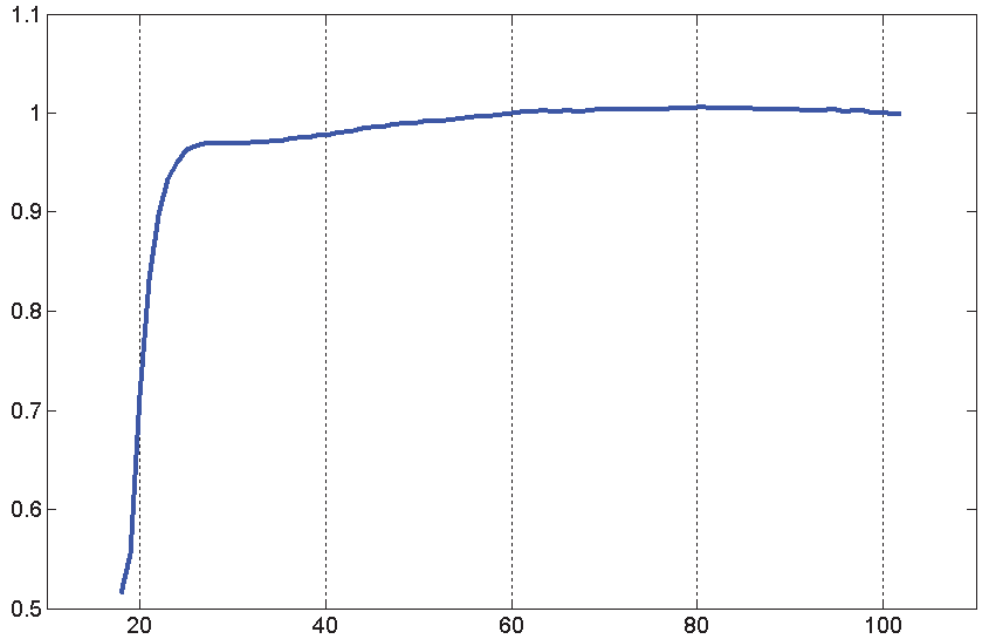

Figure 10. In-silico modeled effect of making vary the delay between the first and the second doses on the immunogenicity induced by the quadrivalent HPV vaccine. **x-axis**: time in days (λ) between the first and the second dose administration, in a 0-λ-180 vaccination schedule. **y-axis**: normalized (with respect to the 0-60-180 vaccination schedule) area under the curve for **zone A**. This curve was obtained by using set of parameters B.

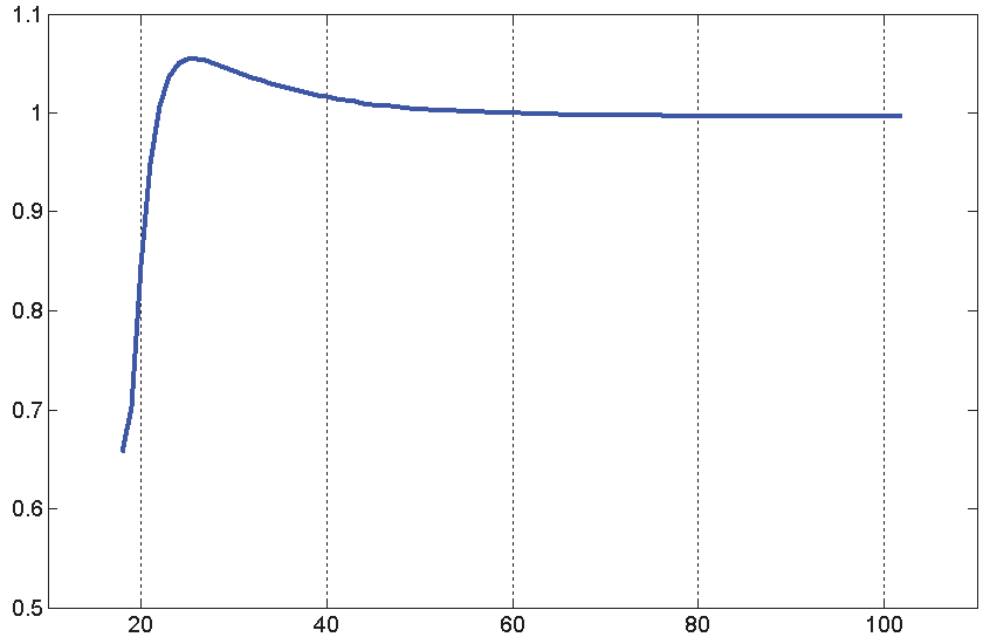

Figure 11. In-silico modeled effect of making vary the delay between the first and the second doses on the immunogenicity induced by the quadrivalent HPV vaccine. **x-axis**: time in days (λ) between the first and the second dose administration, in a 0-λ-180 vaccination schedule. **y-axis**: normalized (with respect to the 0-60-180 vaccination schedule) mean IgG titer for **zone B**. This curve was obtained by using set of parameters B.

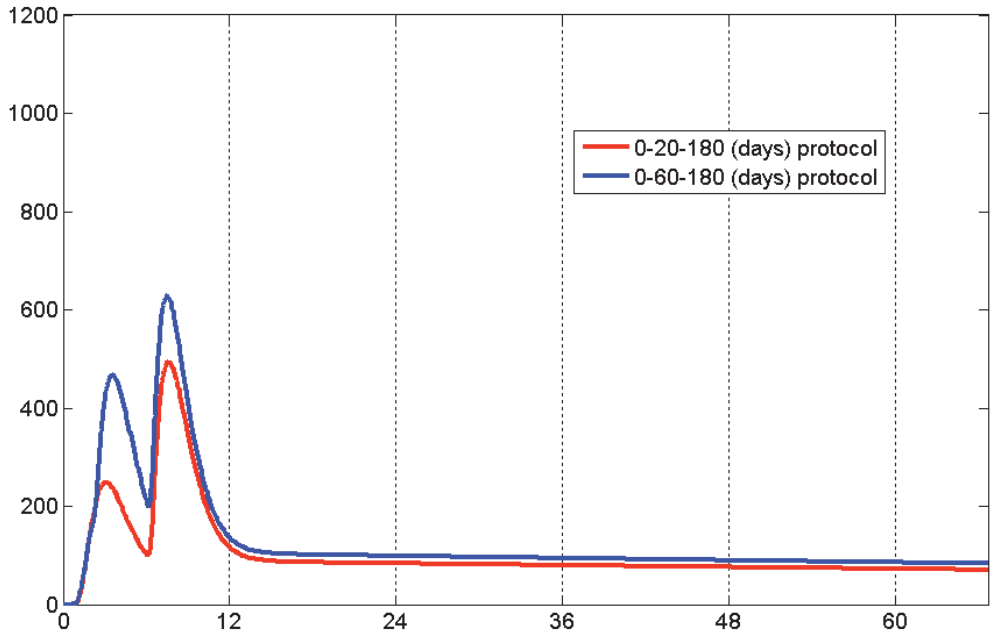

Figure 12. In-silico comparison of two vaccination schedules. **x-axis**: time, in months. **y-axis:** serum HPV-specific IgG titers, in milli-Merck units per mL. Both curves were obtained by using set of pamaters B.

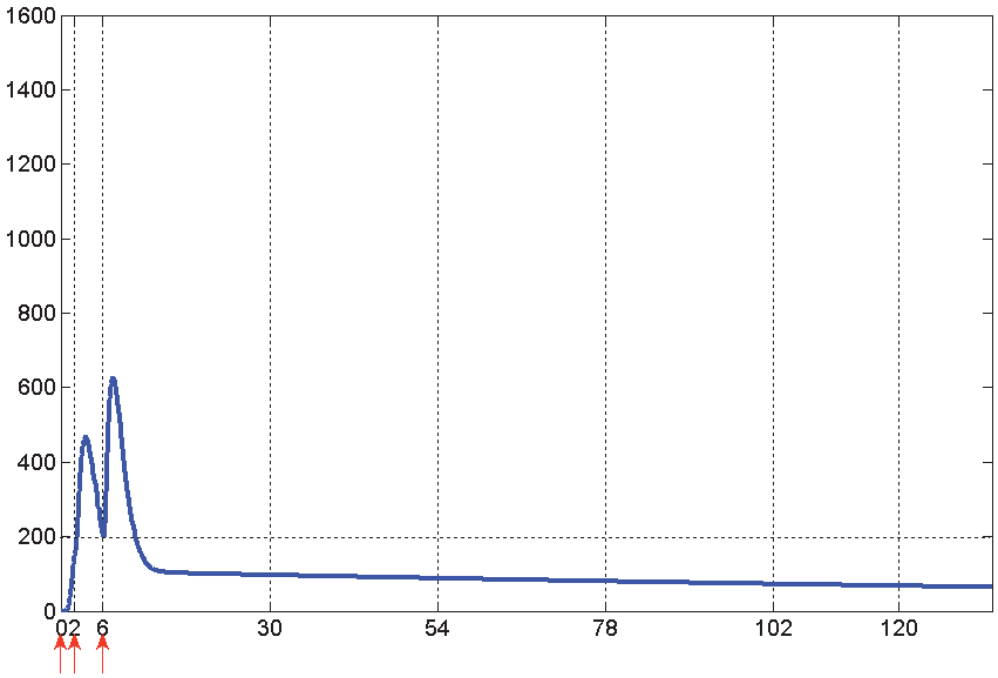

Figure 13. In-silico prediction of the immunoglobulin titer behavior, over a ten-year period of time, following vaccination with the HPV quadrivalent vaccine. **x-axis**: time, in months. **y-axis**: serum HPV-specific IgG titers, in milli-Merck units per mL. This curve was obtained by using set of parameters B. (The red arrows represent the simulated vaccination schedule).

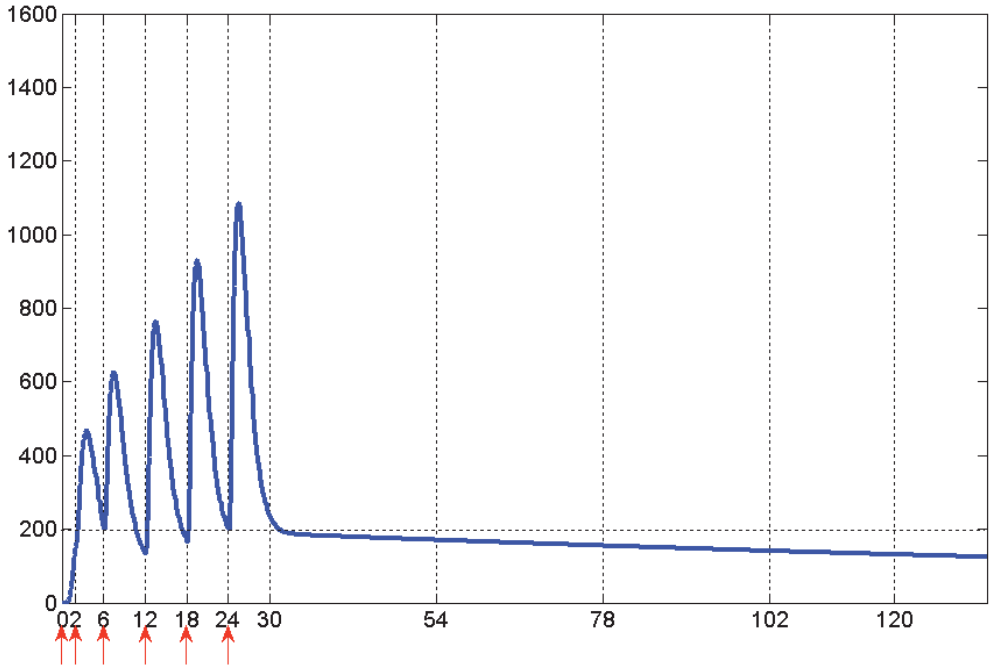

Figure 14. In-silico prediction of the immunoglobulin titer behavior, over a ten-year period of time, following vaccination and consecutive boosting with the HPV quadrivalent vaccine. **x-axis**: time, in months. **y-axis**: serum HPV-specific IgG titers, in milli-Merck units per mL. This curve was obtained by using set of parameters B. (The red arrows represent the simulated vaccination / boosting schedule).

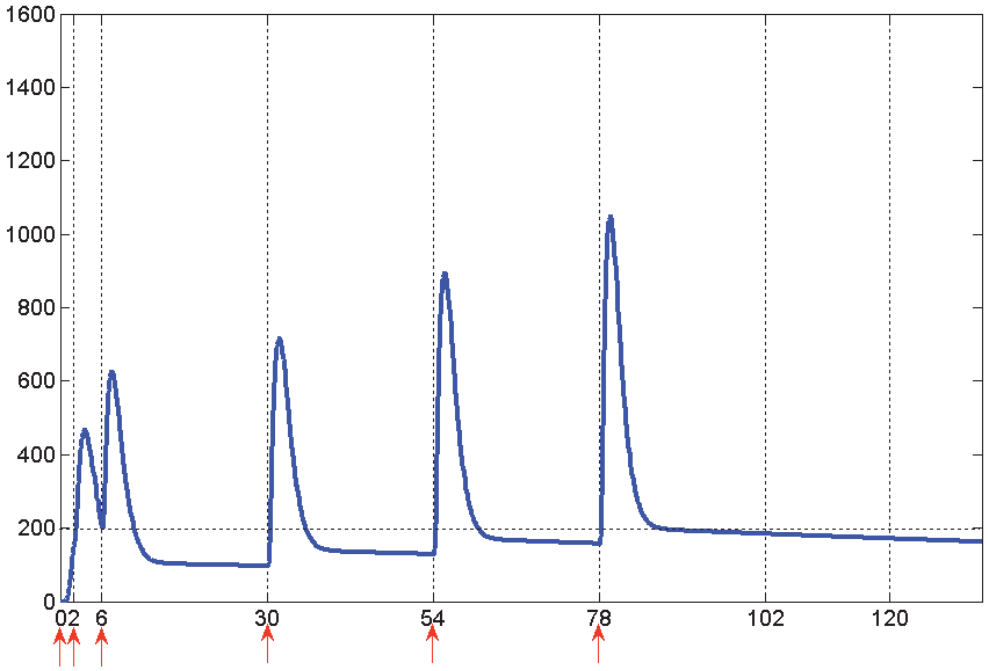

Figure 15. In-silico prediction of the immunoglobulin titer behavior, over a ten-year period of time, following vaccination and posterior boosting with the HPV quadrivalent vaccine. **x-axis**: time, in months. **y-axis**: serum HPV-specific IgG titers, in milli-Merck units per mL. This curve was obtained by using set of parameters B. (The red arrows represent the simulated vaccination / boosting schedule).

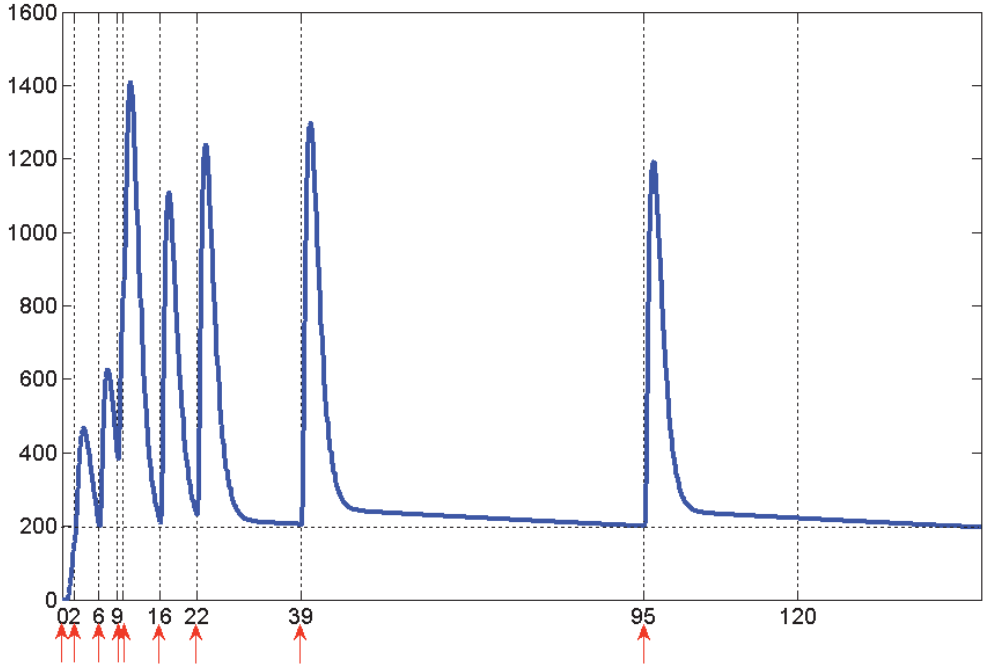

Figure 16. In-silico prediction of the boosting schedule that would be necessary for keeping, as long as possible within a 10-year period of time and through the administration of the smallest possible number of doses, the immunoglobulin titer above a hypothetical titer of 200 mMU/mL. **x-axis**: time, in months. **y-axis**: serum HPV-specific IgG titers, in milli-Merck units per mL. This curve was obtained by using set of parameters B. (The red arrows represent the simulated vaccination / boosting schedule).

CHAPTER 13

IN-SILICO SIMULATIONS OF THE HOST-PATHOGEN INTERACTIONS FOLLOWING A MUCOSAL HPV INFECTION

Here we present the simulations that we conducted by using the multi-agent system that we entirely developed in our laboratory (as explained in chapter 11). The first operation consisted in calibrating the model, which means finding the most appropriate values for the parameters it contains.

The model's parameters are:

- Parameter 1: Latency time needed for viral particles to start a multiplication cycle again.
- Parameter 2: Standard deviation for parameter 1.
- Parameter 3: Viral multiplication capacity.
- Parameter 4: Standard deviation for parameter 3.
- Parameter 5: Cellular multiplication capacity.
- Parameter 6: Latency time needed for cells to start a multiplication cycle again.
- Parameter 7: Standard deviation for parameter 6.
- Parameter 8: Free viral particles' life expectancy.
- Parameter 9: Standard deviation for parameter 8.
- Parameter 10: Free immunoglobulins' life expectancy.
- Parameter 11: Standard deviation for parameter 10.
- Parameter 12: Neutralization capacity of the HPV-L1-specific IgG immunoglobulins.
- Parameter 13: HPV-specific receptor's density on the cellular membrane.
- Parameter 14: Probability that an encounter between a viral particle and its specific receptor on the cell membrane leads to the cell being infected.
- Parameter 15: Immunoglobulins' extravasation capacity
- Parameter 16: Viral particles' capacity to penetrate into the tissue.

- Parameter 17: Immunoglobulins' capacity to transude through the tissue.
- Parameter 18: Viral particles' capacity to cross the tissue.

Three independent rounds of calibration were necessary that can be summarized as follows:

First round of calibration

Entities concerned: The anti-HPV IgG immunoglobulins.

Phenomenon concerned: Extravasation and transudation through the epithelium.

Parameters concerned: 10, 11, 15, 17.

Data used as target during the calibration process: A study[203] was conducted in human beings in which the ratio between the serum and the OMT (i.e. the oral mucosal transudate) IgG immunoglobulin titers was experimentally determined following the administration of the quadrivalent HPV vaccine. It was found to be: $\phi \approx 5.4$.

Description of the calibration process: Let us remember that the model consists of three compartments: i) the "upper free space" which represents the outer mucus-covered surface of the epithelium, ii) the "middle zone" which represents the tissue itself, and iii) the "lower free space" which represents the region where the micro-vessels provide the epithelial cells with blood. This first round of calibration consisted in iteratively: i) reproducing in the lower compartment the dynamics of the serum anti-HPV IgG immunoglobulin titer following vaccination with the quadrivalent HPV vaccine; ii) in determining the resulting titer on the other side of the epithelium; iii) in calculating the in-silico ratio; and iv) in adjusting the four parameters that are concerned in such a way that after each iteration the in-silico ratio gets closer to the published one.

Results presented in figures: 17, 18, 19 and 20.

Second round of calibration

Entities concerned: The epithelial cells.

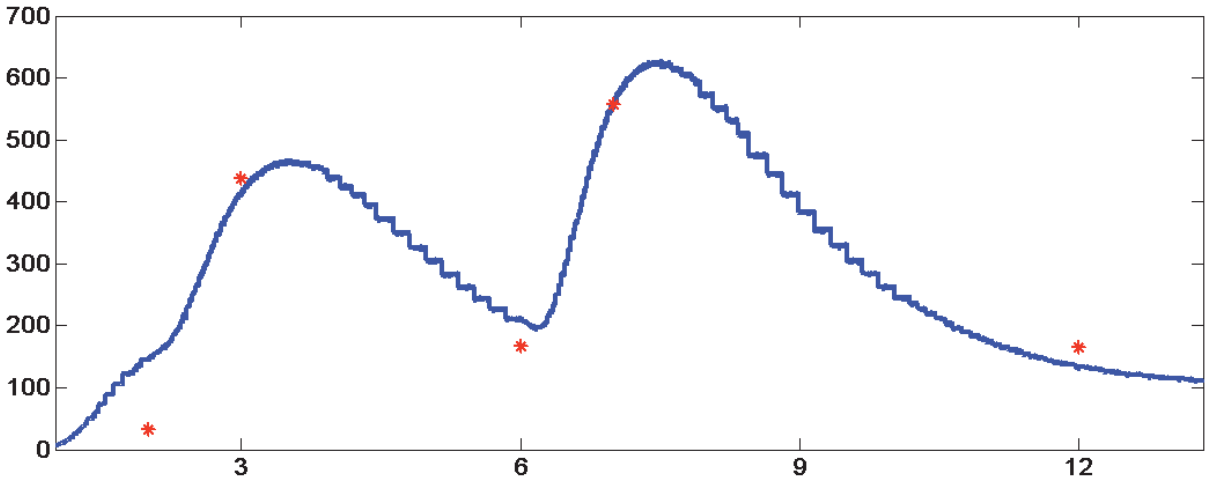

Figure 17. In-silico reproduction (through a multi-agent system approach) of the serum anti-HPV immunoglobulin titers following vaccination with the quadrivalent HPV vaccine (at months 0, 2 and 6). **x-axis**: time, in months, over which the simulation was conducted. **y-axis**: serum HPV-specific IgG titers, in milli-Merck units per mL. The red dots correspond to the observed values as reported in the literature. The discrete values obtained with the mathematical model (blue line in figure 4) were used to feed a procedure devised for creating or deleting agents of the immunoglobulin kind. The blue line in this figure represents the anti-HPV immunoglobulin titer as simulated in the lower free-space compartment, the one used to represent a micro-vessel adjacent to the epithelial tissue. No agents representing viral particles were included in this simulation. This simuation corresponds to the model's **first round of calibration**.

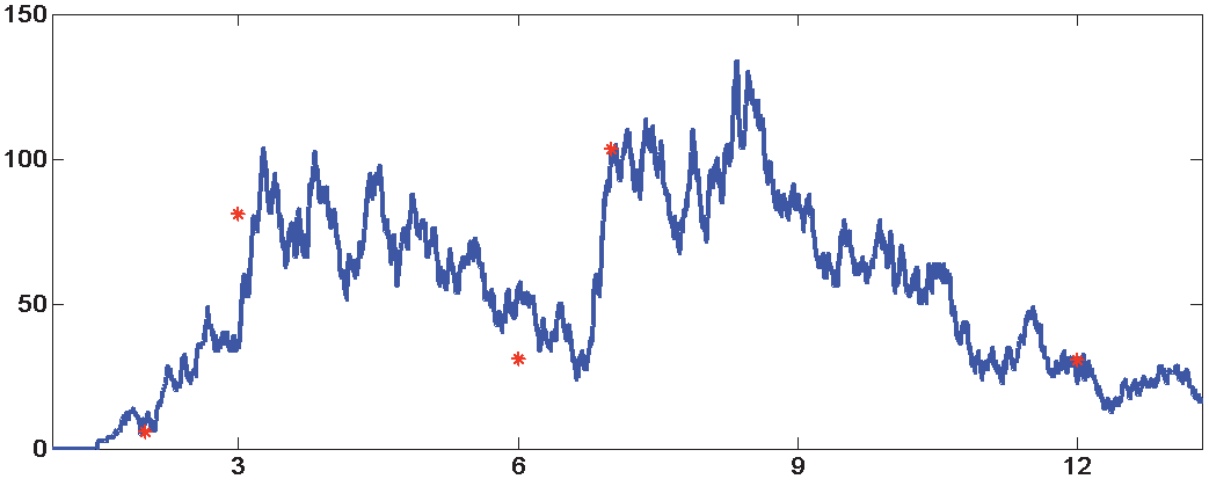

Figure 18. In-silico simulation (through a multi-agent system approach) of the anti-HPV IgG immunoglobulin titers in the upper respiratory tract lumen following intramuscular vaccination (at months 0, 2 and 6) with the quadrivalent HPV vaccine. **x-axis**: time, in months, over which the simulation was conducted. **y-axis**: HPV-specific IgG titers, in milli-Merck units per mL. The red dots correspond to the literature-based estimated titers. Such estimation was conducted as follows: each one of the reported mean values for the serum titers (the red dots in figures 4 and 17) was divided by a factor ($\phi = 5.4$) drawn from the literature[203]. In that study, the authors compared serum versus OMT (oral mucosal transudate) titers following vaccination with the quadrivalent HPV vaccine. No agents representing viral particles were included in this simulation. At t=0 a set of agents representing a 4 x 4 epithelial tissue was set up before letting it evolve freely. Simultaneously, the serum anti-HPV IgG titer was reproduced in the lower free space, as for figure 17. All over the simulation the anti-HPV IgG titer in the upper free space was tracked to yield the blue line in this figure. This simuation corresponds to the model's **first round of calibration**.

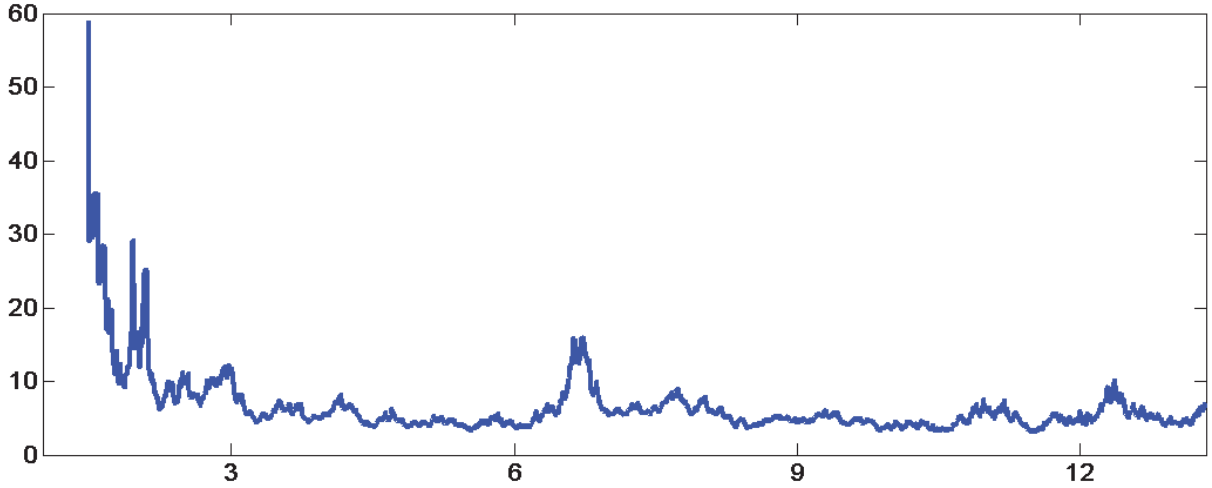

Figure 19. In-silico simulation (through a multi-agent system approach) of the quantitative relationship between the serum and the upper respiratory tract lumen IgG titers following vaccination (at months 0, 2 and 6) with the quadrivalent HPV vaccine. **x-axis**: time, in months, over which the simulation was conducted. **y-axis**: ratio between the serum and the upper respiratory tract lumen IgG titers. This curve was obtained by constantly dividing the results shown in figure 17 by the results shown in figure 18. This simuation corresponds to the model's **first round of calibration**.

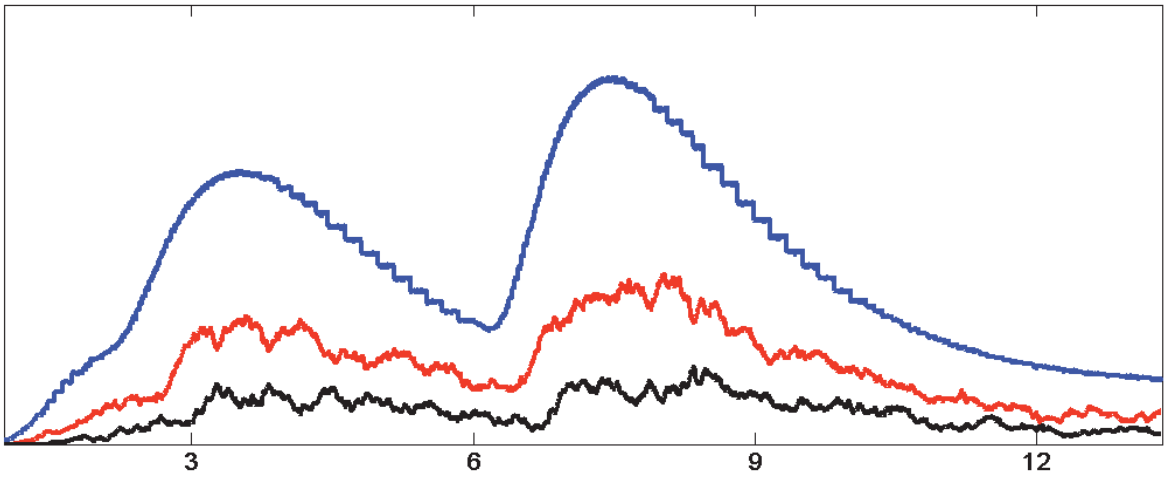

Figure 20. In-silico qualitative comparison (through a multi-agent system approach) of the anti-HPV IgG immunoglobulin titers in blood (blue line), in the mucous epithelial tissue (red line) and in the outer epithelial lumen (black line). **x-axis**: time, in months, over which the simulation was conducted. **y-axis**: relative IgG immunoglobulin titers. This simuation corresponds to the model's **first round of calibration**.

Phenomenon concerned: Stem cells' life cycle and tissular turnover.

Parameters concerned: 5, 6, 7.

Data used as target during the calibration process: In the literature, it is generally accepted that the average time needed for basal cells to cross the epithelium while differentiating to finally reach the outermost layer and die is ≈ 3 weeks[204].

Description of the calibration process: For this phase of the calibration process only agents representing epithelial cells were considered. For each daughter cell, the life span was calculated and the average time over the whole population was tracked and recorded. The concerned parameters were iteratively adjusted so as to reproduce the targeted value.

Results presented in figure: 21.

Third round of calibration

Entities concerned: The viral particles.

Phenomenon concerned: HPV's life cycle.

Parameters concerned: 1, 2, 3, 4, 8, 9, 13, 14, 16, 18.

Data used as target during the calibration process: This was the most delicate part of the calibration process because it was the one that implicated the most parameters and the one for which no relevant data could be found in the literature. For not having to use arbitrary values we used what we call "a rule", rather than data, as the optimization-process target. A rule is a principle to which the in-silico model should freely comply as a sign of biological relevance. In this particular case, we decided to exploit the already-discussed fact the HPV may infect different kinds of epithelia but only succeeds in staying long enough (chronic infection) so as to induce disease in the so-called transformation zones.

Description of the calibration process: For each set of parameters tested, two simulations were conducted in parallel: the first one representing a homogeneous multi-layered squamous epithelium (that we call the square-like architecture), the second one representing a heterogeneous epithelium

in which the junction with a monolayer columnar kind of tissue occurs (that we call the L-like architecture). From the infectious point of view, three different outcomes were possible: i) in both kinds of architectures the virus succeeded in establishing a chronic infection, which was considered to be incompatible with the previously defined rule; ii) in both kinds of architectures the virus failed to establish a chronic infection, which was again considered to be incompatible with the rule; and iii) the virus failed to do so in the former architecture but succeeded in the latter, which is compatible with the rule and therefore leads to the set of parameters not being discarded. Fortunately, the sets of parameters for which the outcome was the third one were rather scarce.

Results presented in figures: 22, 23.

Predictions

Once the model calibrated, we decided to use it in order to simulate what we call the "in-silico neutralization assays", in which the three kinds of agents (those used for representing the epithelial cells, those used for representing the viral particles and those used for representing the anti-HPV immunoglobulins) were allowed, for the very first time, to interact simultaneously. For doing so, we reproduced the simulation conducted during the third round of calibration, more precisely the one in which the squamociliary junction is simulated (through what we call the L-like architecture). Then a series of simulations were conducted in which the serum anti-HPV immunoglobulin titer was progressively increased with the aim of establishing the neutralization threshold (figures 24, 25, 26 and 27). The model suggests that a serum immunoglobulin titer between 100 and 200 mMU/mL would be necessary for preventing the virus from establishing chronic infections in healthy squamociliary junction zones and therefore for preventing JORRP to expand in the respiratory tract. In order to investigate what vaccination/booster schedule would permit to obtain such a therapeutic effect we decided to use the highest value in this immunoglobulin-titer range, as can be seen in figures 13, 14, 15 and 16.

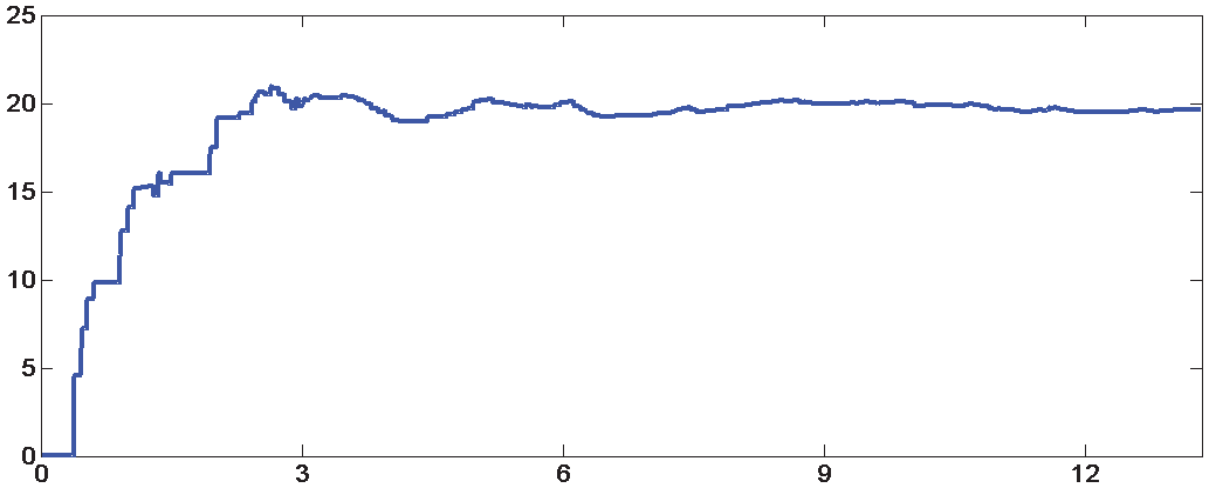

Figure 21. In-silico simulated dynamics of the epithelial-cell turnover process through a multi-agent system approach. **x-axis**: time, in months, over which the simulation was conducted. **y-axis**: time needed for the basal epithelial cells to reach the outermost layer. This simulation was conducted in complete absence of any agent representing viral particles or immunoglogulins. The agents representing the epithelial cells were initially disposed as follows: 4 layers, each one made up of 4 virtual cells, were set up in a square arrangement at t=0. Only the innermost virtual cells were authorized to multiply themselves pushing the rest of cells up. The system was then let to evolve freely. The time required for renewing the virtual tissue is continuously tracked. This simulation corresponds to the model's **second round of calibration**.

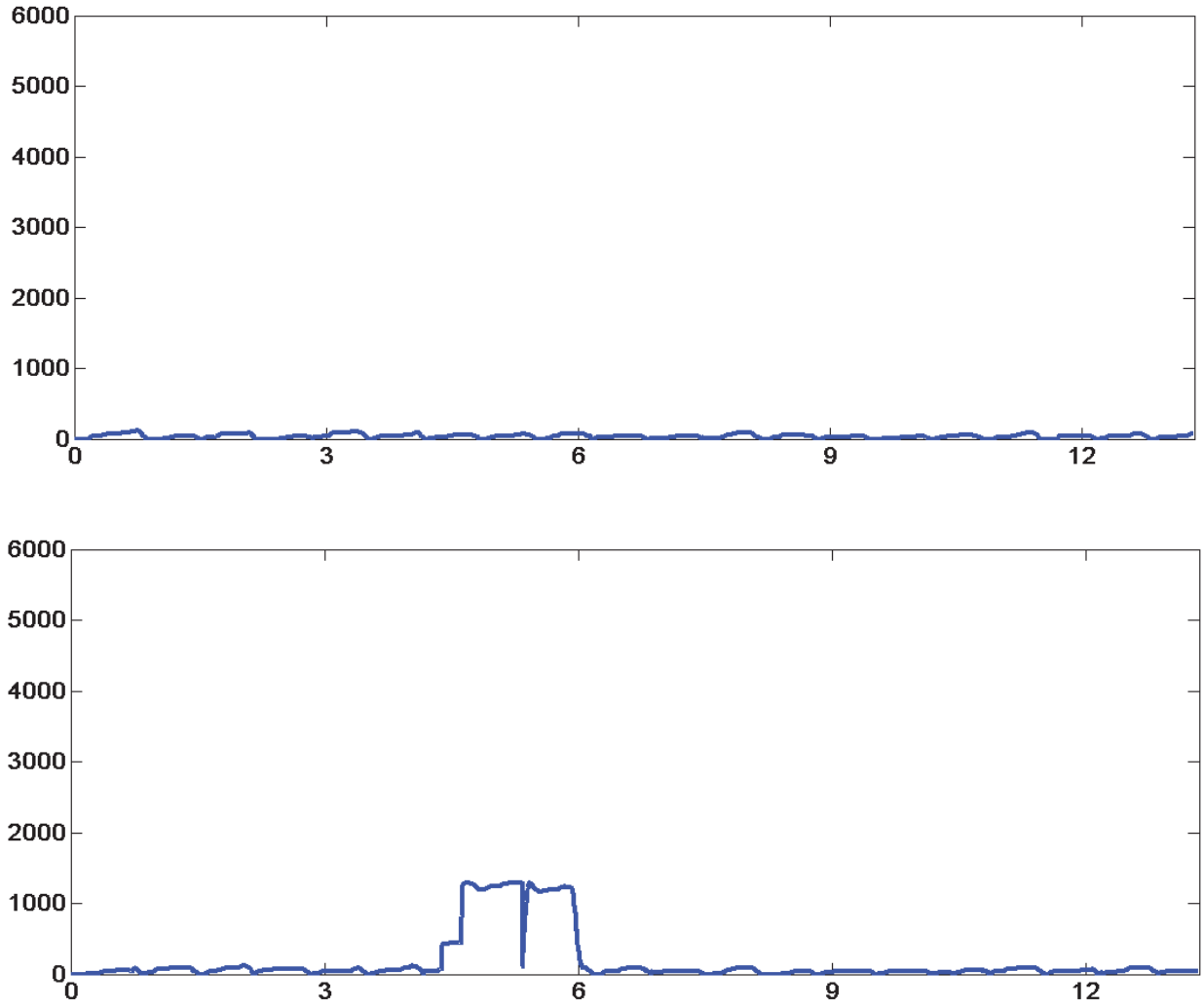

Figure 22. In silico simulation (through a multi-agent system approach) of the viral load evolution in an epithelial tissue sample. **x-axis**: time, in months, over which the simulation was conducted. **y-axis**: viral load, i.e. the number of particles infecting the tissue sample at any given instant of time. A set of virtual epithelial cells was initially arranged in a 4 x 4 **square-like distribution** (i.e. 4 cells in the basal layer bearing three other layers in such a way that a perfect 4-row 4-column structure is obtained). The virtual cells that constitute the innermost layer possess the capacity of multiplying themselves in such a way that the epithelial turnover complies to what was defined in the second round of calibration. No agents representing anti-HPV IgG immunoglobulins were included in this simulation. The tissue sample was subjected to a cyclic viral exposition. The system was let to evolve freely and the viral load was constantly tracked. Both the upper and the lower figures were obtained through the same set-up (the simulation was run twice). It corresponds to the model's **third round of calibration**.

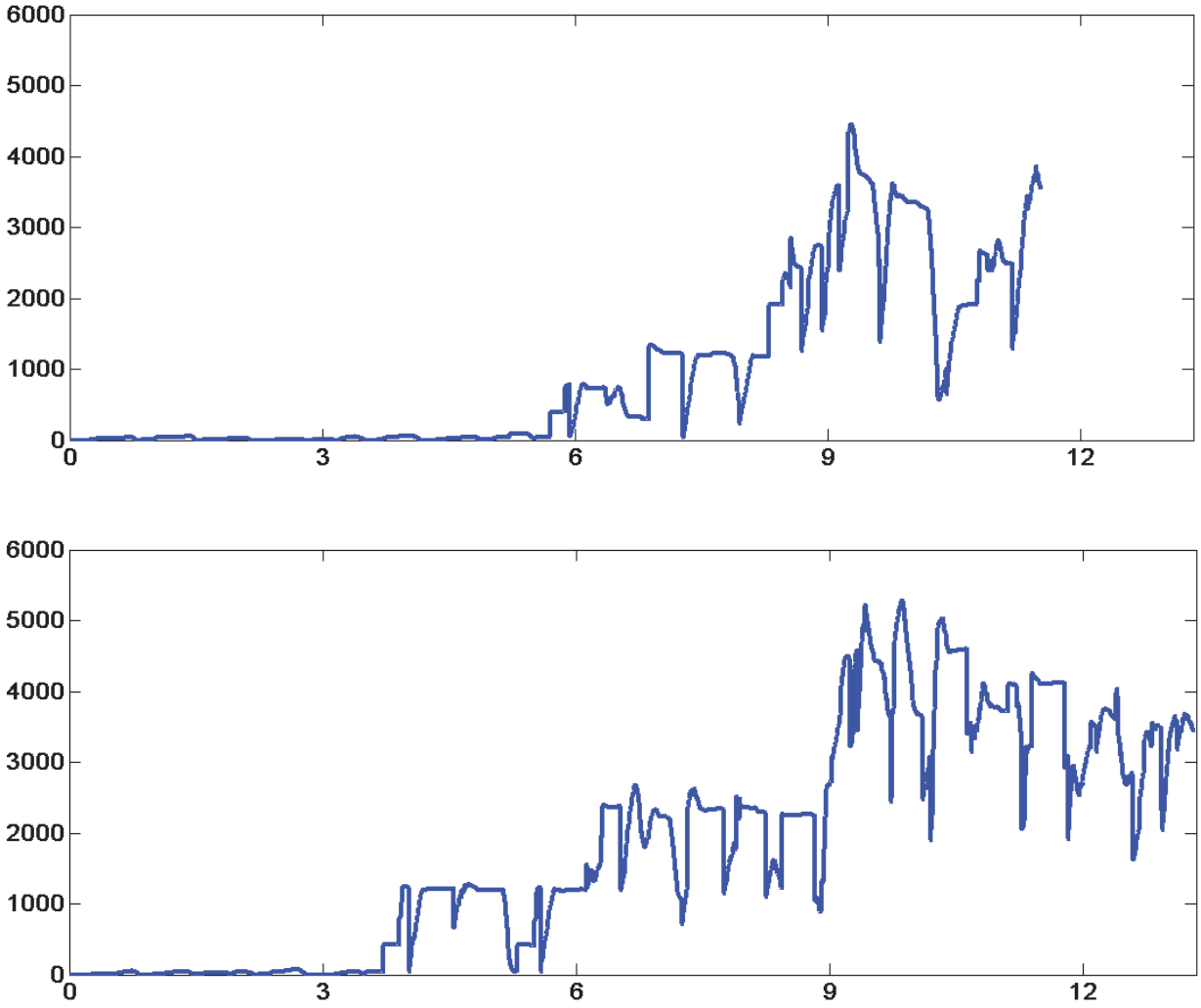

Figure 23. In silico simulation (through a multi-agent system approach) of the viral load evolution in an epithelial tissue sample. **x-axis**: time, in months, over which the simulation was conducted. **y-axis**: viral load, i.e. the number of particles infecting the tissue sample at any given instant of time. A set of virtual epithelial cells was initially arranged in a 4 x 4 **L-like distribution** (i.e. 4 cells in the basal layer bearing other cells in such a way that the first and second columns are made up of 4 cells, while the third and fourth columns are made of only 2 cells). The virtual cells that constitute the innermost layer possess the capacity of multiplying themselves in such a way that the epithelial turnover complies to what was defined in the second round of calibration. No agents representing anti-HPV IgG immunoglobulins were included in this simulation. The tissue sample was subjected to a cyclic viral exposition. The system is let to evolve freely and the viral load was constantly tracked. Both the upper and the lower figures were obtained through the same set-up (the simulation was run twice). It corresponds to the model's **third round of calibration**.

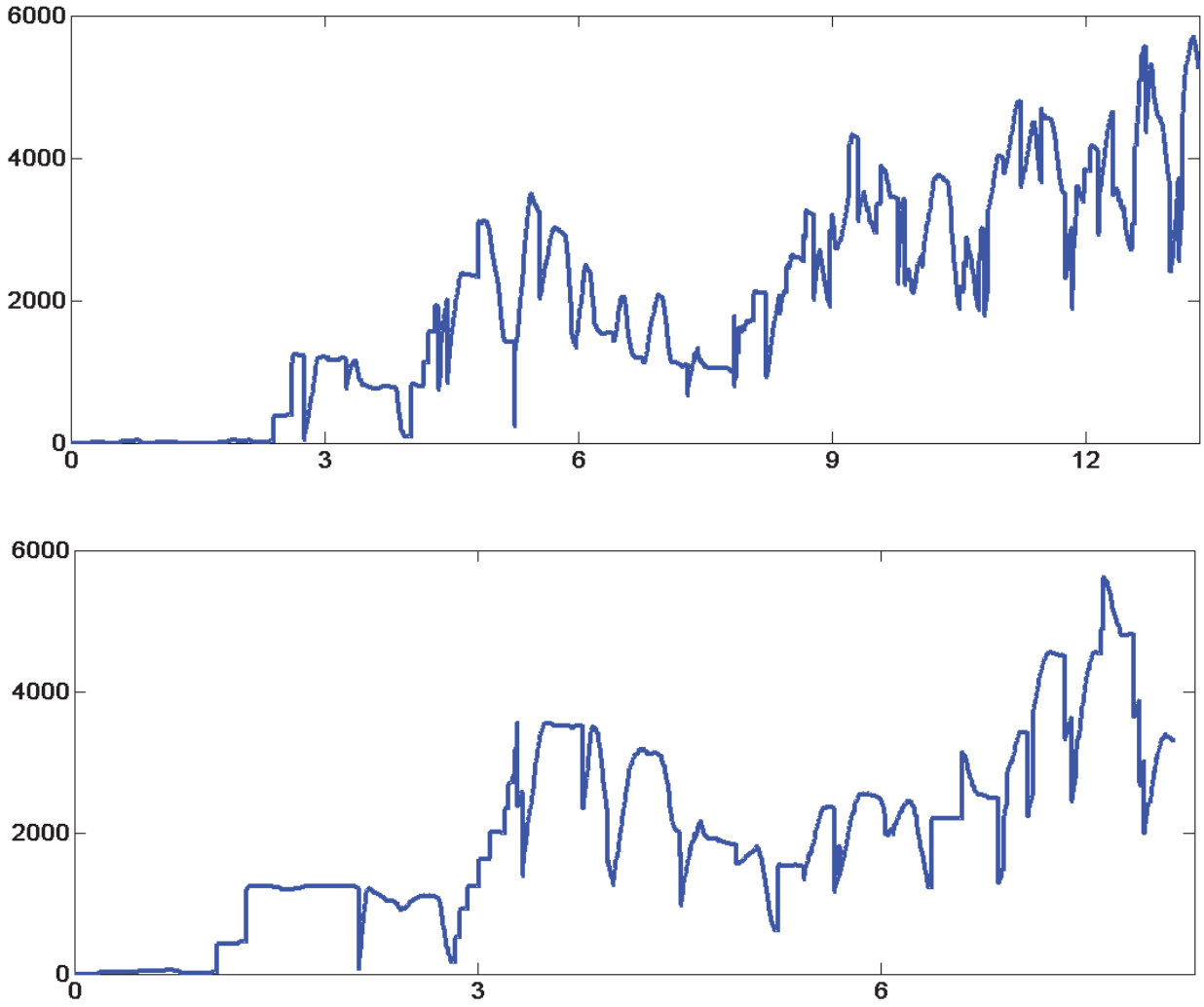

Figure 24. In-silico simulation of the viral load evolution in an epithelial tissue sample through which anti-HPV IgG immunoglobulins transude. **x-axis**: time, in months, over which the simulation was conducted. **y-axis**: viral load, i.e. the number of particles infecting the tissue sample at any given instant of time. Virtual epithelial cells were initially set up in a 4 x 4 L-kind of architecture simulating an epithelial transformation zone. The viral exposition was simulated exactly in the same way as for the third round of calibration. For this particular simulation, **the anti-HPV IgG immunoglobulin titer in the adjacent microvessel was set to be constant at 50 mMU/mL**. Both the upper and the lower figures correspond to the exact same simulation, conducted twice. This simulation corresponds to the in-silico **predictions** made on the intramuscular-vaccination induced immunoglobulins' capacity to interfere with the viral life cycle in the upper respiratory tract mucosa.

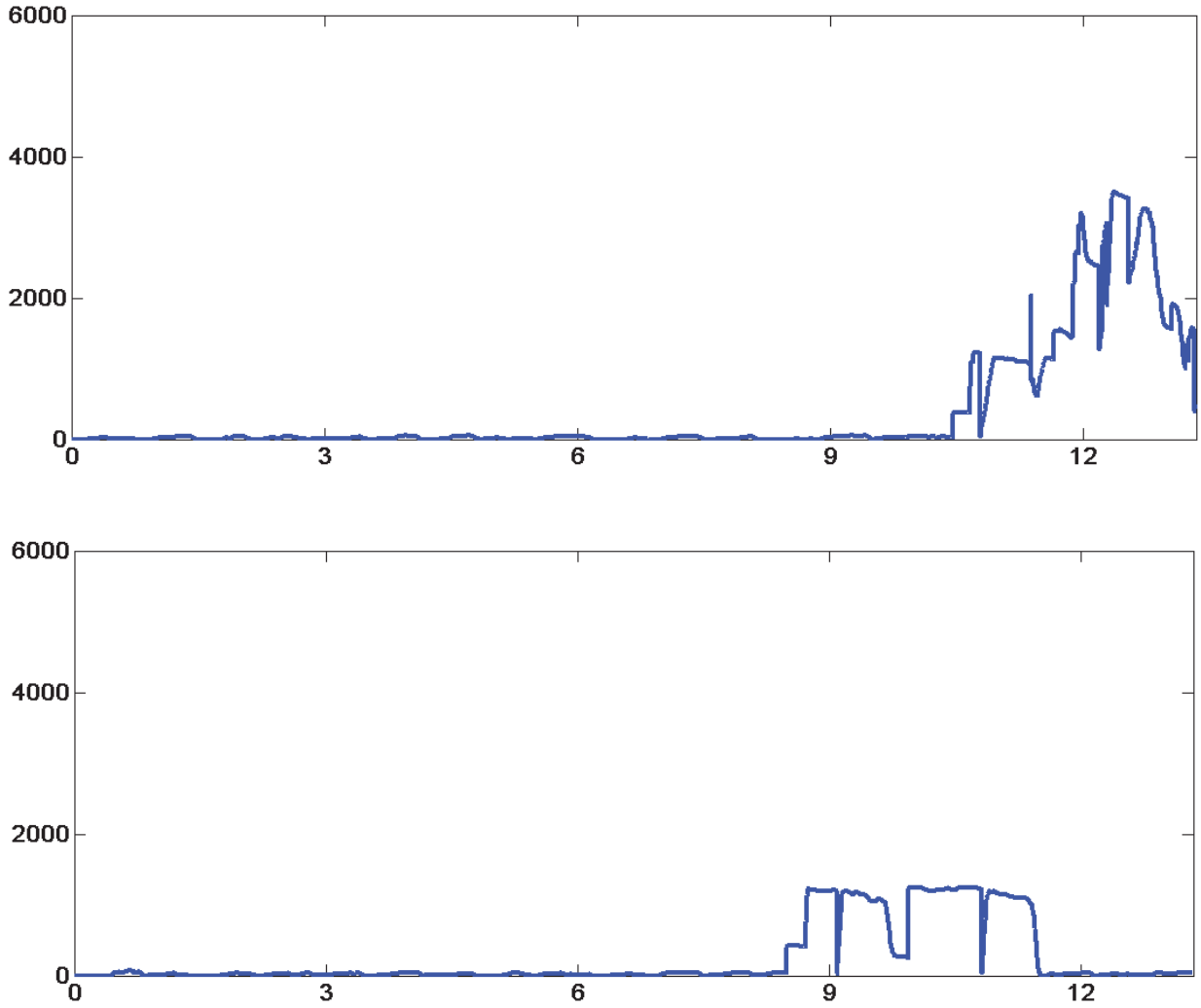

Figure 25. In-silico simulation of the viral load evolution in an epithelial tissue sample through which anti-HPV IgG immunoglobulins transude. **x-axis**: time, in months, over which the simulation was conducted. **y-axis**: viral load, i.e. the number of particles infecting the tissue sample at any given instant of time. Virtual epithelial cells were initially set up in a 4 x 4 L-kind of architecture simulating an epithelial transformation zone. The viral exposition was simulated exactly in the same way as for the third round of calibration. For this particular simulation, **the anti-HPV IgG immunoglobulin titer in the adjacent microvessel was set to be constant at 100 mMU/mL**. Both the upper and the lower figures correspond to the exact same simulation, conducted twice. This simulation corresponds to the in-silico **predictions** made on the intramuscular-vaccination induced immunoglobulins' capacity to interfere with the viral life cycle in the upper respiratory tract mucosa.

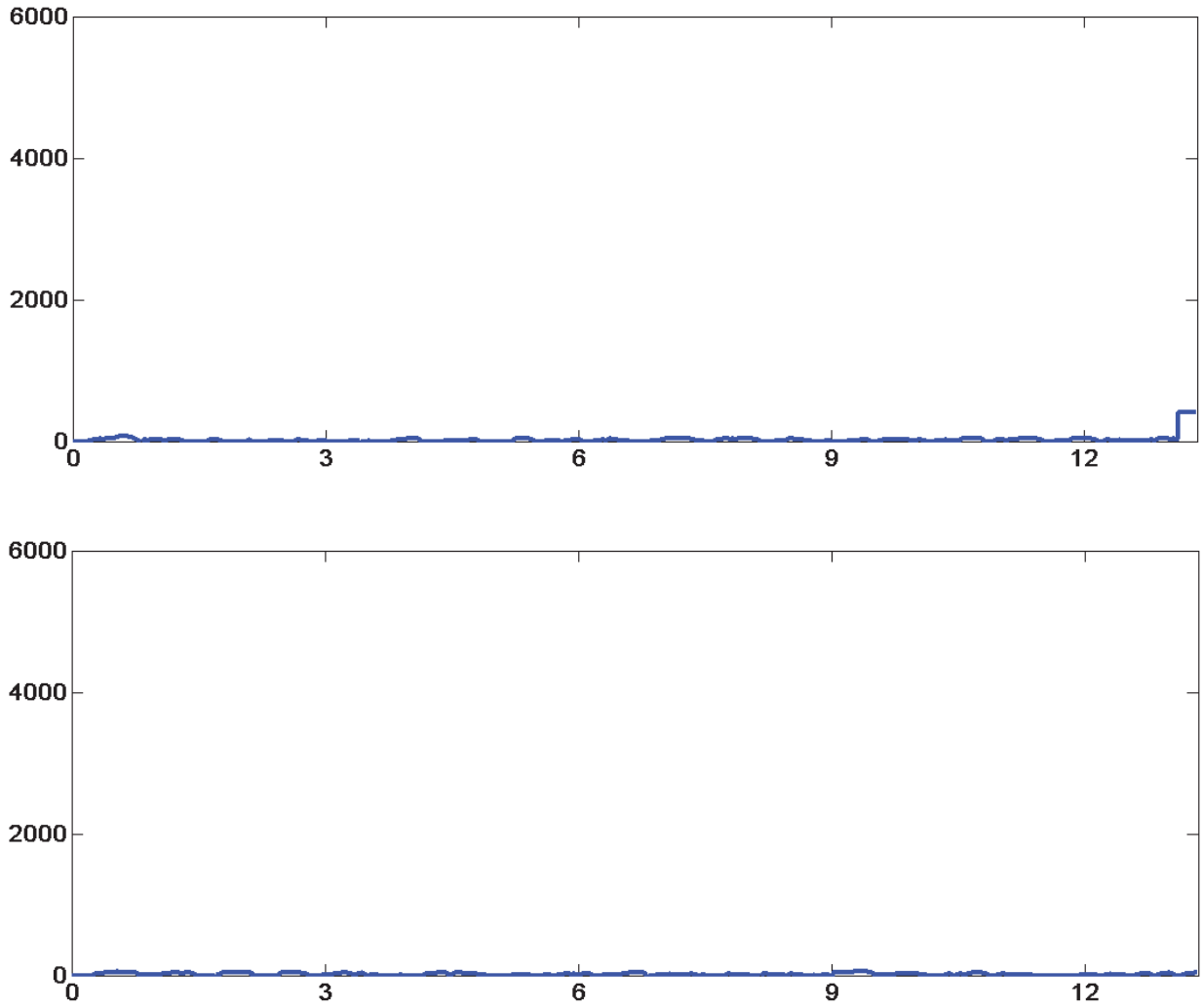

Figure 26. In-silico simulation of the viral load evolution in an epithelial tissue sample through which anti-HPV IgG immunoglobulins transude. **x-axis**: time, in months, over which the simulation was conducted. **y-axis**: viral load, i.e. the number of particles infecting the tissue sample at any given instant of time. Virtual epithelial cells were initially set up in a 4 x 4 L-kind of architecture simulating an epithelial transformation zone. The viral exposition was simulated exactly in the same way as for the third round of calibration. For this particular simulation, **the anti-HPV IgG immunoglobulin titer in the adjacent microvessel was set to be constant at 150 mMU/mL**. Both the upper and the lower figures correspond to the exact same simulation, conducted twice. This simulation corresponds to the in-silico **predictions** made on the intramuscular-vaccination induced immunoglobulins' capacity to interfere with the viral life cycle in the upper respiratory tract mucosa.

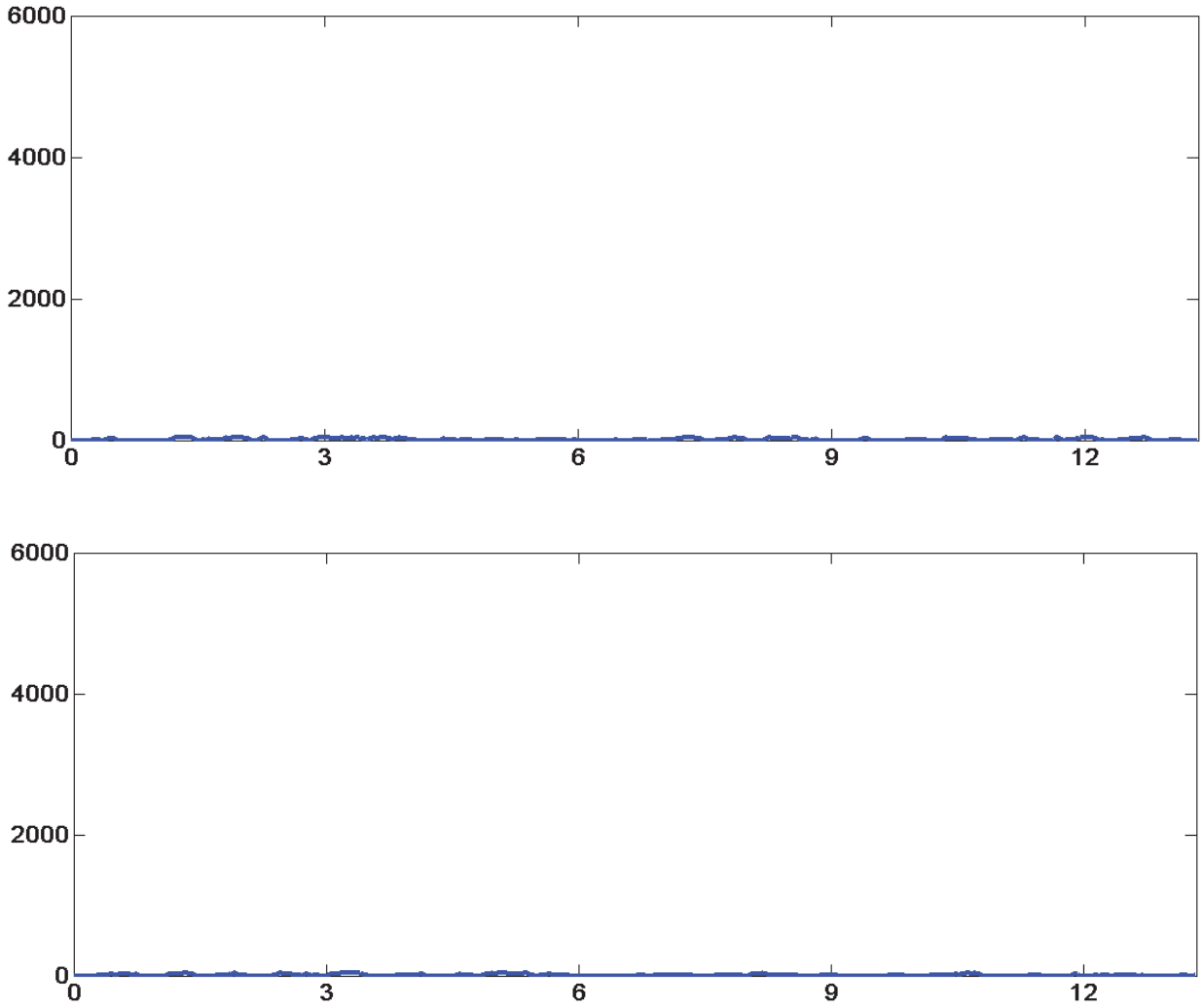

Figure 27. In-silico simulation of the viral load evolution in an epithelial tissue sample through which anti-HPV IgG immunoglobulins transude. **x-axis**: time, in months, over which the simulation was conducted. **y-axis**: viral load, i.e. the number of particles infecting the tissue sample at any given instant of time. Virtual epithelial cells were initially set up in a 4 x 4 L-kind of architecture simulating an epithelial transformation zone. The viral exposition was simulated exactly in the same way as for the third round of calibration. For this particular simulation, **the anti-HPV IgG immunoglobulin titer in the adjacent microvessel was set to be constant at 200 mMU/mL**. Both the upper and the lower figures correspond to the exact same simulation, conducted twice. This simulation corresponds to the in-silico **predictions** made on the intramuscular-vaccination induced immunoglobulins' capacity to interfere with the viral life cycle in the upper respiratory tract mucosa.

CHAPTER 14:

A CONVERSION FACTOR FOR EXPRESSING THE IMMUNOGLOBULIN TITERS IN A MORE STANDARD WAY, A BY-PRODUCT

When Gardasil® and Cervarix® went through the clinical trials phase prior to their approval, the first step towards the assessment of their performance was the evaluation of their immunogenicity, which was done by determining the serum anti-HPV immunoglobulin titers elicited by vaccination. The biochemical techniques for conducting such evaluation have not been standardized so far and, as a consequence, the immunoglobulin titers were (and continue to be, is post-approval studies) expressed differently: in mMU/mL (milli-Merck units per mL) in the case of Gardasil®, in EU/mL (ELISA units per mL) in the case of Cervarix®. Direct comparisons are therefore impossible and a head-to-head clinical study[205], that must have cost a lot, had to be undertaken for this specific purpose. To our knowledge, no factor has been so far proposed to convert any of these arbitrary units into something more conventional, such as for example, ng/mL (nanograms per mL). Based on the analysis of some published data and on some simple calculations we came up with a proposition for such a factor, for the case of Gardasil®. How we did it is presented in the following paragraphs.

In 2005, an article[206], whose most of the authors worked for Merck, was published in which the effect of using their own adjuvant in the formulation of the quadrivalent HPV vaccine was presented. The study was conducted in a group of macaques that they divided into two groups in order to determine the vaccine's immunogenicity with and without the adjuvant. In order to obtain the immunoglobulin titers they used the exact same technique (known as cLIA : competitive Luminex Immuno-Assay) that was used in most (if not all) of Gardasil®'s clinical trials. In the methods section of this article (page 4, left column, first paragraph, line number 16) there is a phrase that, at first sight, would not seem to be extremely significant: "an antibody titer of >200 mMU/mL for HPV 11 has been shown to neutralize ~10^8 virions in the athymic mouse xenograft

assay", and by the end of the phrase there is a bibliographic reference[207]. We analyzed both articles and concluded that what is referenced is not the quantitative result of the neutralization essay but the experimental method used to perform it. The quantitative result would be, in fact, an until-that-moment unpublished result.

A deeper analysis permitted us to obtain the following information about the experimental protocol. For conducting the neutralization essay they first mixed in a test tube: i) a solution containing HPV-11 virions, obtained from HPV-infected human foreskin samples; ii) a solution containing specific IgG immunoglobulins, produced in rabbits; and iii) fragments of HPV-free human foreskin. They kept the mixture during 90 minutes at 37 degrees Celsius, before implanting the foreskin fragments into the renal capsules of athymic mice. Their animal model had developed in such a way that allowed them to determine, through molecular and histological analyses effectuated 10 weeks after, if at the moment of the implantation there were any remaining HPV virions in the foreskin fragments. And since they tested different concentrations of HPV virions, they were able to determine a threshold beyond of which the neutralization takes place.

In the paper by Bryan et al.[207], one can read, in the last paragraph of the results section (page 187): "The estimated neutralizing concentration of HPV 11 L1 VLP-specific IgG was determined to be approximately 700 ng per ml for both anti-HPV 11 A and anti-HPV 11 B sera". And by the end of the same page, one can read "… because the large quantity of purified, concentrated virions used in our experiments (approximately 10^8 virions per implant) may exceed…", which is the same experimental viral load mentioned in the paper by Ruiz et al[206].

Consequently, we propose the immunoglobulin titer of 200 mMU/mL as being functionally equivalent to a 700 ng/mL titer.

SECTION VI

GENERAL DISCUSSION,

CONCLUSIONS AND PERSPECTIVES

CHAPTER 15

GENERAL DISCUSSION

We have presented here an effort for approaching the study of the immunology behind vaccination in an alternative way. 215 years have passed since the occurrence of one of the most later-on-publicized (and therefore best-known) episodes in the history of science: Edward Jenner's experiment of cowpox-residue inoculation on an 8-year old boy with the aim of preventing smallpox. Since then, numerous major scientific breakthroughs have completely changed the way immunology (and life) are studied, and yet, no one, in our days, fully understands how successful vaccines protect, nor why all the vaccine candidates so far tested against several ravaging infectious diseases (such as AIDS, malaria, and others) do not.

Patients suffering from JORRP must be operated several times per year for avoiding critical airway obstruction. If the disease ever expands to the lungs, which, fortunately, is rather rare (it has been estimated that it occurs in approximately 3% of the cases[208]), life expectancy is reduced to only a couple of years. Ultimately, the question of a clinical benefit from prescribing Gardasil® to these patients will have to be brought up and debated on the basis of clinical evidence, which, to date, remains inexistent. We believe that even if a window towards the acquisition of such data existed it would be unreasonable to try to find the optimal vaccination/booster schedule through a (clinical)-trial-and-error kind of strategy. The simulation platform that we propose could represent a shortcut for not having to test hundreds of different vaccination/booster schedules before fate finally decides that is time to get closer to the optimal one. As stated, our simulation platform consists of two models: the first one dealing with the immunology behind vaccination, the second one with the natural history of JORRP. In the following paragraphs, we are going to present the arguments that make us believe in the worth, in the relevance and in the potential of our models. However, such arguments will be presented in a peculiar way: we have decided to play here below the devil's

advocate by pinpointing the reasons why they should be considered worthless, irrelevant and unpromising:

Treatments for JORRP already exist, and the next generation of them, which are currently being tested clinically (e.g. the COX-2 inhibitor Celebrex/Celecoxib), seem to be quite promising. Is there really any space left for even exploring this strange idea of Gardasil® as an adjuvant therapy?

Such space will continue to exist as long as there are patients for whom the option of periodic surgical interventions remains to be the only one, which is currently the case. On the other hand, a phase-II randomized double-blind controlled study (NCT00571701 in the ClinicalTrials.gov register), to be completed in July 2012, should indeed shed some light on the potential efficacy of Celebrex/Celecoxib for treating JORRP. This study was undertaken following the observation that, when compared to healthy laryngeal tissue, the cyclooxigenase-2 (COX-2) enzyme was found to be overexpressed in papillomata collected form JORRP-suffering patients[209], as occurs in several forms of cancer[210,211]. However, we believe that, while waiting for the results of the clinical trial, a quick glimpse at what experience has taught the oncology community about the promise of COX-2 inhibitors as therapeutic agents should warn the JORRP community about the risk of raising false expectations: their clinical efficacy in the treatment of cancer still remains to be demonstrated, specially after the publication of some rather disappointing results for the specific case of prostate cancer[212]. Additionally, doubts concerning their pharmacological safety still subsist: two independent meta-analyses[213,214] published in 2007 with the aim of finishing with the long-lasting debate[215] on the possible lack of cardiovascular safety associated with COX-2 inhibitors present completely opposite conclusions.

HPV vaccines have shown no therapeutic effect in the case of genital infections, why should the outcome for JORRP be different?

Such a conclusion was drawn, among others, from a study[216] in which HPV-DNA-positive-at-enrollment (as determined directly in cervical specimens) 18-to-25-year-old women randomly

received either the bivalent HPV-vaccine or a control hepatitis-A vaccine. After a one-year follow-up, no positive effect (in terms of viral clearance) was associated to the vaccine administration. Two arguments can be evoked as reasons for not extrapolating this failure into the JORRP case: i) women that were not sexually active were excluded from this study, which means that, during the whole follow-up, there was a considerable risk of participants being re-exposed to HPV, making it harder for the organism (with or without any kind of intervention) to get rid of the virus. The chronic re-exposure to HPV is simply not possible in the JORRP case. ii) The presence or absence of HPV-DNA in the infected tissue is not the most suitable marker for establishing if the viral life cycle has been short-circuited or not. HPV is well known for its capacity to establish intracellular latent reservoirs and the only way an action on the immune system would have an effect on them would be through the induction of a cell-mediated HPV-specific immune response, something, that we all know, cannot be attained with the existing HPV vaccines. The therapeutic effect that we pursue depends on HPV's ineluctable need to "travel" as a virion while trying to regain access to the epithelial stem cells (found in the basal layer) in order to complete its life cycle. This need would represent HPV's Achilles' heel to the eyes of the Gardasil®-induced immunoglobulins that would already be there, bathing the ill tissue to prevent the expansion of the disease.

And even if there was a therapeutic effect, what would be its impact? JORRP's incidence seems to be negligible when compared to cervical cancer's.

Cervical cancer affects some 500 thousand women around the world every year[217], which approximately represents 15 per 100 thousand women, while JORRP's incidence has been estimated to be, at least in the USA, of around 4 per 100 thousands infants[218,219]. In the light of these figures three comments are worth to be done: i) fortunately, not even in this aspect (research being oriented on a pathology-incidence basis) our work is statistics-driven; ii) if what we do ever results in a single patient finding some relief to JORRP, all our work will have totally paid off; iii) the immunology behind vaccination (as well as the dynamics of the host-pathogen interactions) are

fundamental research topics for several infectious diseases other than JORRP. Hopefully, the simulation platforms that we have devised will serve as the basis for conducting other research projects.

To what extent the boosting of the humoral response could be restricted by safety issues concerning the repeated administration of Gardasil® to the same patient?

There is no doubt that this factor must absolutely be taken into account, and there is nothing we can say about it on the basis of our simulations. Nonetheless, we can cite some clinical evidence in the form of a study[220] in which some patients received up to 6 doses of an experimental HPV-6b VLP-based vaccine (containing no adjuvant) in an attempt to foster the regression of genital warts. According to their own safety report "…no local, … or systemic adverse reactions were observed or reported by subjects following immunization, beyond the immediate discomfort associated with injection."

The clinical data used to calibrate the model was originally obtain in adults, yet JORRP is a pediatric disease.

Gardasil®, as many other vaccines, follow the simple thumb-rule of "the younger the vaccinee, the stronger the immunogenicity". Ideally, we should have used data drawn from infants rather than from adults to calibrate our model, but, to our knowledge, neither a long-term follow-up of the immunogenicity nor a study of the long-term humoral immune memory have been conducted in children. One possible, rather optimistic, way of considering this discordance would be to say that since JORRP-suffering patients would most likely exhibit a stronger immunogenicity than the one computed by the models, the predicted therapeutic benefit would tend to be underestimated, providing a "safety range" that would compensate any possible uncertainty associated with the models.

Participants in the immunogenicity clinical trial used to calibrate the mathematical model were HPV-naive, while JORRP patients are definitively not. Would not this discordance affect the accuracy of the predicted humoral immune responses?

It is well known that a natural (genital or respiratory) HPV infection has little impact on the systemic immune system. This is thought to be associated to the fact that, while accomplishing their life cycle, HPV viral particles do not kill their host cells, acting as stealthy intruders capable of not triggering any danger (inflammatory) signals. On the other hand, HPV vaccines are administered intramuscularly and therefore all the immune responses they elicit are directly associated with the "systemic" immune system. Previous encounters with the same kind of immunogen do affect the outcome of an immune stimulus, but, since the two stimuli we are dealing with (JORRP-associated natural infection and vaccination with Gardasil®) differ in the physio-anatomic compartments of the immune system they have (or may have) an effect on (the mucosal respiratory-tract-associated immune system versus the systemic immune system), the assumption of JORRP patients being considered as HPV-naive at the systemic level seems to be reasonable and therefore should not be a source of error.

To use 52 parameters for fitting 11 points, what is the sense in that?

We decided that our first action before presenting any arguments against this idea would be actually to do it (to fit the 11 points). We fed the data set that we used to calibrate our model to an over-the-shelf fitting application (MatLab®'s built-in basic fitting tool). We found, against common beliefs that say that high-degrees polynomials can fit anything (as long as you use a sufficient amount of parameters), that for our set of data, an acceptable polynomial fitting could not be obtained (at least, when using up to 10th-degree polynomials). But even if it was not the case, if such a polynomial could be obtained, what could it be used for? For mathematically extending the straight line to which the serocoversion curve clearly tends whenever a 0-60-180-day vaccination schedule is employed? What for? And that would be like the most profound kind of analysis one might intend

to conduct if ever decided to base our research on data fitting, which we do not, of course. For us, data played a secondary role, which was to permit a model to better stick to a well-studied clinical reality.

Would it be really reasonable to consider that the threshold, that defines the minimum serum immunoglobulin titer required for observing a therapeutic effect, will be the same for all JORRP patients?

Both clinical evidence and physiopathological knowledge on this point are scarce (or even inexistent). So the only thing left to do is to muse: it is often argued that each case of JORRP is unique and that, as a consequence, the prognosis (with or without a therapeutic intervention) usually escapes any logic. We believe that there are two different aspects behind the outcome of this disease that should be treated separately: i) the infectious aspect, i.e. the pathogen striving to complete its life cycle within the host; and ii) the disease control aspect, i.e. the host being aware of the presence of (and trying to get rid of) those long-time infected cells that no longer behave normally. Any observed clinical outcome is the result of the superposition of these two different phenomena. Our therapeutic hypothesis concerns exclusively the fate of the underlying HPV infection. We believe that it is rather the fluctuations in the host's natural capacity to maintain the population of abnormal cells under a clinical manifestation level that makes JORRP's natural history to look like a stochastic process. In other words, we believe that the factors that might influence the value of the immunoglobulin titer threshold required for short-circuiting HPV's life cycle (e.g. the local active viral load, the 3D-architecture of the infected tissue, the physicochemical conditions within - and in the neighborhood of - the infected tissue, the virus' ability to employ the host's DNA-associated machinery to multiply itself, the immunoglobulins' capacity to transude through the infected tissue and to neutralize the free viral particles, etc.) should not vary much from one patient to another.

What is the relevance of having simulated the effect of making vary the initial 3-dose vaccination schedule?

The only evidence-based initiative ever undertaken (at least to our knowledge) for exploring the effect of prescribing Gardasil® to patients suffering from some kind of laryngeal papillomatosis is a clinical trial (NCT00829608 in the ClinicalTrials.gov register) centered at the University of Missouri-Columbia, conducted in adults, and expected to have been concluded in June 2010 (after a 1-year clinical follow-up). In this study, the traditional 0-60-180-day vaccination schedule was replaced by a 0-15-30-day alternative one. We believe that these kinds of protocol modifications are not sensible because they imply the refusal of a great deal of already-collected evidence (concerning both the safety and the immunogenicity of the most studied protocol). Besides, we believe that it would be a risk worth to be run if there were any hints pointing towards a better outcome, which is not the case. On the contrary, it has been previously suggested that by reducing the intervals between the vaccine doses there is a considerable risk of falling into a zone of sub-optimal immunogenic performance. Some evidence on this was published more than 20 years ago in the form of a study[221] on the hepatitis-B vaccine. Several similarities exist between the HPV and the hepatitis-B vaccines: i) both of them are administered intramuscularly; ii) the immunogen contained in both vaccines are self-assembling recombinant proteins devised to mimic their respective viral capsids; iii) both their immunization schedules consist of three doses (in fact, the vaccination protocol recommended for Recombivax-HB, the hepatitis-B vaccine used in the just-mentioned study, is exactly the same as the protocol currently recommended for CervarixTM, the other already-in-the-market HPV vaccine: i.e. shots at 0, 30 and 180 days). Thus, by simulating the effect of making vary the initial vaccination protocol we are not inviting others to do so. The fact of having qualitatively reproduced (in-silico) an independently observed and published clinical phenomenon represents for us an indirect argument (indirect because such data do not exist for Gardasil®) for believing in our model's relevance to the fields of immunology and vaccinology.

CHAPTER 16

CONCLUSIONS

The main conclusions are: i) according to our simulations, the minimum serum IgG titer required for hampering the progression of a recurrent respiratory papillomatosis would be 200 mMU/mL ; ii) in order to keep, within a time window of ten years, the anti-HPV IgG titer over the just-mentioned therapeutic-effect threshold, the biggest possible fraction of time, by means of the smallest possible number of booster doses, it would be necessary, according to our simulations, to adopt the following schedule: the basic three-dose classic immunization (at months 0, 2 and 6), followed by three successive booster doses, every six months, until reaching the 24th month, followed by a much-later final booster dose, 18 months later. iii) incidentally, it would seem to be inappropriate, according to our simulations, to modify the classic initial vaccination schedule (at months 0, 2 and 6); and iv) from the immunogenicity point of view, the main effect of administering booster doses (i.e. from the fourth dose on) would be, according to our simulations, higher titer values for the residual IgG's plateau.

CHAPTER 17

PERSPECTIVES

In this project, we devised and implemented a mathematical model of the immunology behind the intramuscular vaccination with Gardasil® as well as a multi-agent system based model of a mucosal HPV infection. We did not pretend to explain all the complexity of such phenomena with our models, nor did we intend to come up with a mathematical representation of the quintessence of the immune system. Our purpose was to develop a to-some-extent predictive tool, capable of operating as close to reality as possible, so that the potential benefit of prescribing Gardasil® to JORRP patients could approximately be estimated.

Now, we hope that in the close future some of the in-silico predictions here presented can be confronted to real data drawn from at least some JORRP patients treated with Gardasil® as an adjuvant therapy.

ACKNOWLEDGMENTS

I wish to gratefully thank all the people and institutions that made possible this adventure, especially:

Pr. François Gueyffier, who, one day, during summer 2006, decided to open the doors of his research team to a foreign engineer who dreamt of biomedical science.

Pr. Jean-Pierre Boissel, for having generously shared with me much of his experience, his thinking, his wisdom.

Sanofi Pasteur MSD, for having generously provided the research grant that made this project possible.

Dr. Benoît Soubeyrand, for having had the courage of co-directing such an exotic project.

Dr. Anne-Carole Jacquard, for having been onboard during most of the journey.

Dr. Yann Leochmac and the other very kind people from Sanofi Pasteur MSD I ever had contact with.

Claude Bernard University and the Institute for Theoretical Medicine, for having permitted me to evolve in a top-level scientific environment for conducting my doctoral research.

The EMET and the APRET teams, because 4 years is a quite a long period of time and it was a great pleasure to share them with all of you.

APPENDICES

APPENDIX 1

LIST OF QUERIES MADE TO THE PUBMED DATABASE

FOR THE REVIEW OF THE LITERATURE PRESENTED IN CHAPTER 4

(QUERIES MADE IN MARCH 2011)

- Query No. 1: "in-silico model [Title/Abstract] AND host-pathogen interactions [Title/Abstract]". Result: 0 articles.
- Query No. 2: "in-silico model [Title/Abstract] AND viral life-cycle [Title/Abstract]". Result: 0 articles.
- Query No. 3: "in-silico model [Title/Abstract] AND natural history [Title/Abstract] AND virus [Title/Abstract]". Result: 0 articles.

- Query No. 4: "computational model [Title/Abstract] AND host-pathogen interactions [Title/Abstract]". Result: 1 article.
- Query No. 5: "computational model [Title/Abstract] AND viral life-cycle [Title/Abstract]". Result: 3 articles.
- Query No. 6: "computational model [Title/Abstract] AND natural history [Title/Abstract] AND virus [Title/Abstract]". Result: 0 articles.

- Query No. 7: "mathematical model [Title/Abstract] AND host-pathogen interactions [Title/Abstract]". Result: 6 articles.
- Query No. 8: "mathematical model [Title/Abstract] AND viral life-cycle [Title/Abstract]". Result: 4 articles.
- Query No. 9: "mathematical model [Title/Abstract] AND natural history [Title/Abstract] AND virus [Title/Abstract]". Result: 8 articles.

- Query No. 10: “in-silico model [Title/Abstract] AND vaccine [Title/Abstract] AND immunogenicity [Title/Abstract]”. Result: 0 articles.
- Query No. 11: “in-silico model [Title/Abstract] AND vaccine [Title/Abstract] AND immune responses [Title/Abstract]”. Result: 1 article.
- Query No. 12: “in-silico model [Title/Abstract] AND vaccine [Title/Abstract] AND immune reactions [Title/Abstract]”. Result: 0 articles.

- Query No. 13: “computational model [Title/Abstract] AND vaccine [Title/Abstract] AND immunogenicity [Title/Abstract]”. Result: 0 articles.
- Query No. 14: “computational model [Title/Abstract] AND vaccine [Title/Abstract] AND immune responses [Title/Abstract]”. Result: 0 articles.
- Query No. 15: “computational model [Title/Abstract] AND vaccine [Title/Abstract] AND immune reactions [Title/Abstract]”. Result: 0 articles.

- Query No. 16: “mathematical model [Title/Abstract] AND vaccine [Title/Abstract] AND immunogenicity [Title/Abstract]”. Result: 9 articles.
- Query No. 17: “mathematical model [Title/Abstract] AND vaccine [Title/Abstract] AND immune responses [Title/Abstract]”. Result: 4 articles.
- Query No. 18: “mathematical model [Title/Abstract] AND vaccine [Title/Abstract] AND immune reactions [Title/Abstract]”. Result: 0 articles.

- Query No 19: “in-silico model [Title/Abstract] AND immune system [Title/Abstract]”. Result: 4 articles.
- Query No 20: “in-silico model [Title/Abstract] AND immune responses [Title/Abstract]”. Result: 2 articles.

- Query No 21: “in-silico model [Title/Abstract] AND immune reactions [Title/Abstract]”. Result: 0 articles.

- Query No 22: “computational model [Title/Abstract] AND immune system [Title/Abstract]”. Result: 13 articles.
- Query No 23: “computational model [Title/Abstract] AND immune responses [Title/Abstract]”. Result: 1 article.
- Query No 24: “computational model [Title/Abstract] AND immune reactions [Title/Abstract]”. Result: 0 articles.

- Query No 25: “mathematical model [Title/Abstract] AND immune system [Title/Abstract]”. Result: 117 articles.
- Query No 26: “mathematical model [Title/Abstract] AND immune responses [Title/Abstract]”. Result: 41 articles.
- Query No 27: “mathematical model [Title/Abstract] AND immune reactions [Title/Abstract]”. Result: 6 articles.

- Query No 28: “in-silico model [Title/Abstract]”. Result: 182 articles.
- Query No 29: “computational model [Title/Abstract]”. Result: 2,880 articles.
- Query No 30: “mathematical model [Title/Abstract]”. Result: 16,426 articles.

- Query No 31: “host-pathogen interactions [Title/Abstract]”. Result: 1,212 articles.
- Query No 32: “viral life-cycle [Title/Abstract]”. Result: 1,114 articles.
- Query No 33: “natural history [Title/Abstract] AND virus [Title/Abstract]”. Result: 2,193 articles.

- Query No 34: “vaccine [Title/Abstract] AND immunogenicity [Title/Abstract]”. Result: 8,849 articles.
- Query No 35: “vaccine [Title/Abstract] AND immune responses [Title/Abstract]”. Result: 9,006 articles.
- Query No 36: “vaccine [Title/Abstract] AND immune reactions [Title/Abstract]”. Result: 88 articles.

- Query No 37: “immune system [Title/Abstract]”. Result: 52,977 articles.
- Query No 38: “immune responses [Title/Abstract]”. Result: 54,012 articles.
- Query No 39: “immune reactions [Title/Abstract]”. Result: 4,261 articles.

Parameter	Value	Units	Equivalence	Origin
d_V	1.16 x 10^{-2}	$days^{-1}$	($t_{1/2}$ = 59,8 days)	est.
d_A	1.16 x 10^{-2}	$days^{-1}$	($t_{1/2}$ = 59,8 days)	est.
d_P	2.31 x 10^{-1}	$days^{-1}$	($t_{1/2}$ = 3,0 days)	lit.[184]
d_H	3.85 x 10^{-2}	$days^{-1}$	($t_{1/2}$ = 18,0 days)	lit.[185]
d_B	1.80 x 10^{-2}	$days^{-1}$	($t_{1/2}$ = 38,5 days)	lit.[186]
d_O	7.20 x 10^{-2}	$days^{-1}$	($t_{1/2}$ = 9,6 days)	est.
d_F	7.20 x 10^{-2}	$days^{-1}$	($t_{1/2}$ = 9,6 days)	est.
d_S	2.89 x 10^{-1}	$days^{-1}$	($t_{1/2}$ = 2,4 days)	est.
d_K	2.89 x 10^{-1}	$days^{-1}$	($t_{1/2}$ = 2,4 days)	est.
d_C	3.30 x 10^{-2}	$days^{-1}$	($t_{1/2}$ = 21,0 days)	lit.[187]

Parameter	Value	Units	Origin
z_{B1}	10	(no units)	est.
z_{B2}	100	(no units)	est.
z_H	100	(no units)	est.
z_M	1000	(no units)	est.
s_B	1800	# of B cells per mL of the corr. comp. per day	calc.
s_H	6930	# of H cells per mL of the corr. comp. per day	calc.

Parameter	Value	Units	Origin
$q_{P/V}$	4.4 x 10^{14}	# of P cells per mole of VLPs	est.
$q_{H/P}$	1	# of H cells per P cell	est.
$q_{B/V}$	2.25 x 10^{16}	# of B cells per mole of VLPs	est.
$q_{B/P}$	1	# of B cells per P cell	est.
$q_{B/H}$	1	# of B cells per H cell	est.
$q_{M/P}$	1	# of M cells per P cell	est.
$q_{V/P}$	2.27 x 10^{-15}	moles of VLPs per P cell	dep.
$q_{V/B}$	4.44 x 10^{-17}	moles of VLPs per B cell	dep.

Parameter	Value	Units	Origin
k_{A2}	1 x 10^{-10}	moles of adj. per mL	est.
ω_B	1 x 10^{-6}	(no units)	est.
ω_H	1 x 10^{-6}	(no units)	est.
τ	1	days	est.
s_P	18480	# of P cells per mL per mL of the corr. comp. per day	calc.

Appendix 2. Parameters that remained constant throughout the calibration process. Origin: lit = literature (for the references, see section 2.3); dep = dependent; calc = calculated; est = estimated; gen. alg. = genetic algorithm. # of … = number of … VLPs = virus-like particles. Types of cells: P cells = antigen-presenting cells; H cells = CD4+ T helper cells; B cells = B-lymphocytes; M cells = memory B-lymphocytes. … per mL of the corr. comp. = per milliliter of the corresponding compartment. Adj. = adjuvant.

	Value ($days^{-1}$)			Equivalent $t_{1/2}$ (days)			
Parameter	**A**	**B**	**C**	**A**	**B**	**C**	**Origin**
d_M	2.61×10^{-4}	1.76×10^{-4}	6.93×10^{-5}	2654,8	3932,3	10000,0	gen. alg.
d_L	6.93×10^{-5}	1.33×10^{-4}	2.61×10^{-4}	10000,0	5209,7	2654,8	gen. alg.
f_V	1.10×10^{-2}	4.50×10^{-3}	1.46×10^{-2}	63,0	154,0	47,5	gen. alg.
f_A	1.46×10^{-2}	4.10×10^{-3}	1.50×10^{-3}	47,5	169,1	462,1	gen. alg.
f_P	8.56×10^{-2}	1.07×10^{-1}	7.14×10^{-2}	8,1	6,5	9,7	gen. alg.
f_H	8.20×10^{-3}	7.40×10^{-3}	8.90×10^{-3}	84,5	93,7	77,9	gen. alg.
f_C	8.60×10^{-3}	1.07×10^{-2}	7.20×10^{-3}	80,6	64,8	96,3	gen. alg.
m_P	1.66×10^{-1}	8.25×10^{-1}	5.05×10^{-1}	4,2	0,8	1,4	gen. alg.
v_S	1.92×10^{-2}	1.42×10^{-2}	9.70×10^{-3}	36	49	71	gen. alg.
v_K	6.70×10^{-3}	8.90×10^{-3}	4.10×10^{-3}	103	78	169	gen. alg.
v_L	1.30×10^{-3}	1.90×10^{-5}	2.09×10^{-2}	533	365	33	gen. alg.
v_M	7.10×10^{-3}	1.06×10^{-2}	2.09×10^{-2}	98	65	33	gen. alg.

		Value			
Parameter	**Units**	**A**	**B**	**C**	**Origin**
n_{B1}	(no units)	45,3	18,4	7,3	gen. alg.
n_{B2}	(no units)	1,0	1,0	12,1	gen. alg.
n_H	(no units)	1,0	2,6	15,2	gen. alg.
n_M	(no units)	2,6	1,0	15,2	gen. alg.

Appendix 3. (First of two parts) Parameters that varied throughout the calibration process (sets of parameters A, B and C). Origin: dep = dependent; gen. alg. = genetic algorithm. # of … = number of … VLPs = virus-like particles. Types of cells: P cells = antigen-presenting cells; H cells = CD4+ T helper cells; B cells = B-lymphocytes; M cells = memory B-lymphocytes. … per mL of the corr. comp. = … per milliliter of the corresponding compartment. Adj. = adjuvant.

Parameter	Units	Value			Origin
		A	B	C	
$k_{P/V}$	(# of P cells per mL of the corr. comp.)$^{-1}$ · (day)$^{-1}$	2.3 x 10^{-5}	2.3 x 10^{-5}	4.5 x 10^{-5}	gen. alg.
$k_{H/P}$	(# of H cells per mL of the corr. comp.)$^{-1}$ · (day)$^{-1}$	6.9 x 10^{-5}	3.1 x 10^{-5}	8.9 x 10^{-5}	gen. alg.
$k_{B/V}$	(# of B cells per mL of the corr. comp.)$^{-1}$ · (day)$^{-1}$	1.5	1.5	0.44	gen. alg.
$k_{B/P}$	(# of B cells per mL of the corr. comp.)$^{-1}$ · (day)$^{-1}$	5.4 x 10^{-3}	6.2 x 10^{-3}	1.2 x 10^{-6}	gen. alg.
$k_{B/H}$	(# of B cells per mL of the corr. comp.)$^{-1}$ · (day)$^{-1}$	14	7.5	8.7	gen. alg.
$k_{M/P}$	(# of M cells per mL of the corr. comp.)$^{-1}$ · (day)$^{-1}$	9.3 x 10^{-3}	1.2 x 10^{-2}	1.2 x 10^{-2}	gen. alg.
$k_{V/P}$	(moles of VLPs per mL of the corr. comp.)$^{-1}$ · (day)$^{-1}$	1.0 x 10^{10}	1.0 x 10^{10}	2.0 x 10^{10}	dep.
$k_{V/B}$	(moles of VLPs per mL of the corr. comp.)$^{-1}$ · (day)$^{-1}$	3.4 x 10^{16}	3.3 x 10^{16}	9.8 x 10^{15}	dep.
r_L	milli-Merck units per B cell per day	165,0	127,8	21,4	gen. alg.
r_S	milli-Merck units per B cell per day	138,4	53,3	122,5	gen. alg.
k_{A1}	(moles of adj. per mL)$^{-1}$	1.29 x 10^{9}	2.58 x 10^{9}	8.39 x 10^{9}	gen. alg.

Appendix 3. (Second of two parts) Parameters that varied throughout the calibration process (sets of parameters A, B and C). Origin: dep = dependent; gen. alg. = genetic algorithm. # of … = number of … VLPs = virus-like particles. Types of cells: P cells = antigen-presenting cells; H cells = CD4+ T helper cells; B cells = B-lymphocytes; M cells = memory B-lymphocytes. … per mL of the corr. comp. = … per milliliter of the corresponding compartment. Adj. = adjuvant.

APPENDIX 4. DETAILED PRESENTATION OF THE MATHEMATICAL MODEL

- A blue line indicates a term.
- A green line indicates a parameter.
- A red one indicates a variable.
- A brief explanatory description is included beneath each equation.

THE VACCINE

$$(1)\quad \frac{d(V^N)}{dt} = \left(-f_V \cdot V^N\right) - \left(d_V \cdot V^N\right) - \left(k_{V/P} \cdot \varphi(A^N) \cdot q_{V/P} \cdot P_N^N \cdot V^N\right) \qquad \varphi(A^N) = \frac{1}{1 + e^{-k_{A1} \cdot (A^N - k_{A2})}}$$

which can be translated as follows: instantaneously, the rate of change in the concentration of the HPV-L1 virus-like particles (VLPs) circulating in the non-lymphoid compartment is defined by:

- First term: The flow of VLPs from the non-lymphoid to the lymphoid compartment.
- Second term: The natural decay of VLPs.
- Third term: The VLP uptake by antigen-presenting cells.

$$(2)\quad \frac{d(V^L)}{dt} = \left(f_V \cdot V^N\right) - \left(d_V \cdot V^L\right) - \left(k_{V/B} \cdot \varphi(A^L) \cdot q_{V/B} \cdot B_N^L \cdot V^L\right) \qquad \varphi(A^L) = \frac{1}{1 + e^{-k_{A1} \cdot (A^L - k_{A2})}}$$

which can be translated as follows: instantaneously, the rate of change in the concentration of the HPV-L1 virus-like particles (VLPs) circulating in the lymphoid compartment is defined by:

- First term: The flow of VLPs from the non-lymphoid to the lymphoid compartment.
- Second term: The natural decay of VLPs.
- Third term: The VLP uptake by HPV-L1-specific B lymphocytes.

$$(3) \quad \frac{d\left(A^N\right)}{dt} = \left(-f_A \cdot A^N\right) - \left(d_A \cdot A^N\right)$$

which can be translated as follows: instantaneously, the rate of change in the concentration of the vaccine adjuvant circulating in the non-lymphoid compartment is defined by:

- First term: The flow of vaccine adjuvant from the non-lymphoid to the lymphoid compartment.
- Second term: The natural decay of the vaccine adjuvant.

$$(4) \quad \frac{d\left(A^L\right)}{dt} = \left(f_A \cdot A^N\right) - \left(d_A \cdot A^L\right)$$

which can be translated as follows: instantaneously, the rate of change in the concentration of the vaccine adjuvant circulating in the lymphoid compartment is defined by:

- First term: The flow of vaccine adjuvant from the non-lymphoid to the lymphoid compartment.
- Second term: The natural decay of the vaccine adjuvant.

ANTIGEN-PRESENTING CELLS

$$(5)\quad \frac{d\left(P_N^N\right)}{dt} = \left(s_P\right) - \left(d_P \cdot P_N^N\right) - \left(k_{P/V} \cdot \varphi\left(A^N\right) \cdot q_{P/V} \cdot V^N \cdot P_N^N\right) \qquad \varphi\left(A^N\right) = \frac{1}{1 + e^{-k_{A1} \cdot \left(A^N - k_{A2}\right)}}$$

which can be translated as follows: instantaneously, the rate of change in the cell-population density of naïve antigen-presenting cells (APCs) circulating in the non-lymphoid compartment is defined by:

- First term: The constant supply of naïve APCs to the non-lymphoid compartment.
- Second term: The natural death of naïve APCs in the non-lymphoid compartment.
- Third term: The transition of APCs in the non-lymphoid compartment from the state of naïve cells to the state of HPV-L1-processing but still tolerogenic cells.

(6) $$\frac{d\left(P_T^N\right)}{dt} = \left(k_{P/V} \cdot \varphi\left(A^N\right) \cdot q_{P/V} \cdot V^N \cdot P_N^N\right) - \left(f_P \cdot P_T^N\right) - \left(d_P \cdot P_T^N\right) \qquad \varphi\left(A^N\right) = \frac{1}{1 + e^{-k_{A1} \cdot \left(A^N - k_{A2}\right)}}$$

which can be translated as follows: instantaneously, the rate of change in the cell-population density of HPV-L1-processing but still tolerogenic antigen-presenting cells (APCs) circulating in the non-lymphoid compartment is defined by:

- First term: The transition of APCs in the non-lymphoid compartment from the state of naïve cells to the state of HPV-L1-processing but still tolerogenic cells.
- Second term: The flow of HPV-L1-processing but still tolerogenic APCs from the non-lymphoid to the lymphoid compartment.
- Third term: The natural death of HPV-L1-processing but still tolerogenic APCs in the non-lymphoid compartment.

(7) $$\frac{d\left(P_T^L\right)}{dt} = \left(f_P \cdot P_T^N\right) - \left(d_P \cdot P_T^L\right) - \left(m_P \cdot P_T^L\right)$$

which can be translated as follows: instantaneously, the rate of change in the cell-population density of HPV-L1-processing but still tolerogenic antigen-presenting cells (APCs) circulating in the lymphoid compartment is defined by:

- First term: The flow of HPV-L1-processing but still tolerogenic APCs from the non-lymphoid to the lymphoid compartment.

- Second term: The natural death of HPV-L1-processing but still tolerogenic APCs in the lymphoid compartment.
- Third term: The maturation of HPV-L1-processing APCs in the lymphoid compartment.

$$(8) \quad \frac{d\left(P_R^L\right)}{dt} = \left(-d_P \cdot P_R^L\right) + \left(m_P \cdot P_T^L\right)$$

which can be translated as follows: instantaneously, the rate of change in the cell-population density of HPV-L1-commited and reactive antigen-presenting cells (APCs) circulating in the lymphoid compartment is defined by:

- First term: The natural death of HPV-L1-commited and reactive APCs in the lymphoid compartment.
- Second term: The maturation of HPV-L1-processing APCs in the lymphoid compartment.

CD4+ HELPER TH2 LYMPHOCYTES

$$(9) \quad \frac{d\left(H_N^L\right)}{dt} = \left(\omega_H \cdot s_H\right) - \left(d_H \cdot H_N^L\right) - \left(k_{H/P} \cdot q_{H/P} \cdot P_R^L \cdot H_N^L\right)$$

which can be translated as follows: instantaneously, the rate of change in the cell-population density of HPV-L1-specific, naïve (i.e. non-effector and non-proliferating), CD4+ helper Th2 lymphocytes, circulating in the lymphoid compartment is defined by:

- First term: The constant supply of naïve CD4+ helper Th2 lymphocytes to the lymphoid compartment.
- Second term: The natural death of naïve CD4+ helper Th2 lymphocytes in the lymphoid compartment.
- Third term: The transition of CD4+ helper Th2 lymphocytes in the lymphoid compartment from the state of naïve cells to the state of primed (i.e. effector and proliferating) cells.

$$(10) \qquad \frac{d\left(H_P^L\right)}{dt} = \left(-f_H \cdot H_P^L\right) - \left(d_H \cdot H_P^L\right) + \left(z_H \cdot k_{H/P} \cdot q_{H/P} \cdot P_R^L\Big|_{t-(n_H \cdot \tau)} \cdot H_N^L\Big|_{t-(n_H \cdot \tau)}\right)$$

which can be translated as follows: instantaneously, the rate of change in the cell-population density of HPV-L1-specific, primed (i.e. effector and proliferating), CD4+ helper Th2 lymphocytes, circulating in the lymphoid compartment is defined by:

- First term: The flow of HPV-L1-specific primed CD4+ helper Th2 lymphocytes from the lymphoid to the non-lymphoid compartment.
- Second term: The natural death of HPV-L1-specific primed CD4+ helper Th2 lymphocytes in the lymphoid compartment.
- Third term: The transition of CD4+ helper Th2 lymphocytes in the lymphoid compartment from the state of naïve cells to the state of primed cells.

$$(11) \qquad \frac{d\left(H_P^N\right)}{dt} = \left(f_H \cdot H_P^L\right) - \left(d_H \cdot H_P^N\right)$$

which can be translated as follows: instantaneously, the rate of change in the cell-population density of HPV-L1-specific, primed (i.e. effector and proliferating), CD4+ helper Th2 lymphocytes, circulating in the non-lymphoid compartment is defined by:

- First term: The flow of HPV-L1-specific primed CD4+ helper Th2 lymphocytes from the lymphoid to the non-lymphoid compartment.
- Second term: The natural death of HPV-L1-specific primed CD4+ helper Th2 lymphocytes in the non-lymphoid compartment.

B LYMPHOCYTES

$$(12)\qquad \frac{d\left(B_N^L\right)}{dt} = \left(\omega_B \cdot s_B\right) - \left(d_B \cdot B_N^L\right) - \left(k_{B/V} \cdot \varphi\left(A^L\right) \cdot q_{B/V} \cdot V^L \cdot B_N^L\right) - \left(k_{B/P} \cdot q_{B/P} \cdot P_R^L \cdot B_N^L\right) \qquad \varphi\left(A^L\right) = \frac{1}{1 + e^{-k_{A1} \cdot \left(A^L - k_{A2}\right)}}$$

which can be translated as follows: instantaneously, the rate of change in the cell-population density of HPV-L1-specific, naïve (i.e. non-effector and non-proliferating) B lymphocytes, circulating in the lymphoid compartment is defined by:

- First term: The constant supply of naïve B lymphocytes to the lymphoid compartment.
- Second term: The natural death of naïve B lymphocytes in the lymphoid compartment.
- Third term: The transition of B lymphocytes from the state of naïve (i.e. non-effector, non-proliferating) cells to the state of pre-primed (i.e. non-effector but proliferating) cells, through the direct interaction with HPV-L1 virus-like particles (VLPs).

- Fourth term: The transition of B lymphocytes from the state of naïve (i.e. non-effector, non-proliferating) cells to the state of pre-primed (i.e. non-effector but proliferating) cells, through the interaction with HPV-L1-commited and reactive antigen-presenting cells (APCs).

$$(13)\quad \frac{d\left(B_O^L\right)}{dt} = \left(-d_O \cdot B_O^L\right) + \left(z_{B1} \cdot k_{B/V} \cdot \varphi\left(A^L\right) \cdot q_{B/V} \cdot V^L\Big|_{t-(n_{B1}\cdot\tau)} \cdot B_N^L\Big|_{t-(n_{B1}\cdot\tau)}\right)$$

$$+\left(z_{B1} \cdot k_{B/P} \cdot q_{B/P} \cdot P_R^L\Big|_{t-(n_{B1}\cdot\tau)} \cdot B_N^L\Big|_{t-(n_{B1}\cdot\tau)}\right) - \left(k_{B/H} \cdot q_{B/H} \cdot H_P^L \cdot B_O^L\right) \qquad \varphi\left(A^L\right) = \frac{1}{1+e^{-k_{A1}\cdot\left(A^L - k_{A2}\right)}}$$

which can be translated as follows: instantaneously, the rate of change in the cell-population density of HPV-L1-specific, pre-primed (i.e. non-effector but proliferating) B lymphocytes, circulating in the lymphoid compartment is defined by:

- First term: The natural death of HPV-L1-specific pre-primed B lymphocytes in the lymphoid compartment.
- Second term: The transition of B lymphocytes from the state of naïve (i.e. non-effector, non-proliferating) cells to the state of pre-primed (i.e. non-effector but proliferating) cells, through the direct interaction with HPV-L1 virus-like particles (VLPs).
- Third term: The transition of B lymphocytes from the state of naïve (i.e. non-effector, non-proliferating) cells to the state of pre-primed (i.e. non-effector but proliferating) cells, through the interaction with HPV-L1-commited and reactive antigen-presenting cells (APCs).
- Fourth term: The transition of B lymphocytes from the state of pre-primed (i.e. non-effector but proliferating) cells to the state of fully primed (effector and proliferating) cells, through the interaction with primed CD4+ helper Th2 lymphocytes.

$$(14)\qquad \frac{d\left(B_F^L\right)}{dt} = \left(-d_F \cdot B_F^L\right) + \left(z_{B2} \cdot k_{B/H} \cdot q_{B/H} \cdot H_P^L\Big|_{t-(n_{B2}\cdot\tau)} \cdot B_O^L\Big|_{t-(n_{B2}\cdot\tau)}\right) - \left(v_S \cdot B_F^L\right) - \left(v_K \cdot B_F^L\right)$$

which can be translated as follows: instantaneously, the rate of change in the cell-population density of HPV-L1-specific, primed (i.e. effector and proliferating) B lymphocytes, circulating in the lymphoid compartment is defined by:

- First term: The natural death of HPV-L1-specific fully primed B lymphocytes in the lymphoid compartment.
- Second term: The transition of HPV-L1-specific B lymphocytes from the state of pre-primed (i.e. non-effector but proliferating) cells to the state of fully primed (effector and proliferating) cells, through the interaction with primed CD4+ helper Th2 lymphocytes.
- Third term: The transition of HPV-L1-specific B lymphocytes from the s state of fully primed (effector and proliferating) cells to the state of plasmocytes.
- Fourth term: The transition of HPV-L1-specific B lymphocytes from the state of fully primed (effector and proliferating) cells to the state of memory-precursor cells.

$$(15)\qquad \frac{d\left(B_S^L\right)}{dt} = \left(v_S \cdot B_F^L\right) - \left(d_S \cdot B_S^L\right) + \left(z_M \cdot k_{M/P} \cdot q_{M/P} \cdot P_R^L\Big|_{t-(n_M\cdot\tau)} \cdot B_M^L\Big|_{t-(n_M\cdot\tau)}\right)$$

which can be translated as follows: instantaneously, the rate of change in the cell-population density of HPV-L1-specific plasmocytes circulating in the lymphoid compartment is defined by:

- First term: The transition of HPV-L1-specific B lymphocytes from the s state of fully primed (effector and proliferating) cells to the state of plasmocytes.
- Second term: The natural death of HPV-L1-specific plasmocytes in the lymphoid compartment.
- Third term: The transition of HPV-L1-specific B lymphocytes from the state of memory (i.e. non-effector, non-proliferating) cells to the state of plasmocytes, through the interaction with HPV-L1-commited and reactive antigen-presenting cells (APCs).

$$(16) \qquad \frac{d\left(B_K^L\right)}{dt} = \left(\overline{v_K} \cdot \overline{B_F^L}\right) - \left(\overline{d_K} \cdot \overline{B_K^L}\right) - \left(\overline{v_M} \cdot \overline{B_K^L}\right) - \left(\overline{v_L} \cdot \overline{B_K^L}\right)$$

which can be translated as follows: instantaneously, the rate of change in the cell-population density of HPV-L1-specific memory-precursor B lymphocytes circulating in the lymphoid compartment is defined by:

- First term: The transition of HPV-L1-specific B lymphocytes from the state of fully primed cells to the state of memory-precursor cells.
- Second term: The natural death of HPV-L1-specific memory-precursor B lymphocytes in the lymphoid compartment.
- Third term: The transition of HPV-L1-specific B lymphocytes from the state of memory-precursor cells to the state of memory cells.
- Fourth term: The transition of HPV-L1-specific B lymphocytes from the state of memory-precursor cells to the state of long-lived bone-marrow cells.

$$(17)\qquad \frac{d\left(B_M^L\right)}{dt} = \left(v_M \cdot B_K^L\right) - \left(d_M \cdot B_M^L\right) - \left(k_{M/P} \cdot q_{M/P} \cdot P_R^L \cdot B_M^L\right)$$

which can be translated as follows: instantaneously, the rate of change in the cell-population density of HPV-L1-specific memory B lymphocytes circulating in the lymphoid compartment is defined by:

- First term: The transition of HPV-L1-specific B lymphocytes from the state of memory-precursor cells to the state of memory cells.
- Second term: The natural death of HPV-L1-specific memory B lymphocytes in the lymphoid compartment.
- Third term: The transition of HPV-L1-specific B lymphocytes from the state of memory (i.e. non-effector, non-proliferating) cells to the state of plasmocytes, through the interaction with HPV-L1-commited and reactive antigen-presenting cells (APCs).

$$(18)\qquad \frac{d\left(B_L^L\right)}{dt} = \left(v_L \cdot B_K^L\right) - \left(d_L \cdot B_L^L\right)$$

which can be translated as follows: instantaneously, the rate of change in the cell-population density of HPV-L1-specific long-lived B lymphocytes residing in the bone-marrow is defined by:

- First term: The transition of HPV-L1-specific B lymphocytes from the state of memory-precursor cells to the state of long-lived bone-marrow cells.
- Second term: The natural death of HPV-L1-specific long-lived B lymphocytes residing in the bone-marrow.

CIRCULATING IgG IMMUNOGLOBULINS

$$(19)\qquad \frac{d\left(C^{L}\right)}{dt} = \left(\overline{r_S \cdot B_S^L}\right) + \left(\overline{r_L \cdot B_L^L}\right) - \left(\overline{d_C \cdot C^L}\right) - \left(\overline{f_C \cdot C^L}\right)$$

which can be translated as follows: instantaneously, the rate of change in the concentration of anti-HPV-L1 IgG immunoglobulins circulating in the lymphoid compartment is defined by:

- First term: The immunoglobulin production capacity of the HPV-L1-specific plasmocytes circulating in the lymphoid compartment.
- Second term: The immunoglobulin production capacity of the HPV-L1-specific long-lived B lymphocytes residing in the bone-marrow.
- First term: The natural decay of the anti-HPV-L1 IgG immunoglobulins circulating in the lymphoid compartment.
- Second term: The flow of anti-HPV-L1 IgG immunoglobulins from the lymphoid to the non-lymphoid compartment.

$$(20)\qquad \frac{d\left(C^{N}\right)}{dt} = \left(\overline{f_C \cdot C^L}\right) - \left(\overline{d_C \cdot C^N}\right)$$

which can be translated as follows: instantaneously, the rate of change in the concentration of anti-HPV-L1 IgG immunoglobulins circulating in the non-lymphoid compartment is defined by:

- First term: The flow of anti-HPV-L1 IgG immunoglobulins from the lymphoid to the non-lymphoid compartment.
- Second term: The natural decay of the anti-HPV-L1 IgG immunoglobulins circulating in the non-lymphoid compartment.

APPENDIX 5

SNAPSHOTS OF THE MULTI-AGENT SIMULATOR

(FIRST OF TWO PARTS)

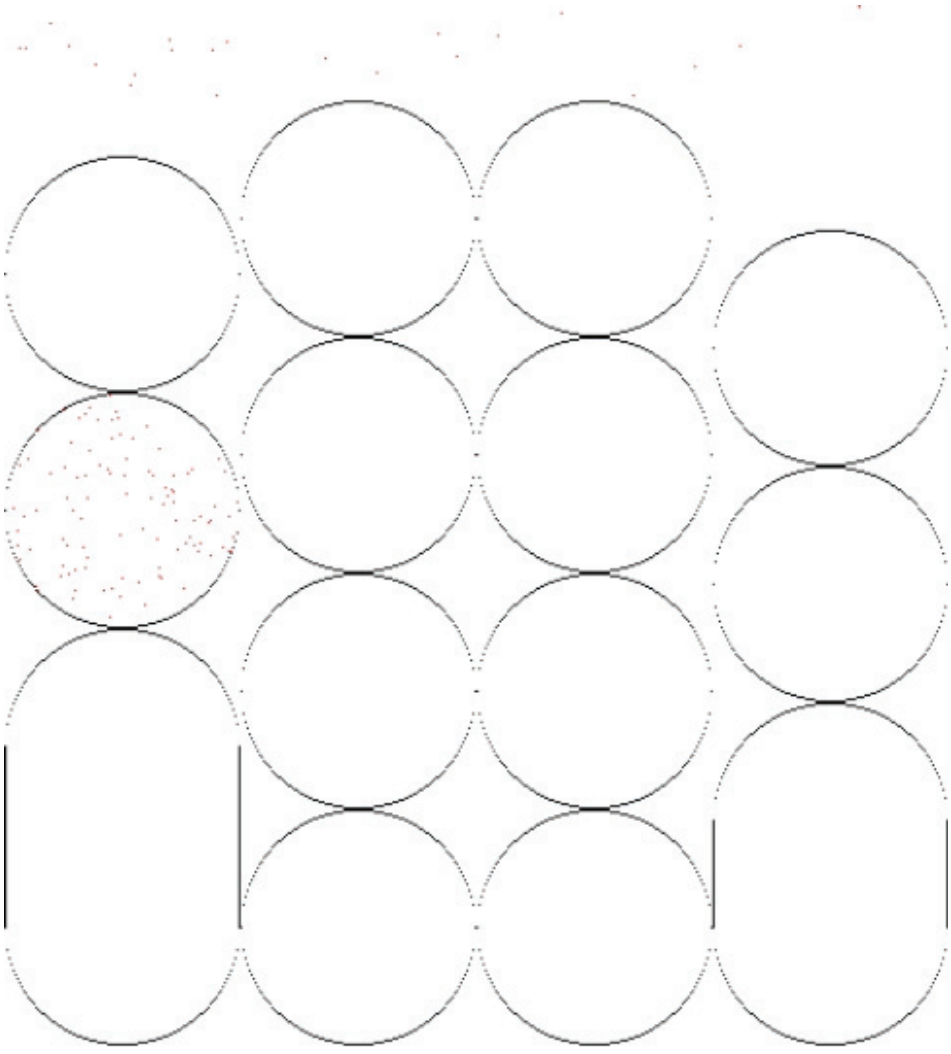

APPENDIX 5

SNAPSHOTS OF THE MULTI-AGENT SIMULATOR

(SECOND OF TWO PARTS)

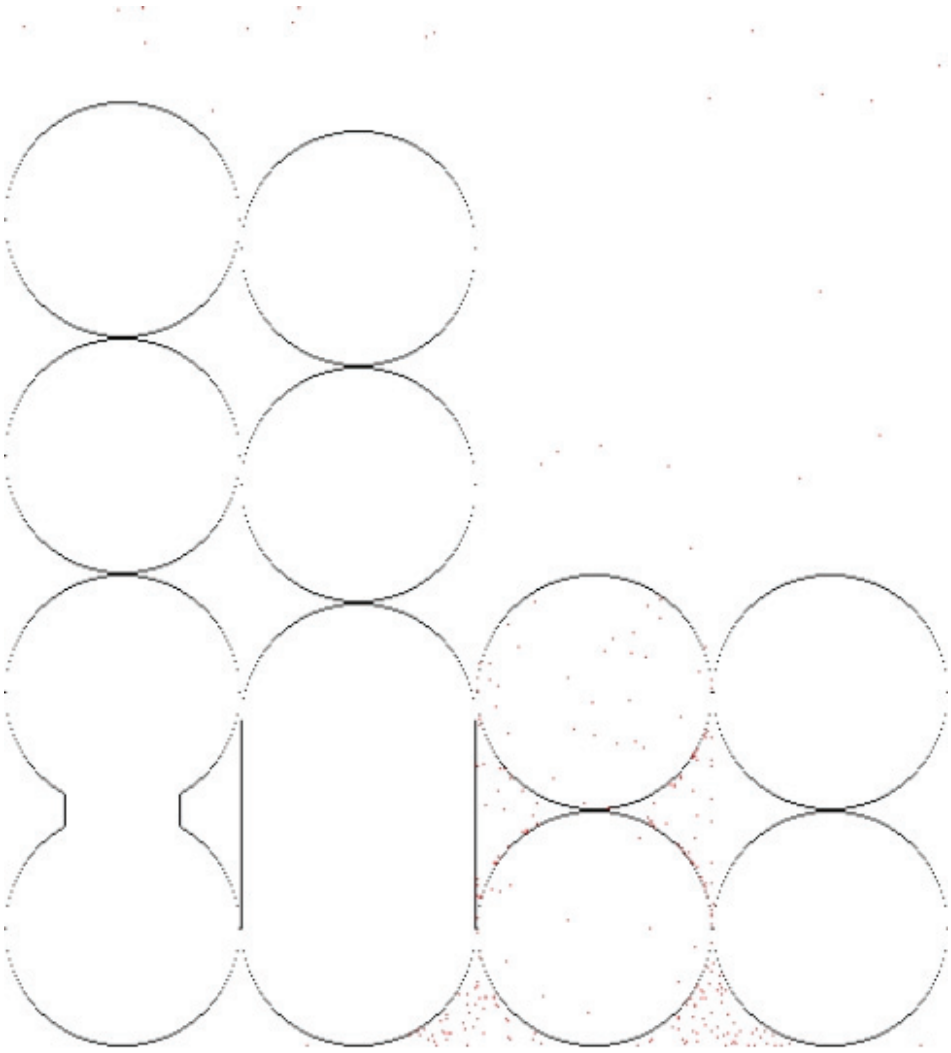

REFERENCES

[1] Cates W, Jr. Estimates of the incidence and prevalence of sexually transmitted diseases in the United States. American Social Health Association Panel. Sex Transm Dis. 1999; 26(4):Suppl:S2-7.
[2] Stanley M, Lowy DR, Frazer I. Chapter 12: Prophylactic HPV vaccines: Underlying mechanisms. Vaccine. 2006 Aug 21;24 Suppl 3:S106-13.
[3] Ada G. Vaccines and vaccination. N Engl J Med. 2001 Oct 4;345(14):1042-53.
[4] Steinbrook R. The potential of human papillomavirus vaccines. N Engl J Med. 2006 Mar 16;354(11):1109-12.
[5] Clifford G, Villa LL et al. Chapter 3: HPV type-distribution in women with and without cervical neoplastic diseases. Vaccine. 2006 Aug 21;24 Suppl 3:S26-34.
[6] Parkin DM, Bray F. Chapter 2: The burden of HPV-related cancers. Vaccine. 2006 Aug 21;24 Suppl 3:S11-25.
[7] Munoz N, Gissmann L et al. Chapter 1: HPV in the etiology of human cancer. Vaccine. 2006 Aug 21;24S3:S1-S10.
[8] Hebner CM, Laimins LA. Human papillomaviruses: basic mechanisms of pathogenesis and oncogenicity. Rev Med Virol. 2006 Mar-Apr;16(2):83-97.
[9] Derkay CS. Task force on recurrent respiratory papillomas. A preliminary report. Arch Otolaryngol Head Neck Surg. 1995 Dec; 121(12):1386-91.
[10] Frazer IH. Prevention of cervical cancer through papillomavirus vaccination. Nat Rev Immunol. 2004 Jan;4(1):46-54.
[11] Stanley M. Immune responses to human papillomavirus. Vaccine. 2006 Mar 30;24 Suppl 1:S16-22.
[12] Koutsky LA, Harper DM. Chapter 13: Current findings from prophylactic HPV vaccine trials. Vaccine. 2006 Aug 21;24 Suppl 3:S114-21.
[13] Nardelli-Haefliger D, De Grandi P et al. Specific antibody levels at the cervix during the menstrual cycle of women vaccinated with human papillomavirus 16 virus-like particles. J Natl Cancer Inst. 2003 Aug 6;95(15):1128-37.
[14] Reeves WC, Unger ER et al. National registry for juvenile-onset recurrent respiratory papillomatosis. Arch Otolaryngol Head Neck Surg. 2003 Sep;129(9):976-82.
[15] Campisi P, Simpson K et al. The epidemiology of juvenile onset recurrent respiratory papillomatosis derived from a population level national database. Laryngoscope. 2010 Jun;120(6):1233-45.
[16] http://rrpr.de/ (last accessed on January 2, 2011)
[17] Armstrong LR, Reeves WC et al. Incidence and prevalence of recurrent respiratory papillomatosis among children in Atlanta and Seattle. Clin Infect Dis. 2000 Jul;31(1):107-9.
[18] Derkay CS. Task force on recurrent respiratory papillomas. A preliminary report. Arch Otolaryngol Head Neck Surg. 1995 Dec;121(12):1386-91.
[19] Bomholt A. Laryngeal papillomas with adult onset. An epidemiological study from the Copenhagen region. Acta Otolaryngol. 1988 Jul-Aug;106(1-2):140-4.
[20] Armstrong LR, Derkay CS, Reeves WC. Initial results from the national registry for juvenile-onset recurrent respiratory papillomatosis. RRP Task Force. Arch Otolaryngol Head Neck Surg. 1999 Jul;125(7):743-8.
[21] Kashima H, Hruban RH et al. Sites of predilection in recurrent respiratory papillomatosis. Ann Otol Rhinol Laryngol. 1993 Aug;102(8 Pt 1):580-3.
[22] Kimberlin DW, Malis DJ. Juvenile onset recurrent respiratory papillomatosis: possibilities for successful antiviral therapy. Antiviral Res. 2000 Feb;45(2):83-93.
[23] Cutts FT, Markowitz L et al. Human papillomavirus and HPV vaccines: a review. Bull World Health Organ. 2007 Sep;85(9):719-26.
[24] Cooper M. Papillomata of the vocal folds: a review. J Speech Hear Disord. 1971 Feb;36(1):51-60.
[25] Soldatski IL, Schepin NV et al. Tracheal, bronchial, and pulmonary papillomatosis in children. Laryngoscope. 2005 Oct;115(10):1848-54.
[26] Cole RR, Myer CM 3rd, Cotton RT. Tracheotomy in children with recurrent respiratory papillomatosis. Head Neck. 1989 May-Jun;11(3):226-30.
[27] Reeves WC, Unger ER et al. National registry for juvenile-onset recurrent respiratory papillomatosis. Arch Otolaryngol Head Neck Surg. 2003 Sep;129(9):976-82.
[28] Zawadzka-Głos L, Brzewski M et al. Lower airway papillomatosis in children. Int J Pediatr Otorhinolaryngol. 2003 Oct;67(10):1117-21.
[29] Derkay CS. Recurrent respiratory papillomatosis. Laryngoscope. 2001 Jan;111(1):57-69.
[30] Abramson AL, Steinberg BM et al. Latent Human Papillomavirus infection is comparable in the larynx and trachea. J Med Virol. 2004 Mar;72(3):473-7.
[31] Cason J, Best JM et al. Perinatal infection and persistence of human papillomavirus types 16 and 18 in infants. J Med Virol. 1995 Nov;47(3):209-18.
[32] Rice PS, Best JM et al. High prevalence of human papillomavirus type 16 infection among children. J Med Virol. 2000 May;61(1):70-5.
[33] Miller CS, Johnstone BM. Human papillomavirus as a risk factor for oral squamous cell carcinoma: a meta-analysis, 1982-1997. Oral Surg Oral Med Oral Pathol Oral Radiol Endod. 2001 Jun;91(6):622-35.
[34] Borkowski G, Luckhaupt H et al. Recurrent respiratory papillomatosis associated with gastroesophageal reflux disease in children. Eur Arch Otorhinolaryngol. 1999;256(7):370-2.

[35] McKenna M, Brodsky L. Extraesophageal acid reflux and recurrent respiratory papilloma in children. Int J Pediatr Otorhinolaryngol. 2005 May;69(5):597-605.
[36] Pignatari SS, De Marco EK et al. Gastroesophageal reflux in patients with recurrent laryngeal papillomatosis. Braz J Otorhinolaryngol. 2007 Mar-Apr;73(2):210-4.
[37] Wiatrak BJ, Lewis L et al. Recurrent respiratory papillomatosis: a longitudinal study comparing severity associated with human papilloma viral types 6 and 11 and other risk factors in a large pediatric population. Laryngoscope. 2004 Nov;114(11 Pt 2 Suppl 104):1-23.
[38] Rabah R, Gregoire L et al. Human papillomavirus-11-associated recurrent respiratory papillomatosis is more aggressive than human papillomavirus-6-associated disease. Pediatr Dev Pathol. 2001 Jan-Feb;4(1):68-72.
[39] Armstrong LR, Derkay CS, Reeves WC. Initial results from the national registry for juvenile-onset recurrent respiratory papillomatosis. RRP Task Force. Arch Otolaryngol Head Neck Surg. 1999 Jul;125(7):743-8.
[40] Goon P, Sudhoff H et al. Recurrent respiratory papillomatosis: an overview of current thinking and treatment. Eur Arch Otorhinolaryngol. 2008 Feb;265(2):147-51.
[41] Dmochowski L, Dreyer DA et al. A study of submicroscopic structure and of virus particles in cells of human laryngeal papillomas. Tex Rep Biol Med. 1964;22:454-91.
[42] Boyle WF, Lennette EH et al. Electron microscopic identification of papova virus in laryngeal papilloma. Laryngoscope. 1973 Jul;83(7):1102-8.
[43] Costa J, Bauer WC et al. Presence of human papilloma viral antigens in juvenile multiple laryngeal papilloma. Am J Clin Pathol. 1981 Feb;75(2):194-7.
[44] Gissmann L, zur Hausen H. Molecular cloning and characterization of human papilloma virus DNA derived from a laryngeal papilloma. J Virol. 1982 Oct;44(1):393-400.
[45] Gissmann L, zur Hausen H et al. Human papillomavirus types 6 and 11 DNA sequences in genital and laryngeal papillomas and in some cervical cancers. Proc Natl Acad Sci U S A. 1983 Jan;80(2):560-3.
[46] Corbitt G, Farrington WT et al. Human papillomavirus (HPV) genotypes associated with laryngeal papilloma. J Clin Pathol. 1988 Mar;41(3):284-8.
[47] Dickens P, Larkin S et al. Human papillomavirus 6, 11, and 16 in laryngeal papillomas. J Pathol. 1991 Nov;165(3):243-6.
[48] Reeves WC, Unger ER et al. National registry for juvenile-onset recurrent respiratory papillomatosis. Arch Otolaryngol Head Neck Surg. 2003 Sep;129(9):976-82.
[49] Bouwes Bavinck JN, Berkhout RJ. HPV infections and immunosuppression. Clin Dermatol. 1997 May-Jun;15(3):427-37.
[50] Sun XW, Wright TC Jr et al. Human papillomavirus infection in women infected with the human immunodeficiency virus. N Engl J Med. 1997 Nov 6;337(19):1343-9.
[51] Palefsky JM, Holly EA. Chapter 6: Immunosuppression and co-infection with HIV. J Natl Cancer Inst Monogr. 2003;(31):41-6.
[52] Scott M, Nakagawa M, Moscicki AB. Cell-mediated immune response to human papillomavirus infection. Clin Diagn Lab Immunol. 2001 Mar;8(2):209-20.
[53] Ferenczy A, Hankins C et al. Human papillomavirus and HIV coinfection and the risk of neoplasias of the lower genital tract: a review of recent developments. CMAJ. 2003 Sep 2;169(5):431-4.
[54] Gerein V, Pfister H et al. Children and partners of patients with recurrent respiratory papillomatosis have no evidence of the disease during long-term observation. Int J Pediatr Otorhinolaryngol. 2006 Dec;70(12):2061-6.
[55] Miller EM. Changes in serum immunity during pregnancy. Am J Hum Biol. 2009 May-Jun;21(3):401-3.
[56] Reinhard G, Ruecker AV et al. Shifts in the TH1/TH2 balance during human pregnancy correlate with apoptotic changes. Biochem Biophys Res Commun. 1998 Apr 28;245(3):933-8.
[57] Hoshimoto K, Inaba N et al. Changes in plasma soluble CD26 and CD30 during pregnancy: markers of Th1/Th2 balance? Gynecol Obstet Invest. 2000;50(4):260-3.
[58] Szekeres-Bartho J. Immunological relationship between the mother and the fetus. Int Rev Immunol. 2002 Nov-Dec;21(6):471-95.
[59] Wiatrak BJ. Overview of recurrent respiratory papillomatosis. Curr Opin Otolaryngol Head Neck Surg. 2003 Dec;11(6):433-41.
[60] Gerein V, Pfister H et al. Children and partners of patients with recurrent respiratory papillomatosis have no evidence of the disease during long-term observation. Int J Pediatr Otorhinolaryngol. 2006 Dec;70(12):2061-6.
[61] Shah KV, Kashima HK et al. Risk factors for juvenile onset recurrent respiratory papillomatosis. Pediatr Infect Dis J. 1998 May;17(5):372-6.
[62] Kashima HK, Shah K et al. A comparison of risk factors in juvenile-onset and adult-onset recurrent respiratory papillomatosis. Laryngoscope. 1992 Jan;102(1):9-13.
[63] Stamataki S, Ferekidis E et al. Juvenile recurrent respiratory papillomatosis: still a mystery disease with difficult management. Head Neck. 2007 Feb;29(2):155-62.
[64] Smith HG, Strong MS et al. Topical chemotherapy of recurrent respiratory papillomatosis. A preliminary report. Ann Otol Rhinol Laryngol. 1980 Sep-Oct;89(5 Pt 1):472-8.

[65] Steinberg BM. Recurrent Respiratory Papillomatosis: Clinical and Molecular Aspects. Contribution to HPV Today: Newsletter on Human Papillomavirus. No 10. January 2007. p. 8-10.
[66] Rosen CA, Bryson PC. Indole-3-carbinol for recurrent respiratory papillomatosis: long-term results. J Voice. 2004 Jun;18(2):248-53.
[67] Gerein V, Pfister H, et al. Use of interferon-alpha in recurrent respiratory papillomatosis: 20-year follow-up. Ann Otol Rhinol Laryngol. 2005 Jun;114(6):463-71.
[68] Szeps M, Dalianis T, et al. Human papillomavirus, viral load and proliferation rate in recurrent respiratory papillomatosis in response to alpha interferon treatment. J Gen Virol. 2005 Jun;86(Pt 6):1695-702.
[69] Shehab N, Sweet BV, Hogikyan ND. Cidofovir for the treatment of recurrent respiratory papillomatosis: a review of the literature. Pharmacotherapy. 2005 Jul;25(7):977-89.
[70] Rogan EG. The natural chemopreventive compound indole-3-carbinol: state of the science. In Vivo. 2006 Mar-Apr;20(2):221-8.
[71] Man LX, Statham MM, Rosen CA. Mucosal bridge and pitting of the true vocal fold: an unusual complication of cidofovir injection. Ann Otol Rhinol Laryngol. 2010 Apr;119(4):236-8.
[72] Harcourt JP, Worley G, Leighton SE. Cimetidine treatment for recurrent respiratory papillomatosis. Int J Pediatr Otorhinolaryngol. 1999 Dec 5;51(2):109-13.
[73] Abramson AL, Steinberg BM et al. Latent Human Papillomavirus infection is comparable in the larynx and trachea. J Med Virol. 2004 Mar;72(3):473-7.
[74] Jahan-Parwar B, Berke GS et al. Development of a canine model for recurrent respiratory papillomatosis. Ann Otol Rhinol Laryngol. 2003 Dec;112(12):1011-3.
[75] Nicholls PK, Stanley MA et al. Naturally occurring, nonregressing canine oral papillomavirus infection: host immunity, virus characterization, and experimental infection. Virology. 1999 Dec 20;265(2):365-74.
[76] DiMasi JA, Hansen RW, Grabowski HG. The price of innovation: new estimates of drug development costs. J Health Econ. 2003 Mar;22(2):151-85.
[77] Witten M. A return to time, cells, systems and aging: II. Relational and reliability theoretic approaches to the study of senescence in living systems. Mech Ageing Dev. 1984 Oct 31;27(3):323-40.
[78] Eisenberg M, Samuels M, DiStefano JJ 3rd. L-T4 bioequivalence and hormone replacement studies via feedback control simulations. Thyroid. 2006 Dec;16(12):1279-92.
[79] Tomb JF, Venter JC et al. The complete genome sequence of the gastric pathogen Helicobacter pylori. Nature. 1997 Aug 7;388(6642):539-47.
[80] Nagel T, Gimbrone MA Jr et al. Vascular endothelial cells respond to spatial gradients in fluid shear stress by enhanced activation of transcription factors. Arterioscler Thromb Vasc Biol. 1999 Aug;19(8):1825-34.
[81] Cooper WG. Roles of evolution, quantum mechanics and point mutations in origins of cancer. Cancer Biochem Biophys. 1993 Jun;13(3):147-70.
[82] Giorgi F, Bruni LE, Maggio R. Receptor oligomerization as a process modulating cellular semiotics. Biosemiotics. 2010 Aug; 3(2):157-76.
[83] Boulé NG, Sigal RJ et al. Effects of exercise on glycemic control and body mass in type 2 diabetes mellitus: a meta-analysis of controlled clinical trials. JAMA. 2001 Sep 12;286(10):1218-27.
[84] Mehl LE, Manchanda S. Use of chaos theory and complex systems modeling to study alcohol effects on fetal condition. Comput Biomed Res. 1993 Oct;26(5):424-48.
[85] Roach JC, Galas DJ et al. Analysis of genetic inheritance in a family quartet by whole-genome sequencing. Science. 2010 Apr 30;328(5978):636-9.
[86] Dietz K, Heesterbeek JA. Daniel Bernoulli's epidemiological model revisited. Math Biosci. 2002 Nov-Dec;180:1-21.
[87] Cojocaru MG, Bauch CT, Johnston MD. Dynamics of vaccination strategies via projected dynamical systems. Bull Math Biol. 2007 Jul;69(5):1453-76.
[88] Noble D. Cardiac action and pacemaker potentials based on the Hodgkin-Huxley equations. Nature. 1960 Nov 5;188:495-7.
[89] Gadêlha H, Kirkman-Brown JC et al. Nonlinear instability in flagellar dynamics: a novel modulation mechanism in sperm migration? J R Soc Interface. 2010 Dec 6;7(53):1689-97.
[90] Fletcher W, Yang Z. INDELible: a flexible simulator of biological sequence evolution. Mol Biol Evol. 2009 Aug;26(8):1879-88.
[91] Calvano SE, Lowry SF et al. A network-based analysis of systemic inflammation in humans. Nature. 2005 Oct 13;437(7061):1032-7.
[92] Heo J, Goddard WA 3rd et al. Prediction of the 3D structure of FMRF-amide neuropeptides bound to the mouse MrgC11 GPCR and experimental validation. Chembiochem. 2007 Sep 3;8(13):1527-39.
[93] Hill AD, Kaznessis YN et al. SynBioSS: the synthetic biology modeling suite. Bioinformatics. 2008 Nov 1;24(21):2551-3.
[94] Bonneau R, Baliga NS et al. A predictive model for transcriptional control of physiology in a free living cell. Cell. 2007 Dec 28;131(7):1354-65.
[95] Schadt EE, Lusis AJ et al. An integrative genomics approach to infer causal associations between gene expression and disease. Nat Genet. 2005 Jul;37(7):710-7.

[96] Querec TD, Pulendran B et al. Systems biology approach predicts immunogenicity of the yellow fever vaccine in humans. Nat Immunol. 2009 Jan;10(1):116-25.
[97] Berger SI, Iyengar R. Role of systems pharmacology in understanding drug adverse events. Wiley Interdiscip Rev Syst Biol Med. 2010 Aug 27.
[98] Germain RN, Fraser ID et al. Systems Biology in Immunology: A Computational Modeling Perspective. Annu Rev Immunol. 2010 Apr 5. [Epub ahead of print]
[99] Louzoun Y. The evolution of mathematical immunology. Immunol Rev. 2007 Apr;216:9-20.
[100] Kim PS, Levy D, Lee PP. Modeling and simulation of the immune system as a self-regulating network. Methods Enzymol. 2009;467:79-109.
[101] Chavali AK, Papin JA et al. Characterizing emergent properties of immunological systems with multi-cellular rule-based computational modeling. Trends Immunol. 2008 Dec;29(12):589-99.
[102] Lundegaard C, Nielsen M et al. Modeling the adaptive immune system: predictions and simulations. Bioinformatics. 2007 Dec 15;23(24):3265-75.
[103] Rapin N, Lund O et al. Modelling the human immune system by combining bioinformatics and systems biology approaches. J Biol Phys. 2006 Oct;32(3-4):335-53.
[104] Forrest S, Beauchemin C. Computer immunology. Immunol Rev. 2007 Apr;216:176-97.
[105] Raman K, Bhat AG, Chandra N. A systems perspective of host-pathogen interactions: predicting disease outcome in tuberculosis. Mol Biosyst. 2010 Mar;6(3):516-30.
[106] Romanyukha AA, Rudnev SG, Sidorov IA. Energy cost of infection burden: an approach to understanding the dynamics of host-pathogen interactions. J Theor Biol. 2006 Jul 7;241(1):1-13.
[107] Sedaghat AR, Siliciano RF et al. Decay dynamics of HIV-1 depend on the inhibited stages of the viral life cycle. Proc Natl Acad Sci U S A. 2008 Mar 25;105(12):4832-7.
[108] Fraser C. HIV recombination: what is the impact on antiretroviral therapy? J R Soc Interface. 2005 Dec 22;2(5):489-503.
[109] Guardiola J, Izzo G, Vecchio A. Simulating the effect of vaccine-induced immune responses on HIV infection. Hum Immunol. 2003 Sep;64(9):840-51.
[110] Bovier PA, Loutan L et al. Predicted 30-year protection after vaccination with an aluminum-free virosomal hepatitis A vaccine. J Med Virol. 2010 Oct;82(10):1629-34.
[111] Wilson JN, Nokes DJ. Do we need 3 doses of hepatitis B vaccine? Vaccine. 1999 Jun 4;17(20-21):2667-73.
[112] Dong X, Androulakis IP et al. Agent-based modeling of endotoxin-induced acute inflammatory response in human blood leukocytes. PLoS One. 2010 Feb 18;5(2):e9249.
[113] Foteinou PT, Androulakis IP et al. Modeling endotoxin-induced systemic inflammation using an indirect response approach. Math Biosci. 2009 Jan;217(1):27-42.
[114] Wang G, Krueger GR, Buja LM. Mathematical model to simulate the cellular dynamics of infection with human herpesvirus-6 in EBV-negative infectious mononucleosis. J Med Virol. 2003 Dec;71(4):569-77.
[115] Marchuk GI, Bocharov GA et al. Mathematical model of antiviral immune response. I. Data analysis, generalized picture construction and parameters evaluation for hepatitis B. J Theor Biol. 1991 Jul 7;151(1):1-40.
[116] Smith AM, McCullers JA, Adler FR. Mathematical model of a three-stage innate immune response to a pneumococcal lung infection. J Theor Biol. 2011 Feb 11. [Epub ahead of print]
[117] Baltcheva I, Le Boudec JY et al. Lifelong dynamics of human CD4+CD25+ regulatory T cells: insights from in vivo data and mathematical modeling. J Theor Biol. 2010 Sep 21;266(2):307-22.
[118] Boissel JP, Dronne MA et al. Modelling methodology in physiopathology. Prog Biophys Mol Biol. 2008 May;97(1):28-39.
[119] The History of inoculation and vaccination for the prevention and treatment of disease. London ; Sydney : Burroughs Wellcome, [1914?] 304 p. [7] p. of plates : ill., maps, ports. (some col.) ; 18 cm. RNB health series.
[120] Frazer IH. Prevention of cervical cancer through papillomavirus vaccination. Nat Rev Immunol. 2004 Jan;4(1):46-54.
[121] Alexopoulou L, Flavell RA et al. Recognition of double-stranded RNA and activation of NF-kappaB by Toll-like receptor 3. Nature. 2001 Oct 18;413(6857):732-8.
[122] Fraillery D, Zosso N, Nardelli-Haefliger D. Rectal and vaginal immunization of mice with human papillomavirus L1 virus-like particles. Vaccine. 2009 Apr 14;27(17):2326-34.
[123] Scott M, Stites DP, Moscicki AB. Th1 cytokine patterns in cervical human papillomavirus infection. Clin Diagn Lab Immunol. 1999 Sep;6(5):751-5.
[124] de Jong A, van der Burg SH et al. Human papillomavirus type 16-positive cervical cancer is associated with impaired CD4+ T-cell immunity against early antigens E2 and E6. Cancer Res. 2004 Aug 1;64(15):5449-55.
[125] García-Piñeres A, Pinto LA et al. Cytokine and chemokine profiles following vaccination with human papillomavirus type 16 L1 Virus-like particles. Clin Vaccine Immunol. 2007 Aug;14(8):984-9.
[126] Lehner T, Anton PA. Mucosal immunity and vaccination against HIV. AIDS. 2002;16 Suppl 4:S125-32.
[127] Delves PJ, Roitt IM. The immune system. First of two parts. N Engl J Med. 2000 Jul 6;343(1):37-49.
[128] Lei YJ, Dong XP et al. Molecular epidemiological study on prevalence of human papillomaviruses in patients with common warts in Beijing area. Biomed Environ Sci. 2009 Feb;22(1):55-61.

[129] Hagiwara K, Hattori A et al. A genotype distribution of human papillomaviruses detected by polymerase chain reaction and direct sequencing analysis in a large sample of common warts in Japan. J Med Virol. 2005 Sep;77(1):107-12.
[130] Aubin F, Chosidow O et al. Presence and persistence of human papillomavirus types 1, 2, and 4 on emery boards after scraping off plantar warts. J Am Acad Dermatol. 2010 Jan;62(1):151-3.
[131] Yoo H, Lee KH et al. Detection and identification of human papillomavirus types isolated from Korean patients with flat warts. Microbiol Immunol. 2005;49(7):633-8.
[132] Rogers HD, Grossman ME et al. Acquired epidermodysplasia verruciformis. J Am Acad Dermatol. 2009 Feb;60(2):315-20.
[133] Begum S, Westra WH et al. Detection of human papillomavirus-16 in fine-needle aspirates to determine tumor origin in patients with metastatic squamous cell carcinoma of the head and neck. Clin Cancer Res. 2007 Feb 15;13(4):1186-91.
[134] Gillison ML, Sidransky D et al. Evidence for a causal association between human papillomavirus and a subset of head and neck cancers. J Natl Cancer Inst. 2000 May 3;92(9):709-20.
[135] Fakhry C, Gillison ML. Clinical implications of human papillomavirus in head and neck cancers. J Clin Oncol. 2006 Jun 10;24(17):2606-11.
[136] Ang KK, Gillison ML et al. Human papillomavirus and survival of patients with oropharyngeal cancer. N Engl J Med. 2010 Jul 1;363(1):24-35.
[137] Saunders NR, Silverman MS et al. Focal epithelial hyperplasia caused by human papillomavirus 13. Pediatr Infect Dis J. 2010 Jun;29(6):550-2.
[138] Falaki F, Pazooki N et al. Detection of human papilloma virus DNA in seven cases of focal epithelial hyperplasia in Iran. J Oral Pathol Med. 2009 Nov;38(10):773-6.
[139] Cuberos V, Sanchez GI et al. Molecular and serological evidence of the epidemiological association of HPV 13 with focal epithelial hyperplasia: a case-control study. J Clin Virol. 2006 Sep;37(1):21-6.
[140] Greenspan D, de Souza Y. Oral "hairy" leucoplakia in male homosexuals: evidence of association with both papillomavirus and a herpes-group virus. Lancet. 1984 Oct 13;2(8407):831-4.
[141] Allam JP, Novak N. Successful treatment of extensive human papillomavirus-associated oral leucoplakia with imiquimod. Br J Dermatol. 2008 Mar;158(3):644-6.
[142] McKay SP, Lancaster WD et al. Human papillomavirus (HPV) transcripts in malignant inverted papilloma are from integrated HPV DNA. Laryngoscope. 2005 Aug;115(8):1428-31.
[143] Beck JC, Bradford CR et al. Presence of human papillomavirus predicts recurrence of inverted papilloma. Otolaryngol Head Neck Surg. 1995 Jul;113(1):49-55.
[144] Furuta Y, Inuyama Y et al. Molecular pathologic study of human papillomavirus infection in inverted papilloma and squamous cell carcinoma of the nasal cavities and paranasal sinuses. Laryngoscope. 1991 Jan;101(1 Pt 1):79-85.
[145] Wiatrak BJ. Overview of recurrent respiratory papillomatosis. Curr Opin Otolaryngol Head Neck Surg. 2003 Dec;11(6):433-41.
[146] Lee JH, Smith RJ. Recurrent respiratory papillomatosis: pathogenesis to treatment. Curr Opin Otolaryngol Head Neck Surg. 2005 Dec;13(6):354-9.
[147] Derkay CS, Wiatrak B. Recurrent respiratory papillomatosis: a review. Laryngoscope. 2008 Jul;118(7):1236-47.
[148] Gallagher TQ, Derkay CS. Recurrent respiratory papillomatosis: update 2008. Curr Opin Otolaryngol Head Neck Surg. 2008 Dec;16(6):536-42.
[149] Kao PC, Blaszyk H et al. Esophageal squamous papillomatosis. Eur J Gastroenterol Hepatol. 2005 Nov;17(11):1233-7.
[150] Mosca S, Balzano A et al. Squamous papilloma of the esophagus: long-term follow up. J Gastroenterol Hepatol. 2001 Aug;16(8):857-61.
[151] Kibria R, Ali S et al. Esophageal squamous papillomatosis with dysplasia. Is there a role of balloon-based radiofrequency ablation therapy? Acta Gastroenterol Belg. 2009 Jul-Sep;72(3):373-6.
[152] Muñoz N, Meijer CJ et al. Epidemiologic classification of human papillomavirus types associated with cervical cancer. N Engl J Med. 2003 Feb 6;348(6):518-27.
[153] Muñoz N, Bosch X, Kaldor JM. Does human papillomavirus cause cervical cancer? The state of the epidemiological evidence. Br J Cancer. 1988 Jan;57(1):1-5.
[154] Bosch FX, Shah KV et al. Prevalence of human papillomavirus in cervical cancer: a worldwide perspective. International biological study on cervical cancer (IBSCC) Study Group. J Natl Cancer Inst. 1995 Jun 7;87(11):796-802.
[155] Walboomers JM, Muñoz N et al. Human papillomavirus is a necessary cause of invasive cervical cancer worldwide. J Pathol. 1999 Sep;189(1):12-9.
[156] Smith JS, Clifford GM et al. Human papillomavirus type distribution in invasive cervical cancer and high-grade cervical lesions: a meta-analysis update. Int J Cancer. 2007 Aug 1;121(3):621-32.
[157] Dürst M, zur Hausen H et al. A papillomavirus DNA from a cervical carcinoma and its prevalence in cancer biopsy samples from different geographic regions. Proc Natl Acad Sci U S A. 1983 Jun;80(12):3812-5.
[158] Boshart M, zur Hausen H et al. A new type of papillomavirus DNA, its presence in genital cancer biopsies and in cell lines derived from cervical cancer. EMBO J. 1984 May;3(5):1151-7.

[159] Tsunokawa Y, Sugimura T et al. Presence of human papillomavirus type-16 and type-18 DNA sequences and their expression in cervical cancers and cell lines from Japanese patients. Int J Cancer. 1986 Apr 15;37(4):499-503.
[160] Moscicki AB, Villa LL et al. Chapter 5: Updating the natural history of HPV and anogenital cancer. Vaccine. 2006 Aug 21;24 Suppl 3:S42-51.
[161] Doorbar J. Molecular biology of human papillomavirus infection and cervical cancer. Clin Sci (Lond). 2006 May;110(5):525-41.
[162] Muñoz N, Gissmann L et al. Chapter 1: HPV in the etiology of human cancer. Vaccine. 2006 Aug 31;24 Suppl 3:S3/1-10. Epub 2006 Jun 23..
[163] Quayle AJ. The innate and early immune response to pathogen challenge in the female genital tract and the pivotal role of epithelial cells. J Reprod Immunol. 2002 Oct-Nov;57(1-2):61-79.
[164] Wira CR, Shen L et al. Innate and adaptive immunity in female genital tract: cellular responses and interactions. Immunol Rev. 2005 Aug;206:306-35.
[165] Mestecky J, Moldoveanu Z, Russell MW. Immunologic uniqueness of the genital tract: challenge for vaccine development. Am J Reprod Immunol. 2005 May;53(5):208-14.
[166] Frazer IH. Prevention of cervical cancer through papillomavirus vaccination. Nat Rev Immunol. 2004 Jan;4(1):46-54.
[167] Ulmer JB, Valley U, Rappuoli R. Vaccine manufacturing: challenges and solutions. Nat Biotechnol. 2006 Nov;24(11):1377-83.
[168] Abadie V, Combadière B et al. Original encounter with antigen determines antigen-presenting cell imprinting of the quality of the immune response in mice. PLoS One. 2009 Dec 7;4(12):e8159.
[169] Pulendran B. Learning immunology from the yellow fever vaccine: innate immunity to systems vaccinology. Nat Rev Immunol. 2009 Oct;9(10):741-7.
[170] Steinman RM, Hemmi H. Dendritic cells: translating innate to adaptive immunity. Curr Top Microbiol Immunol. 2006;311:17-58.
[171] Shi Y, Devadas S et al. Granulocyte-macrophage colony-stimulating factor (GM-CSF) and T-cell responses: what we do and don't know. Cell Res. 2006 Feb;16(2):126-33.
[172] Zubler RH. Naive and memory B cells in T-cell-dependent and T-independent responses. Springer Semin Immunopathol. 2001 Dec;23(4):405-19.
[173] Delves PJ, Roitt IM. The immune system. Second of two parts. N Engl J Med. 2000 Jul 13;343(2):108-17.
[174] Gourley TS, Ahmed R et al. Generation and maintenance of immunological memory. Semin Immunol. 2004 Oct;16(5):323-33.
[175] Wrammert J, Ahmed R. Maintenance of serological memory. Biol Chem. 2008 May;389(5):537-9.
[176] Amanna IJ, Carlson NE, Slifka MK. Duration of humoral immunity to common viral and vaccine antigens. N Engl J Med. 2007 Nov 8;357(19):1903-15.
[177] Kim PS, Lee PP, Levy D. Modeling regulation mechanisms in the immune system. J Theor Biol. 2007 May 7;246(1):33-69.
[178] Gudmundsdottir H, Wells AD, Turka LA. Dynamics and requirements of T cell clonal expansion in vivo at the single-cell level: effector function is linked to proliferative capacity. J Immunol. 1999 May 1;162(9):5212-23.
[179] Heinrich PC, Schaper F et al. Principles of interleukin (IL)-6-type cytokine signalling and its regulation. Biochem J. 2003 Aug 15;374(Pt 1):1-20.
[180] Krammer PH, Arnold R, Lavrik IN. Life and death in peripheral T cells. Nat Rev Immunol. 2007 Jul;7(7):532-42.
[181] Sakaguchi S, Powrie F. Emerging challenges in regulatory T cell function and biology. Science. 2007 Aug 3;317(5838):627-9.
[182] Harro CD, Lowy DR et al. Safety and immunogenicity trial in adult volunteers of a human papillomavirus 16 L1 virus-like particle vaccine. J Natl Cancer Inst. 2001 Feb 21;93(4):284-92.
[183] Shampine LF, Thompson S. Solving DDEs in MATLAB. Applied Numerical Mathematics 37 (2001) 441–458.
[184] Minors DS. Physiology of red and white blood cells. Anaesthesia & intensive care medicine. Volume 5, Issue 5, 1 May 2004, Pages 174-178
[185] Scott JL, Davidson JG et al. Leukocyte labeling with 51 chromium. IV. The kinetics of chronic lymphocytic leukemic lymphocytes. Blood. 1973 Jan;41(1):155-62.
[186] Fulcher DA, Basten A. B cell life span: a review. Immunol Cell Biol. 1997 Oct;75(5):446-55.
[187] Amanna IJ, Carlson NE, Slifka MK. Duration of humoral immunity to common viral and vaccine antigens. N Engl J Med. 2007 Nov 8;357(19):1903-15.
[188] Gray D. Immunological memory: a function of antigen persistence. Trends Microbiol. 1993 May;1(2):39-41; discussion 41-2.
[189] Oehen S, Zinkernagel RM et al. Antivirally protective cytotoxic T cell memory to lymphocytic choriomeningitis virus is governed by persisting antigen. J Exp Med. 1992 Nov 1;176(5):1273-81.
[190] Gray D, Matzinger P. T cell memory is short-lived in the absence of antigen. J Exp Med. 1991 Nov 1;174(5):969-74.
[191] Bellier B, Klatzmann D et al. Turning immunological memory into amnesia by depletion of dividing T cells. Proc Natl Acad Sci U S A. 2003 Dec 9;100(25):15017-22.

[192] Maruyama M, Lam KP, Rajewsky K. Memory B-cell persistence is independent of persisting immunizing antigen. Nature. 2000 Oct 5;407(6804):636-42.
[193] Müllbacher A. The long-term maintenance of cytotoxic T cell memory does not require persistence of antigen. J Exp Med. 1994 Jan 1;179(1):317-21.
[194] Hem SL. Elimination of aluminum adjuvants. Vaccine. 2002 May 31;20 Suppl 3:S40-3.
[195] HogenEsch H. Mechanisms of stimulation of the immune response by aluminum adjuvants. Vaccine. 2002 May 31;20 Suppl 3:S34-9.
[196] Ho F, Khan M et al. Distinct short-lived and long-lived antibody-producing cell populations. Eur J Immunol. 1986 Oct;16(10):1297-301.
[197] Jacob J, Kassir R, Kelsoe G. In situ studies of the primary immune response to (4-hydroxy-3-nitrophenyl)acetyl. I. The architecture and dynamics of responding cell populations. J Exp Med. 1991 May 1;173(5):1165-75.
[198] Zubler RH. Naive and memory B cells in T-cell-dependent and T-independent responses. Springer Semin Immunopathol. 2001 Dec;23(4):405-19.
[199] Olsson SE et al. Induction of immune memory following administration of a prophylactic quadrivalent human papillomavirus (HPV) types 6/11/16/18 L1 virus-like particle (VLP) vaccine. Vaccine. 2007 Jun 21;25(26):4931-9.
[200] Villa LL et al. High sustained efficacy of a prophylactic quadrivalent human papillomavirus types 6/11/16/18 L1 virus-like particle vaccine through 5 years of follow-up. Br J Cancer. 2006 Dec 4;95(11):1459-66.
[201] Wiatrak BJ, Lewis L et al. Recurrent respiratory papillomatosis: a longitudinal study comparing severity associated with human papilloma viral types 6 and 11 and other risk factors in a large pediatric population. Laryngoscope. 2004 Nov;114(11 Pt 2 Suppl 104):1-23.
[202] Einstein MH, Dubin G et al. Comparison of the immunogenicity and safety of CervarixTM and Gardasil® human papillomavirus (HPV) cervical cancer vaccines in healthy women aged 18-45 years. Hum Vaccin. 2009 Oct;5(10):705-19.
[203] Rowhani-Rahbar A et al. Antibody responses in oral fluid after administration of prophylactic human papillomavirus vaccines. J Infect Dis. 2009 Nov 1;200(9):1452-5.
[204] Stanley M. Immune responses to human papillomavirus. Vaccine. 2006 Mar 30;24 Suppl 1:S16-22.
[205] Einstein MH, Dubin G et al. Comparison of the immunogenicity and safety of CervarixTM and Gardasil® human papillomavirus (HPV) cervical cancer vaccines in healthy women aged 18-45 years. Hum Vaccin. 2009 Oct;5(10):705-19.
[206] Ruiz W, Esser MT et al. Kinetics and isotype profile of antibody responses in rhesus macaques induced following vaccination with HPV 6, 11, 16 and 18 L1-virus-like particles formulated with or without Merck aluminum adjuvant. J Immune Based Ther Vaccines. 2005 Apr 20;3(1):2.
[207] Bryan JT, Brown DR et al. Human papillomavirus type 11 neutralization in the athymic mouse xenograft system: correlation with virus-like particle IgG concentration. J Med Virol. 1997 Nov;53(3):185-8.
[208] Gélinas JF, Manoukian J, Côté A. Lung involvement in juvenile onset recurrent respiratory papillomatosis: a systematic review of the literature. Int J Pediatr Otorhinolaryngol. 2008 Apr;72(4):433-52.
[209] Wu R, Steinberg BM et al. Epidermal growth factor-induced cyclooxygenase-2 expression is mediated through phosphatidylinositol-3 kinase, not mitogen-activated protein/extracellular signal-regulated kinase kinase, in recurrent respiratory papillomas. Clin Cancer Res. 2005 Sep 1;11(17):6155-61.
[210] Aparicio Gallego G, Antón Aparicio LM et al. Cyclooxygenase-2 (COX-2): a molecular target in prostate cancer. Clin Transl Oncol. 2007 Nov;9(11):694-702.
[211] Mann JR, DuBois RN. Cyclooxygenase-2 and gastrointestinal cancer. Cancer J. 2004 May-Jun;10(3):145-52.
[212] Smith MR, Kantoff PW et al. Celecoxib versus placebo for men with prostate cancer and a rising serum prostate-specific antigen after radical prostatectomy and/or radiation therapy. J Clin Oncol. 2006 Jun 20;24(18):2723-8.
[213] White WB, Verburg KM et al. Risk of cardiovascular events in patients receiving celecoxib: a meta-analysis of randomized clinical trials. Am J Cardiol. 2007 Jan 1;99(1):91-8.
[214] Chen LC, Ashcroft DM. Risk of myocardial infarction associated with selective COX-2 inhibitors: meta-analysis of randomised controlled trials. Pharmacoepidemiol Drug Saf. 2007 Jul;16(7):762-72.
[215] Khanna D, Khanna PP, Furst DE. COX-2 controversy: where are we and where do we go from here? Inflammopharmacology. 2005;13(4):395-402.
[216] Hildesheim A et al. Effect of human papillomavirus 16/18 L1 viruslike particle vaccine among young women with preexisting infection: a randomized trial. JAMA. 2007 Aug 15;298(7):743-53.
[217] Cutts FT et al. Human papillomavirus and HPV vaccines: a review. Bull World Health Organ. 2007 Sep;85(9):719-26.
[218] Derkay CS. Task force on recurrent respiratory papillomas. A preliminary report. Arch Otolaryngol Head Neck Surg. 1995 Dec;121(12):1386-91.
[219] Reeves WC, Unger ER, et al. National registry for juvenile-onset recurrent respiratory papillomatosis. Arch Otolaryngol Head Neck Surg. 2003 Sep;129(9):976-82.
[220] Frazer IH et al. HPV6b virus like particles are potent immunogens without adjuvant in man. Vaccine. 2000 Jan 6;18(11-12):1051-8.

[221] Jilg W, Schmidt M, Deinhardt F. Vaccination against hepatitis B: comparison of three different vaccination schedules. J Infect Dis. 1989 Nov;160(5):766-9.

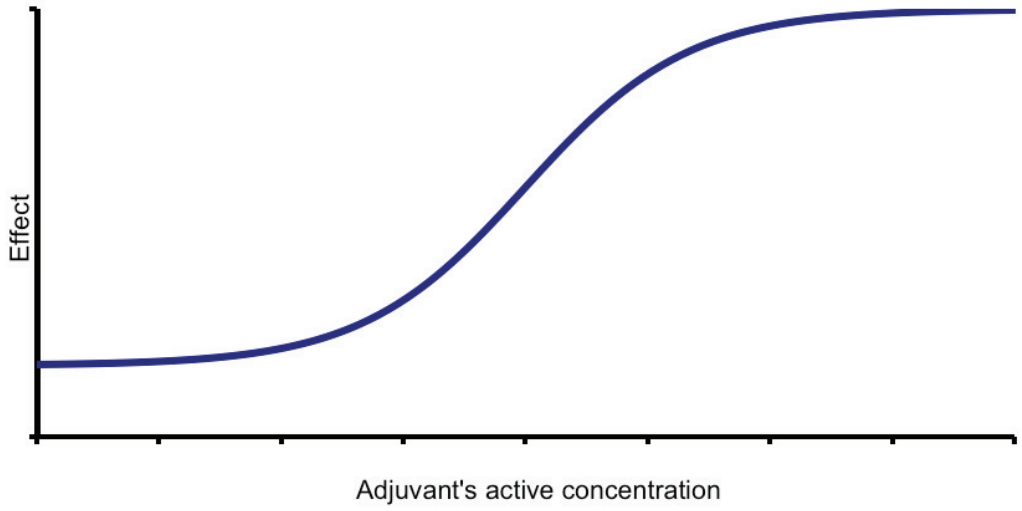

Figure 2. Schematic representation of the relationship used for computing the adjuvant's effect on the induced immune response. By using this empirical function we hypothesize the existence of a lower and an upper threshold. The former should reflect the fact that even when administered with no adjuvant the vaccine remains immunogenic, while the latter indicates the existence of a limit beyond of which no increase in the adjuvant's concentration would result in a higher immunogenicity. The quantitative characterization of this relationship constitutes one of the major challenges for the model's calibration process.

Implementing the model

The model contains a total of fifty-six parameters, which constitute the bricks permitting the establishment of quantitative relationships (equations) between the twenty variables. Once all the equations finely chipped and crafted, and the dimensional coherence of each one of them verified, the model (extensively presented in appendix 4) found itself ready for being implemented, calibrated and exploited. For doing so, we employed a Matlab® (2006R) simulation environment.

Conducting a simulation implies four fundamental steps: i) Attributing each one of the fifty-six parameters a value. ii) Defining the system's history (i.e. the behavior of each one of the twenty variables for any $t < t_0$; $t_0 = 0$). We did so by assuming that before any perturbation occurs (i.e. before the vaccine administration is simulated) the system finds itself in a steady state in which all the variables exhibit constant values (estimated through a procedure later explained in this

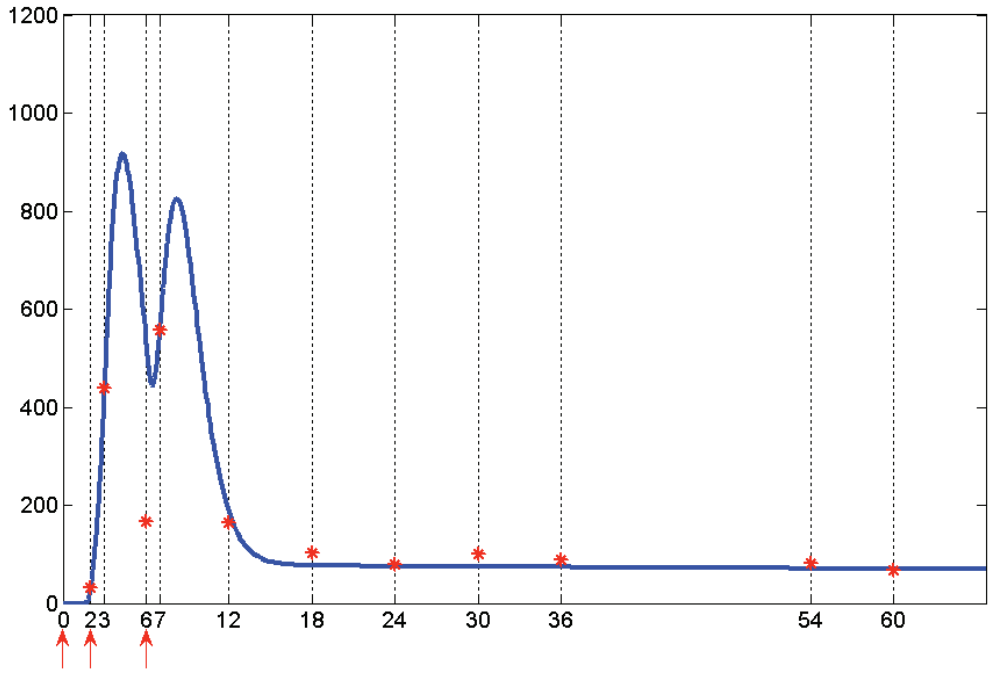

Figure 3. In-silico modeled (blue line) versus observed (red dots) immunogenicity of the quadrivalent HPV vaccine. **x-axis**: time, in months. **y-axis**: serum HPV-specific IgG titers, in milli-Merck units per mL. This curve was obtained during the model **calibration** process by using **set of parameters A**. (The red arrows represent the simulated vaccination schedule).

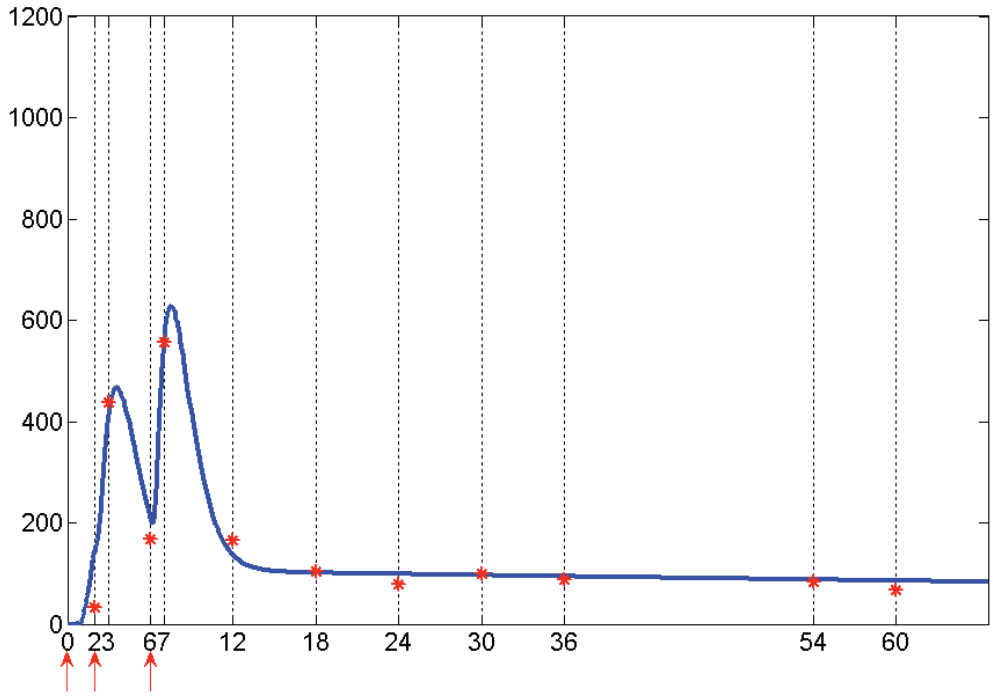

Figure 4. In-silico modeled (blue line) versus observed (red dots) immunogenicity of the quadrivalent HPV vaccine. **x-axis**: time, in months. **y-axis**: serum HPV-specific IgG titers, in milli-Merck units per mL. This curve was obtained during the model **calibration** process by using **set of parameters B**. (The red arrows represent the simulated vaccination schedule).

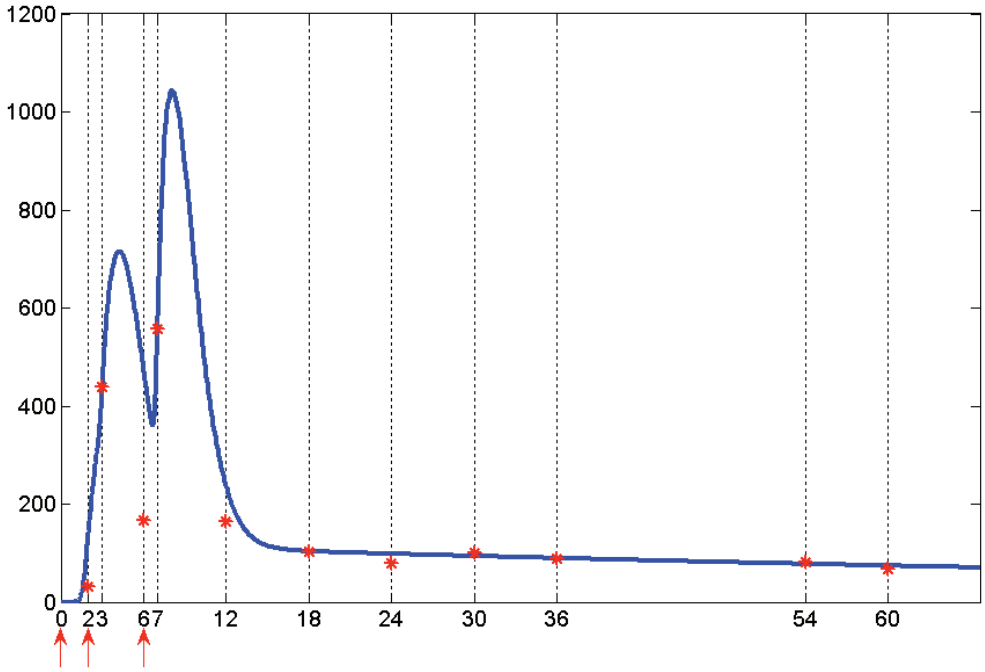

Figure 5. In-silico modeled (blue line) versus observed (red dots) immunogenicity of the quadrivalent HPV vaccine. **x-axis**: time, in months. **y-axis**: serum HPV-specific IgG titers, in milli-Merck units per mL. This curve was obtained during the model **calibration** process by using **set of parameters C**. (The red arrows represent the simulated vaccination schedule).

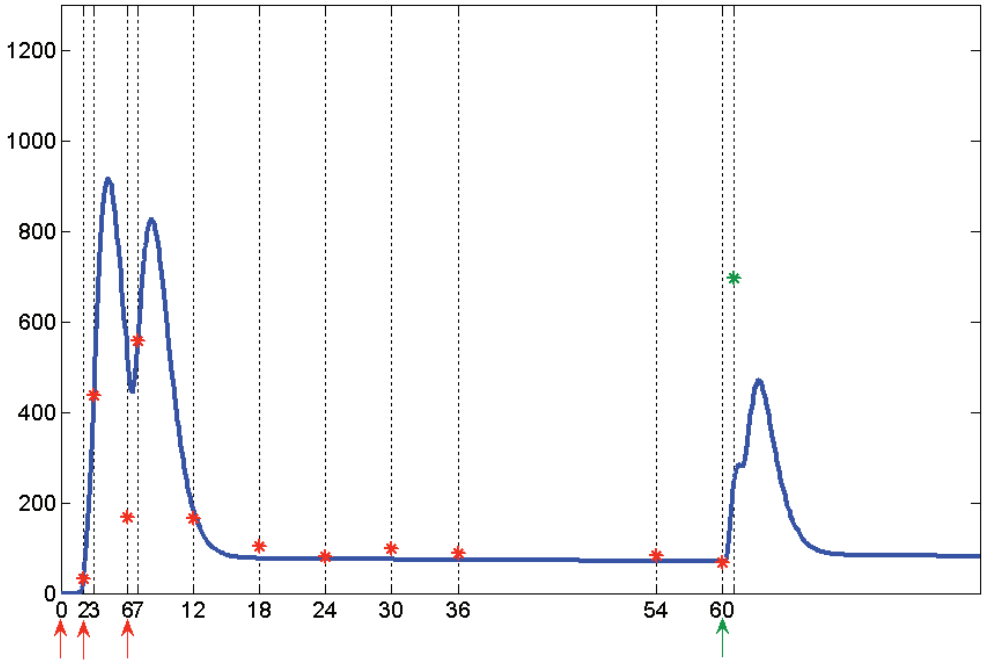

Figure 6. In-silico modeled (blue line) versus observed (green dot) immunogenic response following the late administration of a fourth dose (green arrow) of the quadrivalent HPV vaccine. **x-axis**: time in months. **y-axis**: serum HPV-specific IgG titers, in milli-Merck units per mL. This curve was obtained during the model **validation** process by using set of **parameters A**.

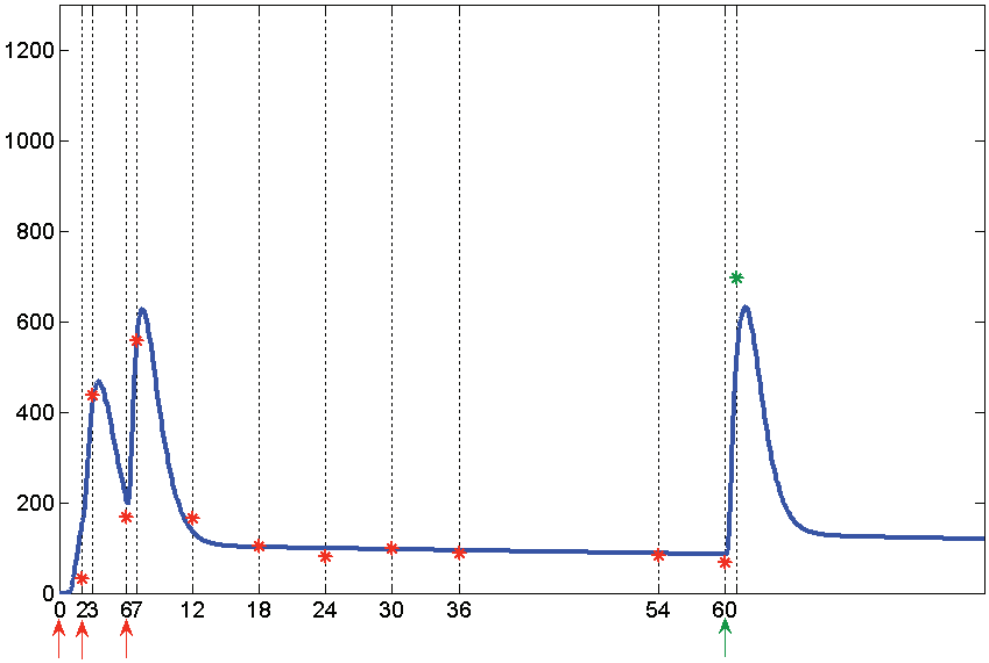

Figure 7. In-silico modeled (blue line) versus observed (green dot) immunogenic response following the late administration of a fourth dose (green arrow) of the quadrivalent HPV vaccine. **x-axis**: time in months. **y-axis**: serum HPV-specific IgG titers, in milli-Merck units per mL. This curve was obtained during the model **validation** process by using set of **parameters B**.

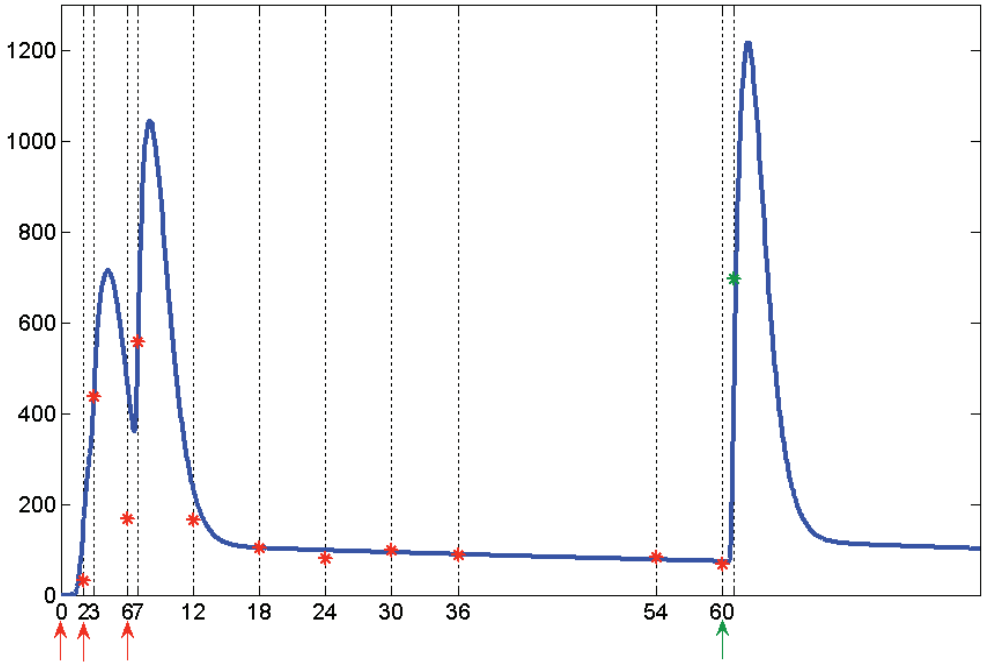

Figure 8. In-silico modeled (blue line) versus observed (green dot) immunogenic response following the late administration of a fourth dose (green arrow) of the quadrivalent HPV vaccine. **x-axis**: time in months. **y-axis**: serum HPV-specific IgG titers, in milli-Merck units per mL. This curve was obtained during the model **validation** process by using set of **parameters C**.

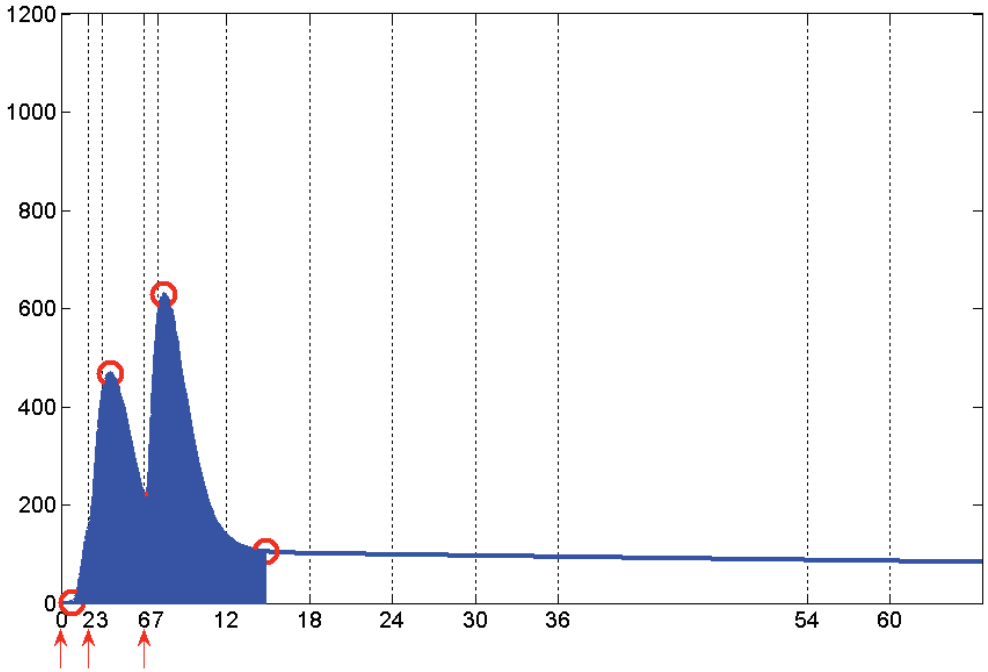

Figure 9. Schematic representation of the procedure used for quantitatively characterizing the modeled immunogenicity induced by the quadrivalent HPV vaccine. **x axis**: time, in months. **y axis**: serum HPV-specific IgG titers, in milli-Merck units per mL. Zone A (the blue shaded area) is defined as the double bell-shaped portion in which the highest IgG titers are observed. Zone B is defined as the remaining portion in which a less-intense plateau-like behavior takes place. The quantitative characterization consists in calculating the area under the curve for zone A and in calculating the mean IgG titer for zone B.

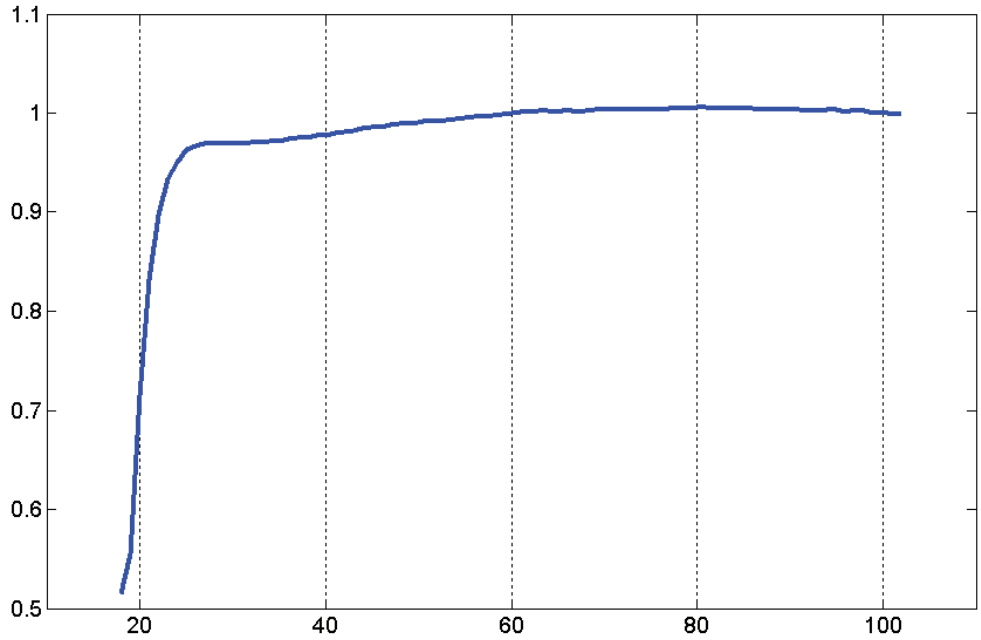

Figure 10. In-silico modeled effect of making vary the delay between the first and the second doses on the immunogenicity induced by the quadrivalent HPV vaccine. **x-axis**: time in days (λ) between the first and the second dose administration, in a 0-λ-180 vaccination schedule. **y-axis**: normalized (with respect to the 0-60-180 vaccination schedule) area under the curve for **zone A**. This curve was obtained by using set of parameters B.

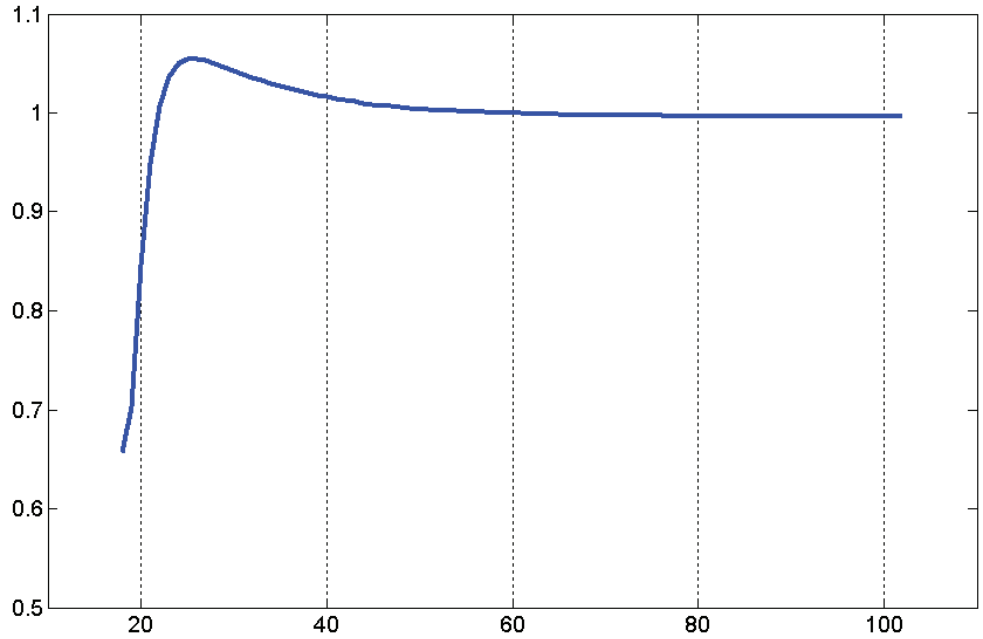

Figure 11. In-silico modeled effect of making vary the delay between the first and the second doses on the immunogenicity induced by the quadrivalent HPV vaccine. **x-axis**: time in days (λ) between the first and the second dose administration, in a 0-λ-180 vaccination schedule. **y-axis**: normalized (with respect to the 0-60-180 vaccination schedule) mean IgG titer for **zone B**. This curve was obtained by using set of parameters B.

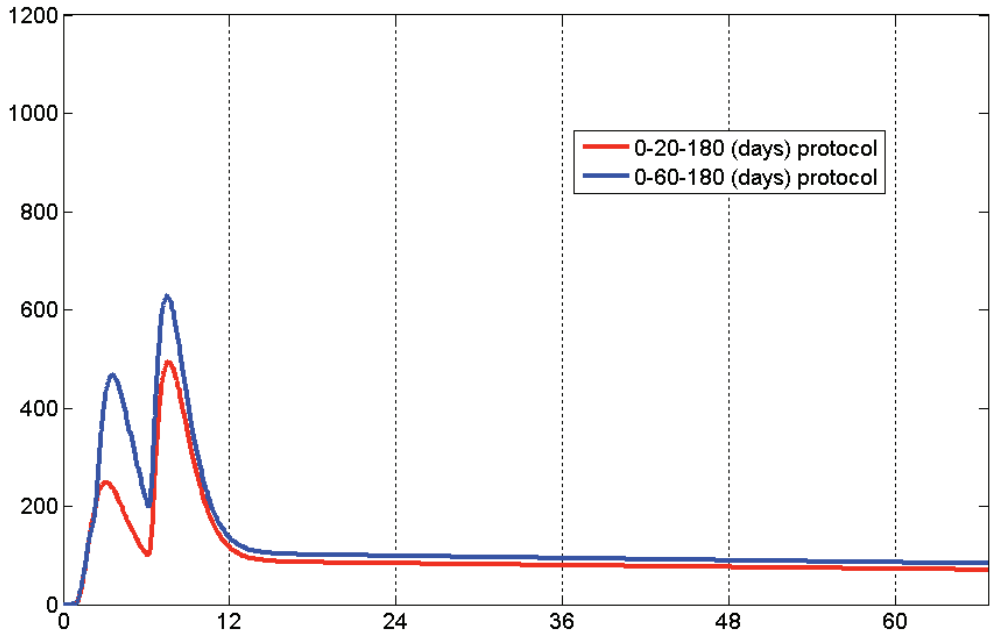

Figure 12. In-silico comparison of two vaccination schedules. **x-axis**: time, in months. **y-axis:** serum HPV-specific IgG titers, in milli-Merck units per mL. Both curves were obtained by using set of pamaters B.

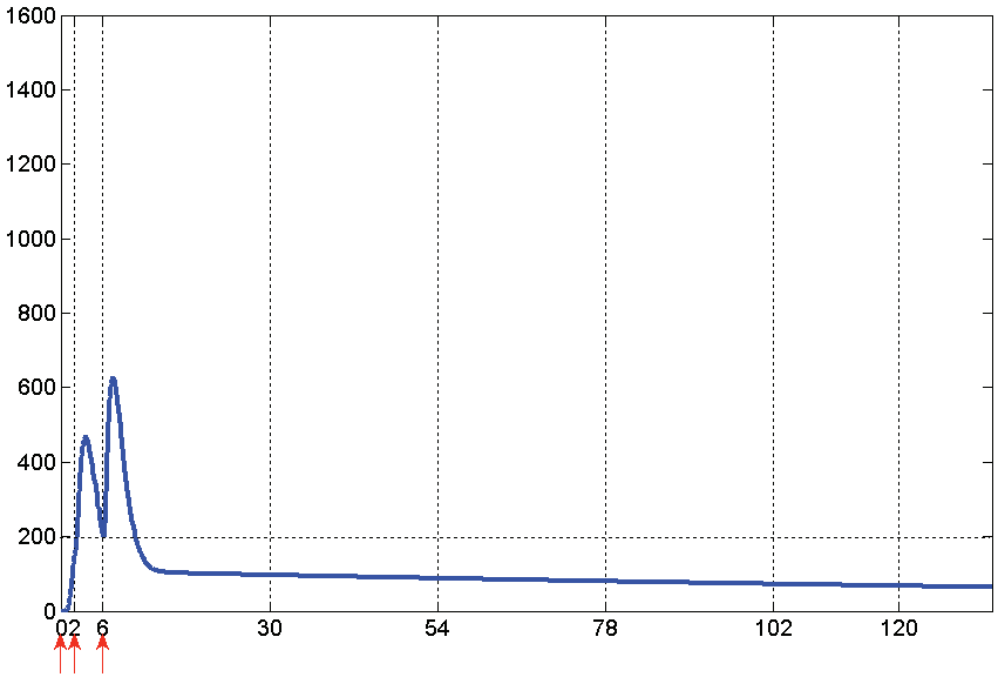

Figure 13. In-silico prediction of the immunoglobulin titer behavior, over a ten-year period of time, following vaccination with the HPV quadrivalent vaccine. **x-axis**: time, in months. **y-axis**: serum HPV-specific IgG titers, in milli-Merck units per mL. This curve was obtained by using set of parameters B. (The red arrows represent the simulated vaccination schedule).

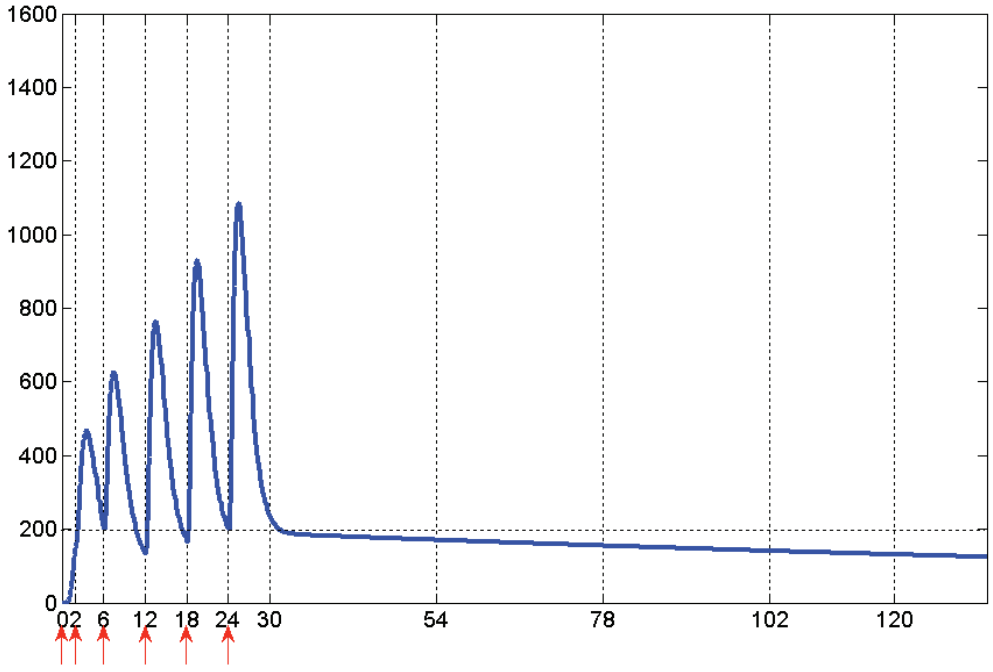

Figure 14. In-silico prediction of the immunoglobulin titer behavior, over a ten-year period of time, following vaccination and consecutive boosting with the HPV quadrivalent vaccine. **x-axis**: time, in months. **y-axis**: serum HPV-specific IgG titers, in milli-Merck units per mL. This curve was obtained by using set of parameters B. (The red arrows represent the simulated vaccination / boosting schedule).

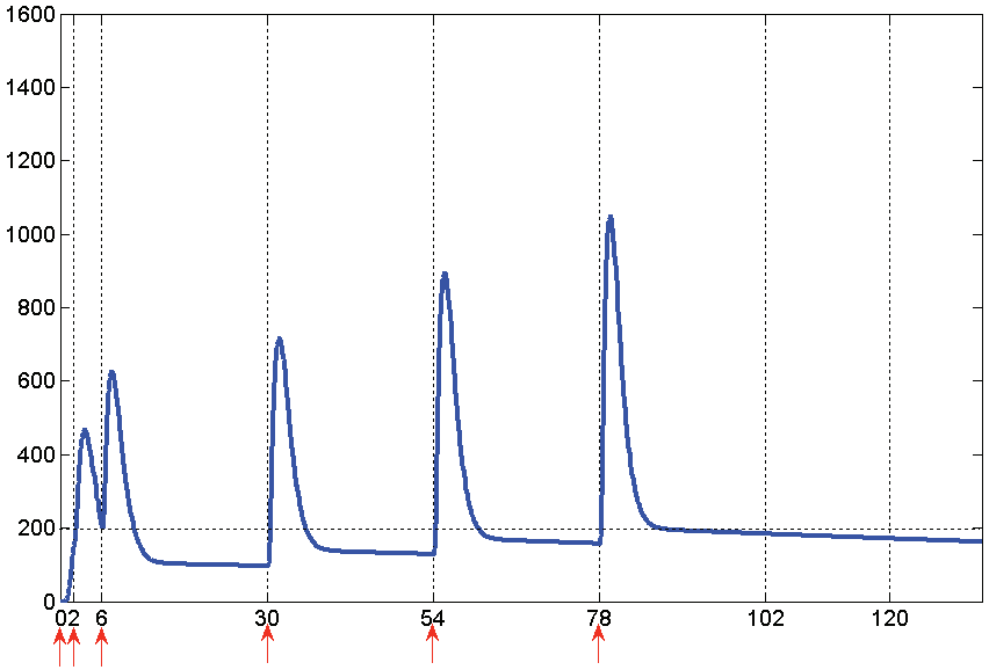

Figure 15. In-silico prediction of the immunoglobulin titer behavior, over a ten-year period of time, following vaccination and posterior boosting with the HPV quadrivalent vaccine. **x-axis**: time, in months. **y-axis**: serum HPV-specific IgG titers, in milli-Merck units per mL. This curve was obtained by using set of parameters B. (The red arrows represent the simulated vaccination / boosting schedule).

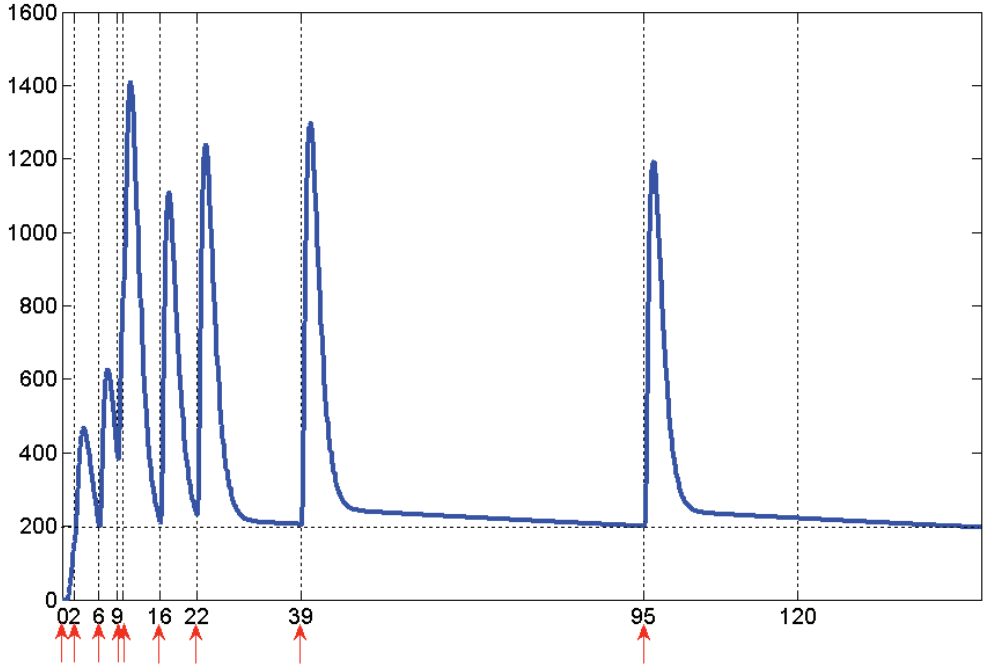

Figure 16. In-silico prediction of the boosting schedule that would be necessary for keeping, as long as possible within a 10-year period of time and through the administration of the smallest possible number of doses, the immunoglobulin titer above a hypothetical titer of 200 mMU/mL. **x-axis**: time, in months. **y-axis**: serum HPV-specific IgG titers, in milli-Merck units per mL. This curve was obtained by using set of parameters B. (The red arrows represent the simulated vaccination / boosting schedule).

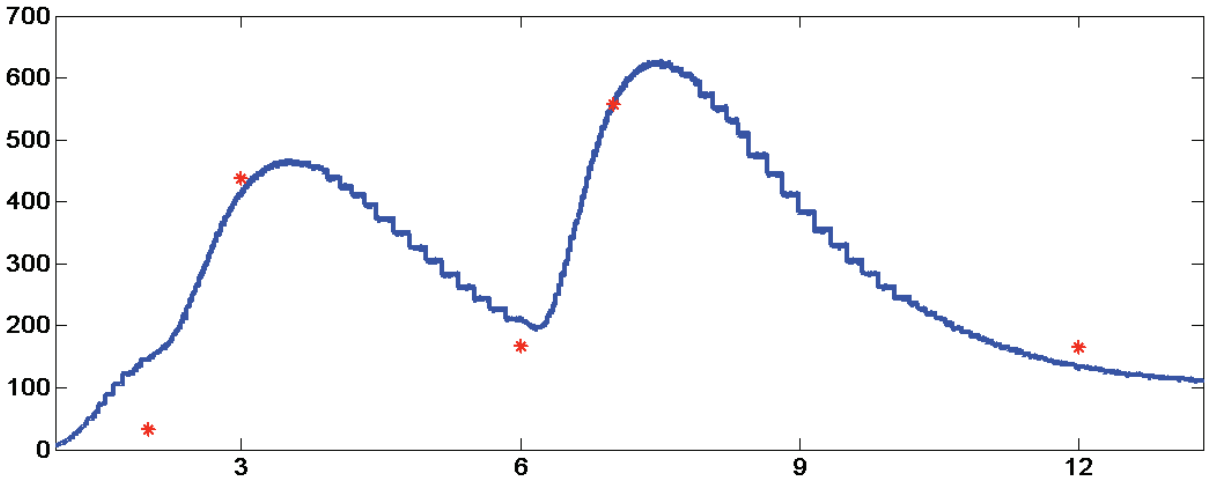

Figure 17. In-silico reproduction (through a multi-agent system approach) of the serum anti-HPV immunoglobulin titers following vaccination with the quadrivalent HPV vaccine (at months 0, 2 and 6). **x-axis**: time, in months, over which the simulation was conducted. **y-axis**: serum HPV-specific IgG titers, in milli-Merck units per mL. The red dots correspond to the observed values as reported in the literature. The discrete values obtained with the mathematical model (blue line in figure 4) were used to feed a procedure devised for creating or deleting agents of the immunoglobulin kind. The blue line in this figure represents the anti-HPV immunoglobulin titer as simulated in the lower free-space compartment, the one used to represent a micro-vessel adjacent to the epithelial tissue. No agents representing viral particles were included in this simulation. This simuation corresponds to the model's **first round of calibration**.

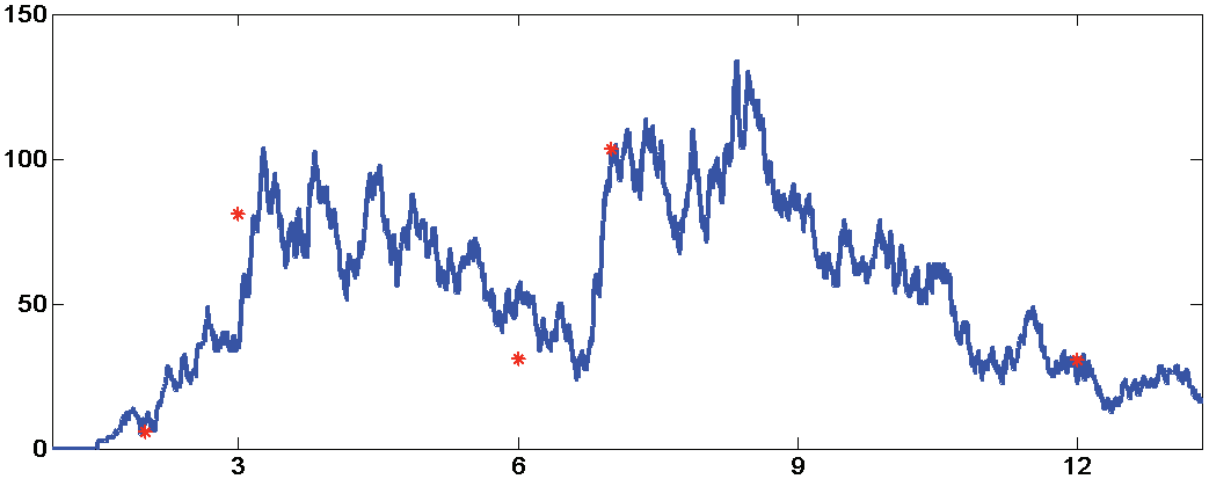

Figure 18. In-silico simulation (through a multi-agent system approach) of the anti-HPV IgG immunoglobulin titers in the upper respiratory tract lumen following intramuscular vaccination (at months 0, 2 and 6) with the quadrivalent HPV vaccine. **x-axis**: time, in months, over which the simulation was conducted. **y-axis**: HPV-specific IgG titers, in milli-Merck units per mL. The red dots correspond to the literature-based estimated titers. Such estimation was conducted as follows: each one of the reported mean values for the serum titers (the red dots in figures 4 and 17) was divided by a factor ($\phi = 5.4$) drawn from the literature[203]. In that study, the authors compared serum versus OMT (oral mucosal transudate) titers following vaccination with the quadrivalent HPV vaccine. No agents representing viral particles were included in this simulation. At t=0 a set of agents representing a 4 x 4 epithelial tissue was set up before letting it evolve freely. Simultaneously, the serum anti-HPV IgG titer was reproduced in the lower free space, as for figure 17. All over the simulation the anti-HPV IgG titer in the upper free space was tracked to yield the blue line in this figure. This simuation corresponds to the model's **first round of calibration**.

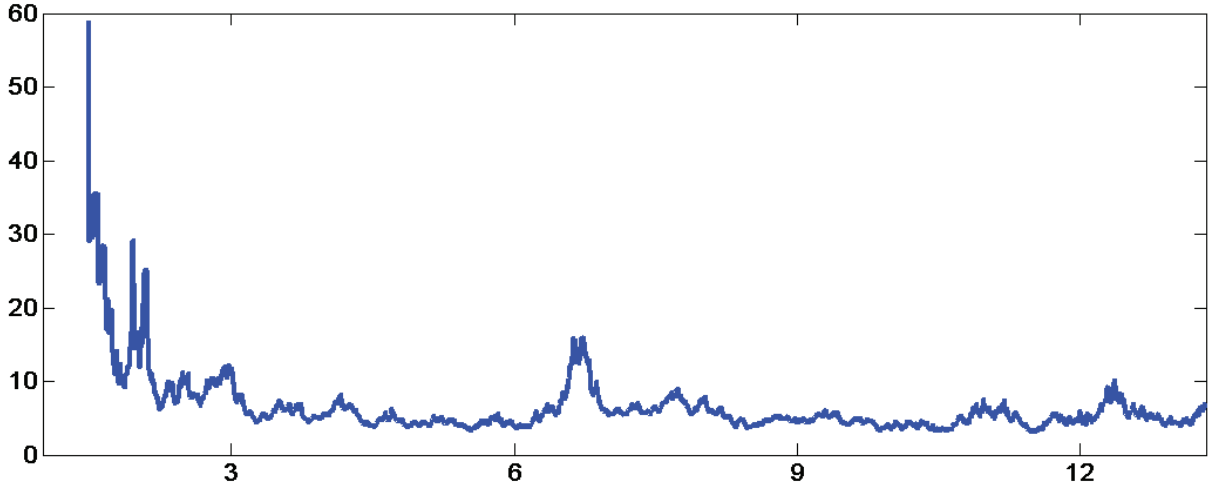

Figure 19. In-silico simulation (through a multi-agent system approach) of the quantitative relationship between the serum and the upper respiratory tract lumen IgG titers following vaccination (at months 0, 2 and 6) with the quadrivalent HPV vaccine. **x-axis**: time, in months, over which the simulation was conducted. **y-axis**: ratio between the serum and the upper respiratory tract lumen IgG titers. This curve was obtained by constantly dividing the results shown in figure 17 by the results shown in figure 18. This simuation corresponds to the model's **first round of calibration**.

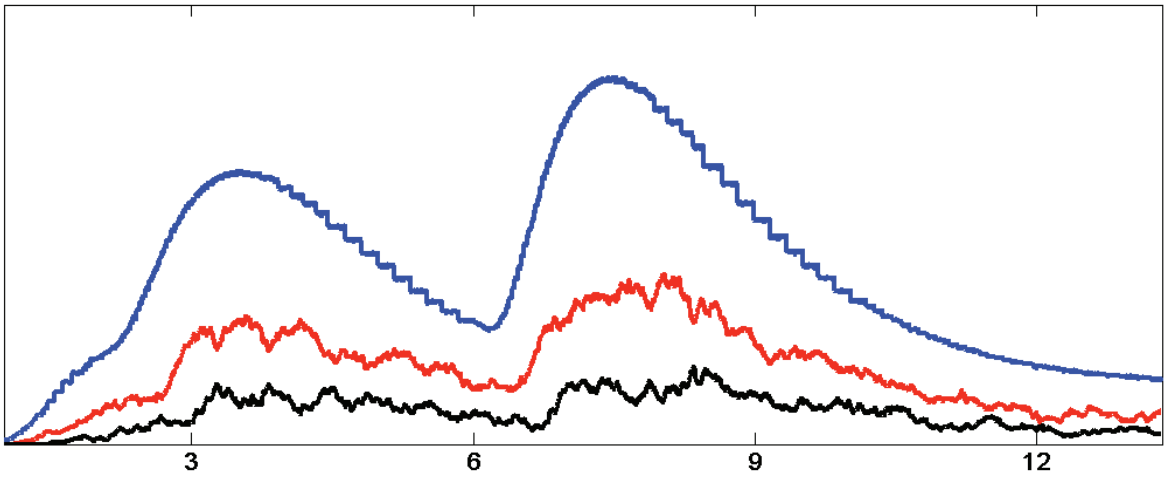

Figure 20. In-silico qualitative comparison (through a multi-agent system approach) of the anti-HPV IgG immunoglobulin titers in blood (blue line), in the mucous epithelial tissue (red line) and in the outer epithelial lumen (black line). **x-axis**: time, in months, over which the simulation was conducted. **y-axis**: relative IgG immunoglobulin titers. This simuation corresponds to the model's **first round of calibration**.

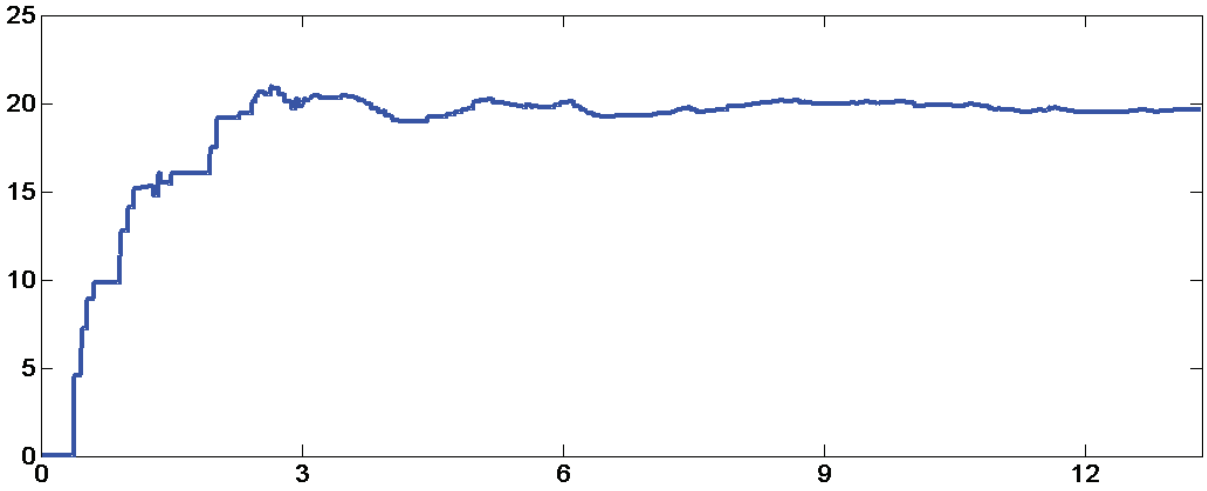

Figure 21. In-silico simulated dynamics of the epithelial-cell turnover process through a multi-agent system approach. **x-axis**: time, in months, over which the simulation was conducted. **y-axis**: time needed for the basal epithelial cells to reach the outermost layer. This simulation was conducted in complete absence of any agent representing viral particles or immunoglogulins. The agents representing the epithelial cells were initially disposed as follows: 4 layers, each one made up of 4 virtual cells, were set up in a square arrangement at t=0. Only the innermost virtual cells were authorized to multiply themselves pushing the rest of cells up. The system was then let to evolve freely. The time required for renewing the virtual tissue is continuously tracked. This simulation corresponds to the model's **second round of calibration**.

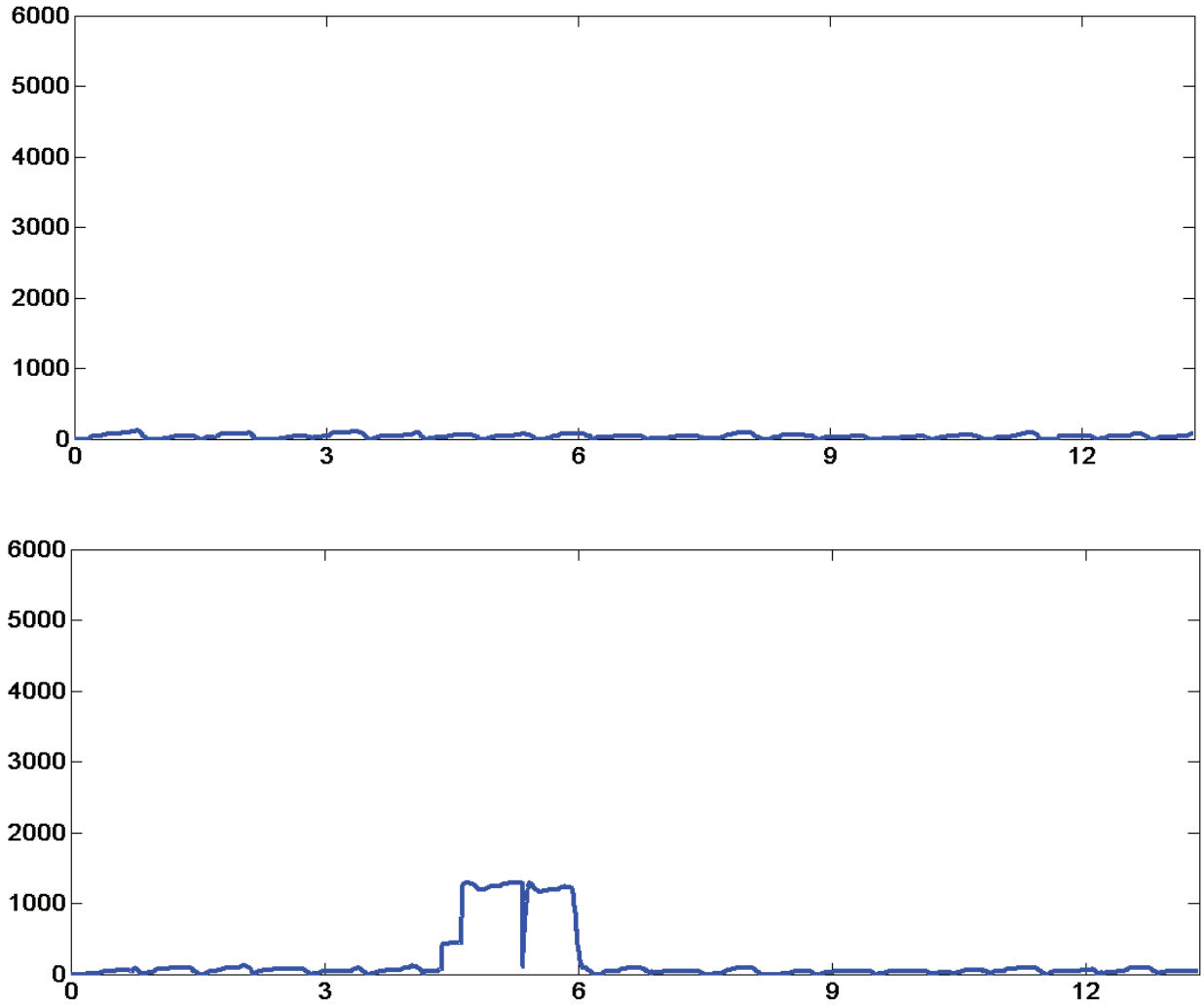

Figure 22. In silico simulation (through a multi-agent system approach) of the viral load evolution in an epithelial tissue sample. **x-axis**: time, in months, over which the simulation was conducted. **y-axis**: viral load, i.e. the number of particles infecting the tissue sample at any given instant of time. A set of virtual epithelial cells was initially arranged in a 4 x 4 **square-like distribution** (i.e. 4 cells in the basal layer bearing three other layers in such a way that a perfect 4-row 4-column structure is obtained). The virtual cells that constitute the innermost layer possess the capacity of multiplying themselves in such a way that the epithelial turnover complies to what was defined in the second round of calibration. No agents representing anti-HPV IgG immunoglobulins were included in this simulation. The tissue sample was subjected to a cyclic viral exposition. The system was let to evolve freely and the viral load was constantly tracked. Both the upper and the lower figures were obtained through the same set-up (the simulation was run twice). It corresponds to the model's **third round of calibration**.

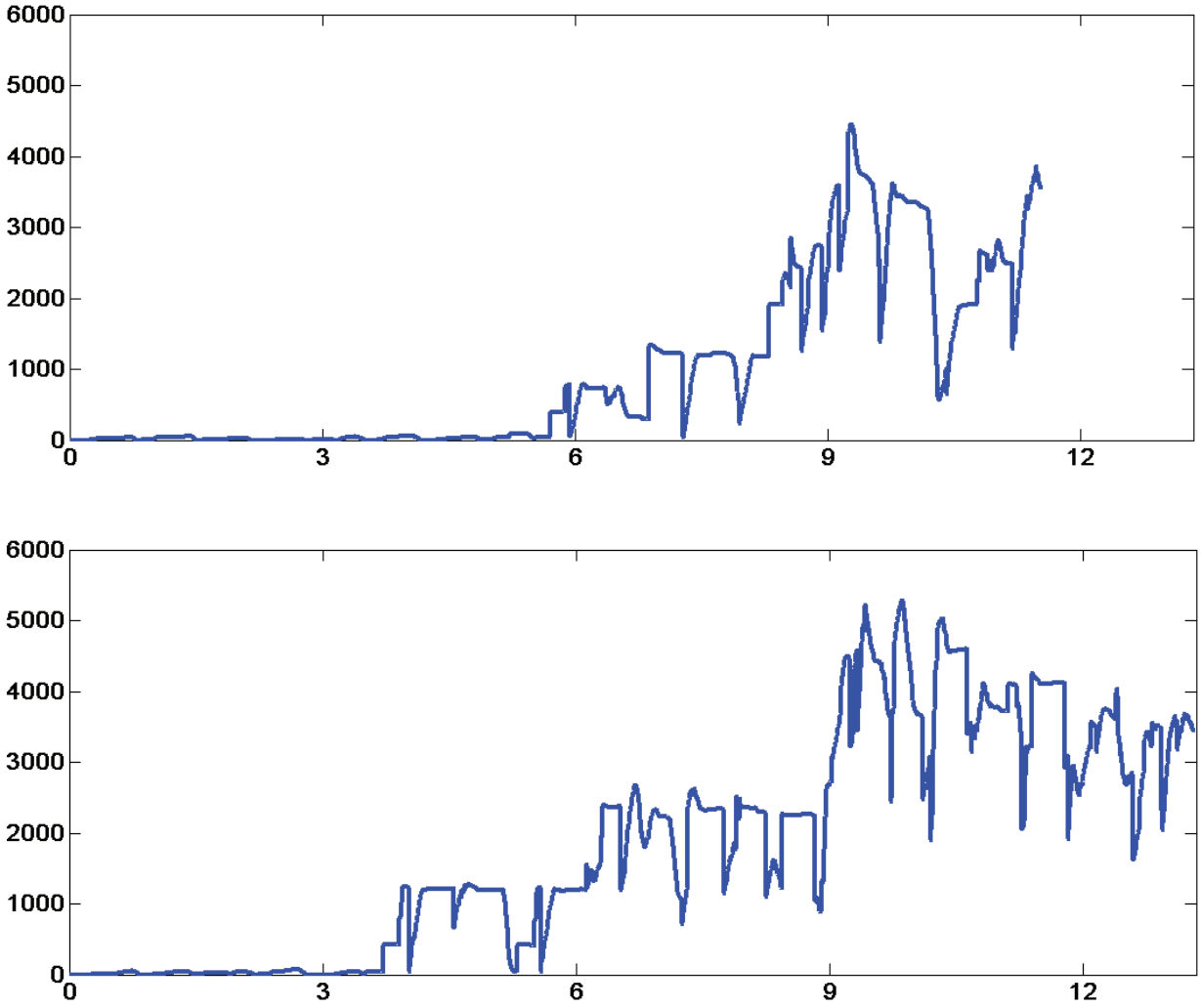

Figure 23. In silico simulation (through a multi-agent system approach) of the viral load evolution in an epithelial tissue sample. **x-axis**: time, in months, over which the simulation was conducted. **y-axis**: viral load, i.e. the number of particles infecting the tissue sample at any given instant of time. A set of virtual epithelial cells was initially arranged in a 4 x 4 **L-like distribution** (i.e. 4 cells in the basal layer bearing other cells in such a way that the first and second columns are made up of 4 cells, while the third and fourth columns are made of only 2 cells). The virtual cells that constitute the innermost layer possess the capacity of multiplying themselves in such a way that the epithelial turnover complies to what was defined in the second round of calibration. No agents representing anti-HPV IgG immunoglobulins were included in this simulation. The tissue sample was subjected to a cyclic viral exposition. The system is let to evolve freely and the viral load was constantly tracked. Both the upper and the lower figures were obtained through the same set-up (the simulation was run twice). It corresponds to the model's **third round of calibration**.

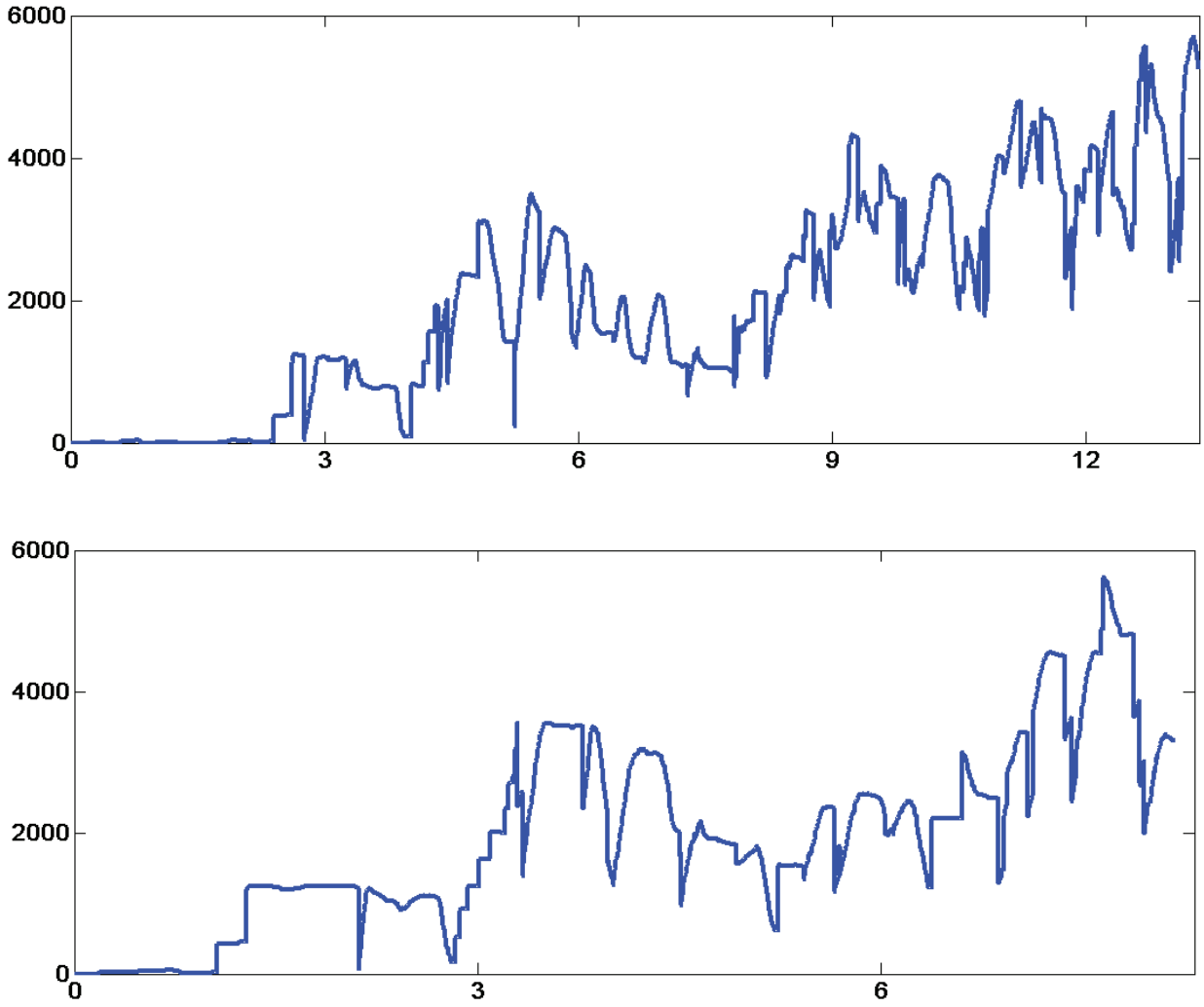

Figure 24. In-silico simulation of the viral load evolution in an epithelial tissue sample through which anti-HPV IgG immunoglobulins transude. **x-axis**: time, in months, over which the simulation was conducted. **y-axis**: viral load, i.e. the number of particles infecting the tissue sample at any given instant of time. Virtual epithelial cells were initially set up in a 4 x 4 L-kind of architecture simulating an epithelial transformation zone. The viral exposition was simulated exactly in the same way as for the third round of calibration. For this particular simulation, **the anti-HPV IgG immunoglobulin titer in the adjacent microvessel was set to be constant at 50 mMU/mL**. Both the upper and the lower figures correspond to the exact same simulation, conducted twice. This simulation corresponds to the in-silico **predictions** made on the intramuscular-vaccination induced immunoglobulins' capacity to interfere with the viral life cycle in the upper respiratory tract mucosa.

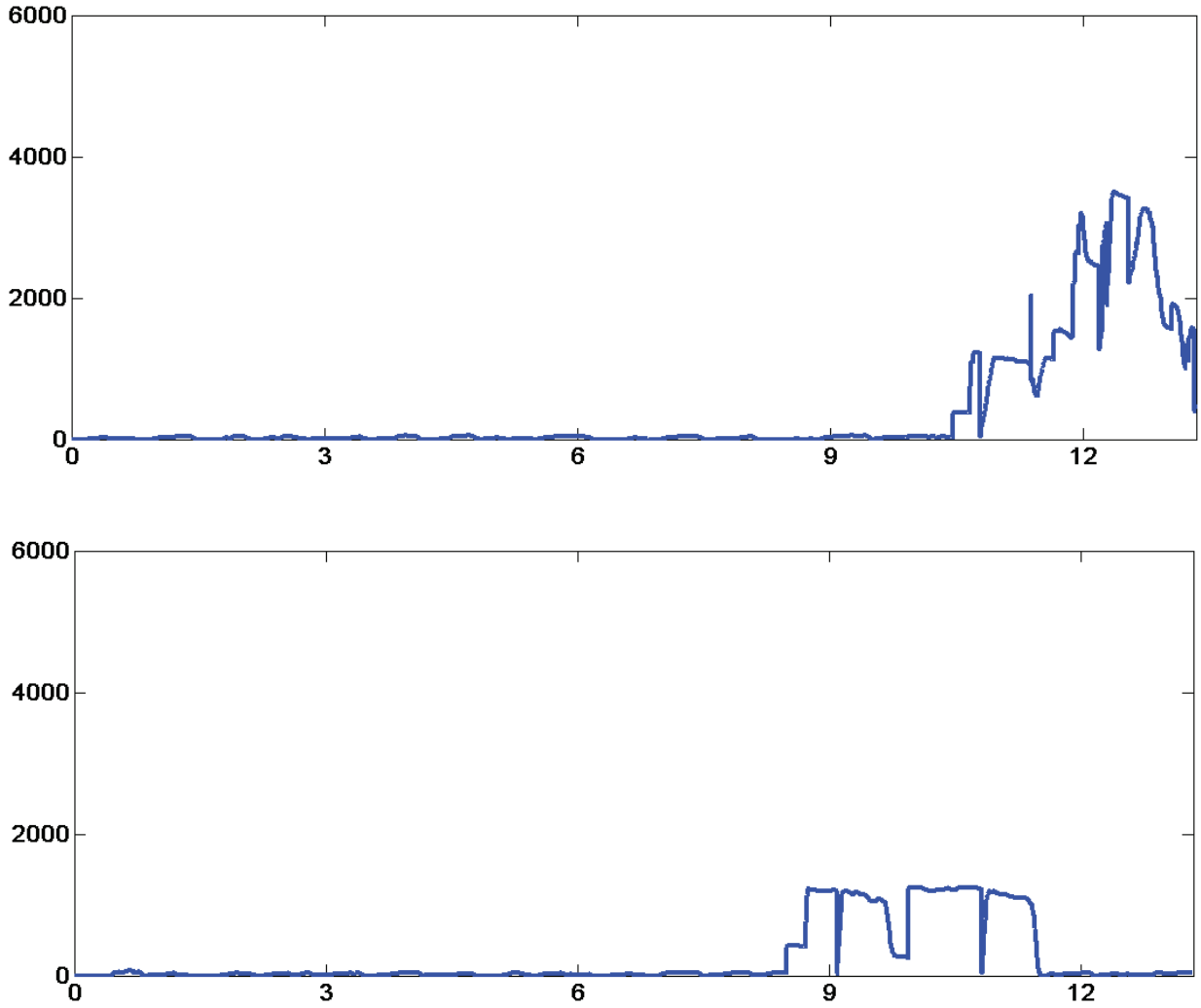

Figure 25. In-silico simulation of the viral load evolution in an epithelial tissue sample through which anti-HPV IgG immunoglobulins transude. **x-axis**: time, in months, over which the simulation was conducted. **y-axis**: viral load, i.e. the number of particles infecting the tissue sample at any given instant of time. Virtual epithelial cells were initially set up in a 4 x 4 L-kind of architecture simulating an epithelial transformation zone. The viral exposition was simulated exactly in the same way as for the third round of calibration. For this particular simulation, **the anti-HPV IgG immunoglobulin titer in the adjacent microvessel was set to be constant at 100 mMU/mL**. Both the upper and the lower figures correspond to the exact same simulation, conducted twice. This simulation corresponds to the in-silico **predictions** made on the intramuscular-vaccination induced immunoglobulins' capacity to interfere with the viral life cycle in the upper respiratory tract mucosa.

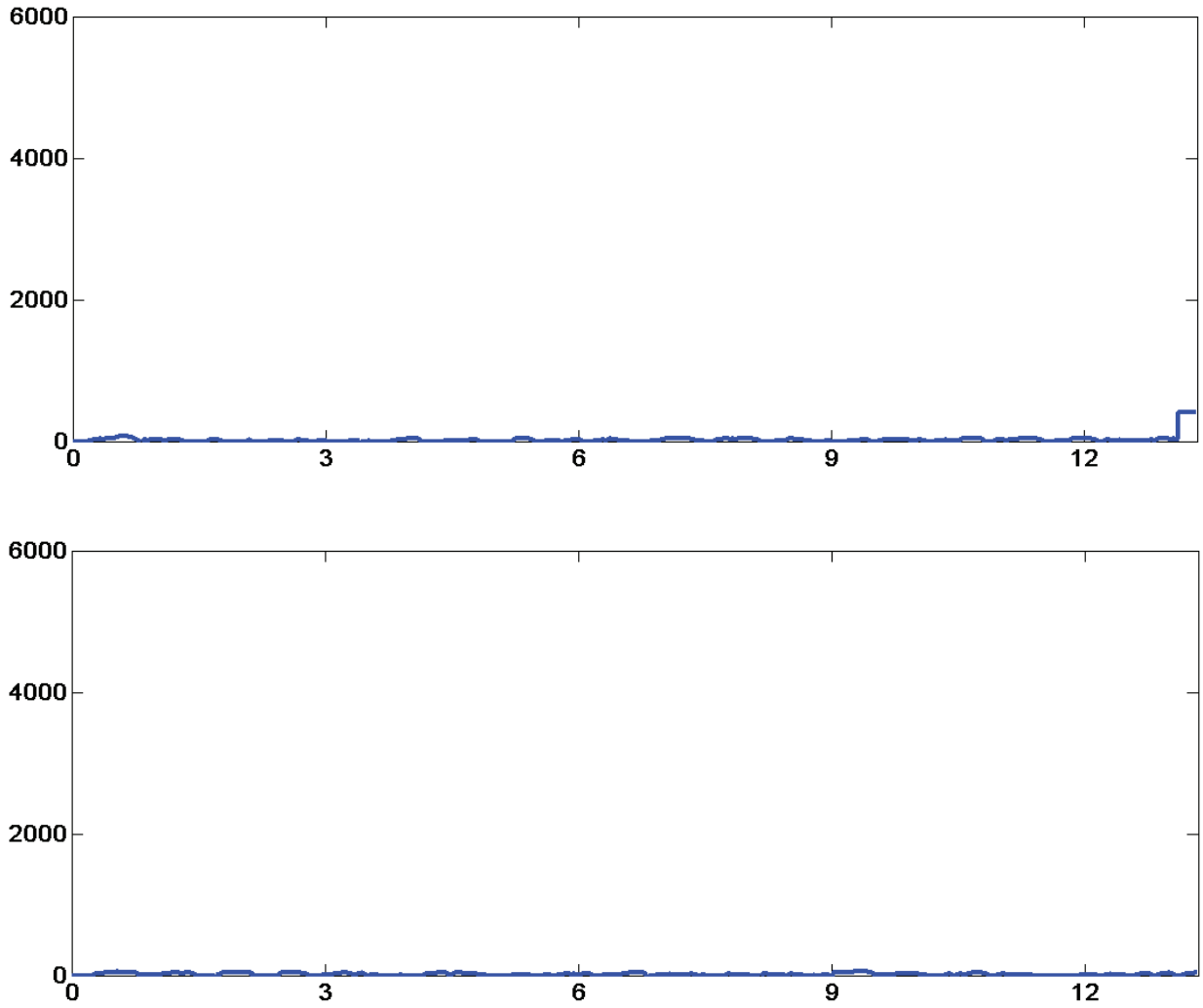

Figure 26. In-silico simulation of the viral load evolution in an epithelial tissue sample through which anti-HPV IgG immunoglobulins transude. **x-axis**: time, in months, over which the simulation was conducted. **y-axis**: viral load, i.e. the number of particles infecting the tissue sample at any given instant of time. Virtual epithelial cells were initially set up in a 4 x 4 L-kind of architecture simulating an epithelial transformation zone. The viral exposition was simulated exactly in the same way as for the third round of calibration. For this particular simulation, **the anti-HPV IgG immunoglobulin titer in the adjacent microvessel was set to be constant at 150 mMU/mL**. Both the upper and the lower figures correspond to the exact same simulation, conducted twice. This simulation corresponds to the in-silico **predictions** made on the intramuscular-vaccination induced immunoglobulins' capacity to interfere with the viral life cycle in the upper respiratory tract mucosa.

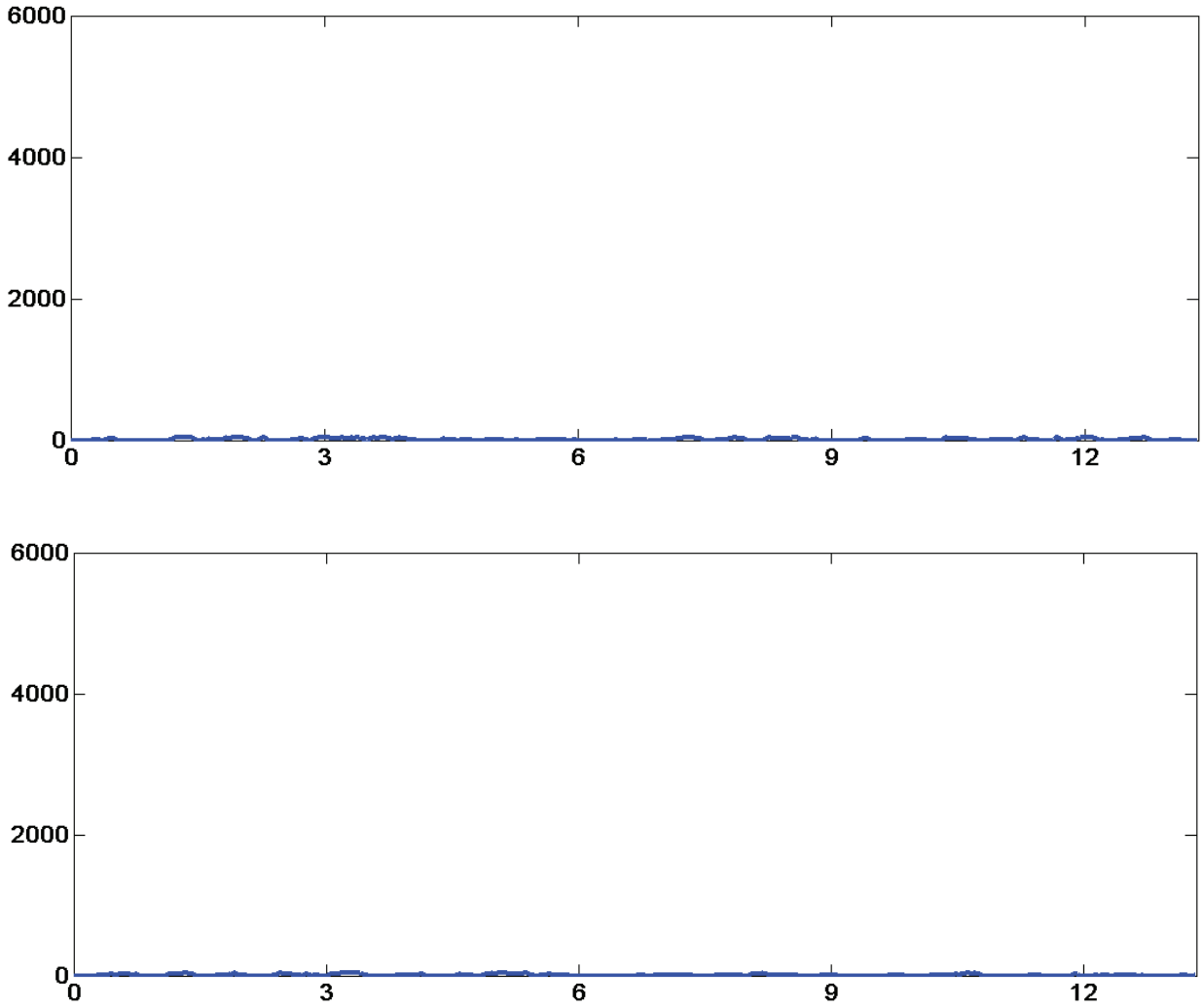

Figure 27. In-silico simulation of the viral load evolution in an epithelial tissue sample through which anti-HPV IgG immunoglobulins transude. **x-axis**: time, in months, over which the simulation was conducted. **y-axis**: viral load, i.e. the number of particles infecting the tissue sample at any given instant of time. Virtual epithelial cells were initially set up in a 4 x 4 L-kind of architecture simulating an epithelial transformation zone. The viral exposition was simulated exactly in the same way as for the third round of calibration. For this particular simulation, **the anti-HPV IgG immunoglobulin titer in the adjacent microvessel was set to be constant at 200 mMU/mL**. Both the upper and the lower figures correspond to the exact same simulation, conducted twice. This simulation corresponds to the in-silico **predictions** made on the intramuscular-vaccination induced immunoglobulins' capacity to interfere with the viral life cycle in the upper respiratory tract mucosa.